The influence of calcium on biofilm processes
by Mukesh Harilal Turakhia

A thesis submitted in partial fulfillment of the requirements for the degree of Doctor of Philosophy in Chemical Engineering
Montana State University

Abstract:
Bacteria exhibit a tendency for adsorbing to and colonizing surfaces which are submerged in aquatic environments. Adsorption is mediated by extracellular polymeric material which is formed by the bacteria and extends from the cell to the attachment surface. The attached cells reproduce and form additional extracellular polymer increasing the mass of the deposit. The cellular-extracellular matrix is termed a bipfilm.

The purpose of this study was to investigate the effect of calcium on cellular reproduction and extracellular polymer formation by Pseudomonas aeruginosa in a biofilm.

Experiments were conducted with a pure culture of Ps. aeruginosa using fixed film bioreactors with glucose serving as the limiting nutrient.

Results indicate calcium increases the rate and extent of cellular carbon accumulation at the surface. However, there was no effect of calcium on the amount of polymer carbon accumulated on the surface. Results also suggest that free calcium (or calcium-assisted ligands) is essential to the structural integrity of the biofilm. The energy required for biochemical conversion of glucose into biomass by suspended or immobilized culture of Ps. aeruginosa was constant and was independent of time, biomass concentration, specific cellular growth rate, and calcium concentration in the medium.

THE INFLUENCE OF CALCIUM ON BIOFILM PROCESSES

by

Mukesh Harilal Turakhia

A thesis submitted in partial fulfillment
of the requirements for the degree

of

Doctor of Philosophy

in

Chemical Engineering

MONTANA STATE UNIVERSITY
Bozeman, Montana

March 1986

APPROVAL

of a thesis submitted by

Mukesh Harilal Turakhia

This thesis has been read by each member of the thesis committee and been found to be satisfactory regarding content, English usage, format, citations, bibliographic style, and consistency, and is ready for submission to the College of Graduate Studies.

5 March 1986
Date

W. G. Charachis
Chairperson, Graduate Committee

Approved for Major Department

5 March 1986
Date

John T. Sears
Head, Major Department

Approved for College of Graduate Studies

March 10, 1986
Date

Henry L. Parsons
Graduate Dean

STATEMENT OF PERMISSION TO USE

In presenting this thesis in partial fulfillment of the requirements for a doctoral degree at Montana State University, I agree that the Library shall make it available to borrowers under rules of the Library. I further agree that copying of this thesis is allowable only for scholarly purposes, consistent with "fair use" as prescribed in the U.S. Copyright Law. Requests for extensive copying or production of this thesis should be referred to University Microfilms International, 300 North Zeeb Road, Ann Arbor, Michigan 48106, to whom I have granted "the exclusive right to reproduce and distribute copies of the dissertation in and from microfilm and the right to reproduce and distribute by abstract in any format."

Signature Mukesh Turakhia

Date 5 March 1986

ACKNOWLEDGMENTS

I wish to express my appreciation to the following:

Bill Characklis for his support, guidance, and encouragement which made my graduate educational experience productive and enjoyable.

Keith Cooksey, Gordon McFeters, and Dan Goodman for their advice and critical comments relating to my thesis.

The "slime gang": Rune, Andy, Maarten, Bjorn, Pam, Nick, Frank, Joe, Chris, and Rich for being an interesting group with whom to work and interact.

Lyman Fellows, Gordon Williamson, and Stuart Aasgaard for their help in maintenance of various equipment.

The staff and students of the Chemical Engineering, Civil Engineering, and Microbiology Departments whom I have not mentioned but have directly or indirectly contributed to this project.

I-Hsing Tsao for biofilm elemental analysis, Robert Kultgen for drafting some of the figures, and Wanda Myers for typing this thesis.

Naval Post Graduate Foundation for providing partial financial support through The Carl E. Menneken Fellowship.

Montana State University Engineering Experiment Station, National Science Foundation, and Office of Naval Research for partial financial support.

TABLE OF CONTENTS

TABLE OF CONTENTS (Continued)

LIST OF TABLES

LIST OF TABLES (Continued)

LIST OF FIGURES

LIST OF FIGURES (Continued)

LIST OF FIGURES (Continued)

LIST OF FIGURES (Continued)

ABSTRACT

Bacteria exhibit a tendency for adsorbing to and colonizing surfaces which are submerged in aquatic environments. Adsorption is mediated by extracellular polymeric material which is formed by the bacteria and extends from the cell to the attachment surface. The attached cells reproduce and form additional extracellular polymer increasing the mass of the deposit. The cellular-extracellular matrix is termed a biofilm.

The purpose of this study was to investigate the effect of calcium on cellular reproduction and extracellular polymer formation by *Pseudomonas aeruginosa* in a biofilm.

Experiments were conducted with a pure culture of *Ps. aeruginosa* using fixed film bioreactors with glucose serving as the limiting nutrient.

Results indicate calcium increases the rate and extent of cellular carbon accumulation at the surface. However, there was no effect of calcium on the amount of polymer carbon accumulated on the surface. Results also suggest that free calcium (or calcium-assisted ligands) is essential to the structural integrity of the biofilm. The energy required for biochemical conversion of glucose into biomass by suspended or immobilized culture of *Ps. aeruginosa* was constant and was independent of time, biomass concentration, specific cellular growth rate, and calcium concentration in the medium.

INTRODUCTION

Microorganisms, primarily bacteria, exhibit a tendency for adsorbing to and colonizing surfaces which are submerged in aquatic environments. The immobilized cells grow, reproduce, and produce extracellular polymeric substances (EPS) which frequently extend from the cell, forming a tangled mass of fibers lending structure to the entire assemblage which shall be termed a biofilm.

Biofilms serve beneficial purposes in natural environments and in some modulated systems. For example, biofilms are responsible for removing organic or inorganic "contaminants" from natural streams and in wastewater treatment processes (e.g., trickling filters and rotating biological contactors). Biofilms can, however, impair the performance of process equipment. They can impede the flow of heat across the surface, increase fluid frictional resistance at the surface, and increase the corrosion rate at the surface. Fouling of heat exchange equipment was estimated to cost the United States billions of dollars annually (Lund and Sandu, 1981).

Most studies on the effect of dissolved constituents on biofilm formation have been limited to the effect of organic constituents. There is little or no information on the effect of dissolved inorganic constituents. There are a number of inorganic components which can have an effect. However, the scope of this study was limited to the effect of calcium on biofilm formation.

The presence of calcium in the microbial growth medium has been shown to (1) influence microbial adsorption to the solid substratum, (2) be required for cellular growth and reproduction, (3) influence the composition of EPS. Published reports on the influence of calcium on the above processes is contradictory and the majority of the studies were conducted in quiescent conditions where the cells are not subject to shear stress. Understanding the role of calcium in biofilm processes may be useful in ecosystem analysis, control of biofouling in heat exchangers and/or pipelines, operation of fixed film biological wastewater treatment processes and increasing the rate or strength of cell immobilization in a biofilm reactor for biotechnology applications.

The major emphasis of this study was to determine the influence of calcium on (1) cellular reproduction and polymer formation in a biofilm, and (2) the cohesive strength of biofilm. *Pseudomonas aeruginosa* was used as a test organism because this organism has been extensively studied both in continuous flow stirred tank reactors, i.e., chemostats, and in biofilm reactors. Specific cellular growth rates and EPS formation rates are known under defined experimental conditions in chemostat and biofilm environments (Robinson et al., 1984; Bakke et al., 1984).

Research Goal and Objectives

The goal of this research was to determine the role of calcium in the formation and maintenance of a biofilm. To accomplish this goal, the following objectives were established:

1. Determine the influence of calcium on cellular reproduction and extracellular polymer formation by *Pseudomonas aeruginosa* in a biofilm.
2. Determine the influence of calcium on biofilm cohesiveness.
3. Determine the influence of calcium on the net accumulation rate of biofilm resulting from processes and characteristics in Objectives (1) and (2).

LITERATURE REVIEW

Biofilm Formation: A Process Analysis

The adsorption of bacteria is a general phenomenon encountered in natural environments with important ecological implications. Bacterial adsorption to surface offers advantages in terms of nutrient availability, particularly in fast flowing and nutrient deficient habitats. The adsorbed cells reproduce and form extracellular polymers leading to the formation of a biofilm. Accumulation of biofilm at the surface is the net result of the following fundamental processes (Characklis, 1981):

1. Adsorption of organic molecules to the surface forming a conditioned surface.
2. Transport of microbial cells to the conditioned surface.
3. Microbial adsorption to the conditioned surface.
4. Microbial transformation (growth, reproduction, etc.) at the surface resulting in the formation of biofilm.
5. Partial detachment of biofilm due to fluid shear stress.

Biofilm formation is not a sequence of the above rate processes occurring individually but rather the net result of these processes occurring simultaneously. At specific times in the overall development, certain rate processes contribute more than the others. This literature review will focus on the influence of calcium on the processes involved in the formation of biofilm.

Organic Adsorption

Adsorption of an organic monolayer occurs within minutes of exposure of an initially "clean" surface to an aqueous environment containing dissolved organics, microorganisms, and nutrients. This adsorption changes the properties of the wetted surface and actually conditions the surface for subsequent attachment and colonization (Loeb and Neihof, 1975; Baier and Depalma, 1977). These conditioning films have been investigated by various means. Baier and various co-workers have characterized these acquired films as negatively charged (poly-anionic) polysaccharides or glycoproteins (Baier, 1980, Baier and Weiss, 1975; Marshall, 1979).

There appears to be no evidence, however, that microorganisms can only attach to conditioned surfaces. Also, little is known regarding the influence of calcium on organic adsorption.

Transport of Microbial Cells

Microbial cells (0.5 - 10.0 μm) can be transported from the bulk fluid to the wetted surface by several mechanisms, including the following: diffusion (Brownian), gravity, thermophoresis, taxis, and fluid dynamic forces (inertia, drag, drainage, and downsweeps).

In general, the transport of microbial cells from the bulk fluid to the wetted surface depends on fluid flow conditions and is not known to be influenced by the presence of calcium in the bulk fluid.

Microbial Adsorption

Once bacterial cells have been transported to the wetted surface, two types of adsorption are possible; reversible and irreversible (Marshall et al., 1971; Zobell, 1943). Reversible adsorption is characterized by an initially weak adsorption of a cell which still exhibits Brownian motion and is readily removed by mild rinsing. Conversely, irreversible adsorption is a permanent bonding to the surface, usually aided by the production of EPS (Fletcher, 1980). Cells attached in this way can only be removed by rather severe mechanical or chemical treatment.

Calcium and Microbial Adsorption

The role of cations in the adsorption of a cell to the substratum is presently unknown. Roux (1894) reported the necessity for divalent cations, notably Ca^{2+}, in cellular adsorption. Calcium has been shown to be necessary for adsorption of aquatic bacteria (Marshall et al., 1971; Fletcher and Floodgate, 1973; Stanley, 1983) and marine diatoms (Cooksey, 1981). For example, a marine pseudomonad would not irreversibly adsorb in the absence of Ca^{2+} and Mg^{2+}, but would adsorb when either of the cations were present (Marshall et al., 1971). Stanley (1983) observed that *Ps. aeruginosa* adsorbed poorly in distilled water with adsorption increasing as calcium chloride concentration was increased to 10 mM.

Fletcher (1980) observed the influence of cations on the adsorption process by "chemically treating" free-living cells and

observing any influence on their subsequent adsorption to surfaces. The adsorption of a marine pseudomonad (Fletcher, 1980) was inhibited by the presence of EDTA (ethylenediaminetetra-acetic acid) suggesting that the chelant removed surface-bound divalent cations conceivably involved in intercellular-ionic bridging. Fletcher (1980) noted that lanthanum decreased bacterial adsorption and postulated that lanthanum prevented adsorption through interaction with and subsequent denaturation of EPS. Lanthanum is known to inhibit calcium transport into cells, and to displace calcium from cellular membranes (Weiss, 1974), so that the effect observed by Fletcher (1980) may have been related to the diminution of the flux of calcium to the intracellular space.

Divalent cations, calcium in particular, have been shown to influence microbial adsorption. However, the role of cations in the adsorption process is much disputed. It has been suggested that cations influence adsorption (1) by directly influencing cell physiology or membrane permeability (Drapeau and MacLeod, 1965), and (2) directly by their accumulation at the cell surface where they mediate the formation of the electric double layer (Shaw, 1970). Moscona (1968) suggested that the removal and/or absence of divalent cations inhibits adsorption via calcium sensitive ligands. It has also been suggested that divalent cations, especially calcium, can form bridges between negatively charged substrata and microorganisms, can stabilize the structure of EPS (Fletcher and Floodgate, 1973), or cause precipitation of EPS in the space between a cell and a substratum (Rutter, 1980). Further evidence for the involvement of calcium in the adsorption process comes from the use of complexing agents EDTA

(Fletcher, 1980) and EGTA (Appendix H). The chelant did not remove cells irreversibly adsorbed (ethylene glycol-bis(β-aminoethyl ether)-N, N-tetraacetic acid) to the surface (Fletcher, 1980; Appendix H) suggesting that calcium was not involved in the adsorption of cells to the substratum.

Microbial Transformation

The attached microorganisms assimilate nutrients, reproduce, and form extracellular polymers. The combined result of these processes is the formation of biofilm. The characteristic of the biofilm accumulated will depend on the microbial species, the polymers produced, and the environmental conditions.

Biofilm studies thus far (Kornegay and Andrews, 1967; Lamotta, 1967; Zelver, 1979; Trulear and Characklis, 1982) relied on a relatively unstructured approach to the analysis of biomass components. The biotic component was generally characterized only in terms of cell number and cell mass with little attention to the physiological state of the organisms, although there have been some limited attempts at distinguishing between reproduction and polymer formation (Trulear, 1983; Bakke et al., 1984). Trulear (1983) and Bakke et al. (1984) have used process analysis techniques in experimental biofilm reactors to quantify the fundamental rate processes within a biofilm at steady state. Their results suggest the following:

1. *Ps. aeruginosa* does not behave differently in biofilms than in suspension at steady state. The biofilm activity measurements in

this study were made *in situ*, and without significant diffusional resistance.

2. Intrinsic rate and stoichiometric coefficients derived in the chemostat can, therefore, be used to describe steady state biofilm processes.

Process analysis techniques can be useful in determining the effect of calcium on cellular reproduction and polymer formation. The effect of calcium on microbial transformation within a biofilm can also be inferred from more easily observed rate processes such as substrate consumption and oxygen consumption. However, the observed rate processes are not a sufficient criterion for comparing microbial activity under different experimental conditions because they are the net result of several fundamental processes.

Calcium and Microbial Growth

Calcium plays a vital function inside the cell. The concept of calcium as intracellular messenger and/or regulator was proposed 30-40 years ago (Campbell, 1983). For example, Hojeberg and Rydstrom (1977) suggested that calcium is a potent positive effector of nicotinamide nucleotide transhydrogenase in *Ps. aeruginosa*. Several extracellular degradative enzymes in both eucaryotes and procaryotes require calcium for stability and/or maximal activity (Campbell, 1983).

Calcium is required for growth and function of many bacterial species (Campbell, 1983, Weinberg, 1977). Marshall et al. (1971) reported that omission of calcium and magnesium from artificial sea water prevented growth and polymer production of *Pseudomonas* R3.

Shooter and Wyatt (1955) investigated the mineral requirements of Staphylococcus pyogenes and found that calcium and magnesium were needed for growth. Kenward et al. (1979) reported that inclusion of calcium and/or magnesium in the media had no effect on the exponential growth rate (0.66 h^{-1}) of Ps. aeruginosa. Calcium was shown to be necessary for the growth of marine Bdellovibrio sp. (Huang and Staff, 1973; Bell and Lantham, 1975).

Calcium appears to be exclusively extracellular and is not accumulated by a normal growing cell (Silver, 1977; Belliveau and Lanyi, 1978; Wacker and William, 1968). A special situation of calcium accumulation occurs during unusual conditions such as bacterial sporulation. Similarly, a number of different major ions (e.g., magnesium, iron, sodium, and potassium) were shown to be required for growth (Shankar and Bard, 1952; Weinberg, 1977; Shooter and Wyatt, 1955).

Very little is known regarding the effect of calcium on specific cellular growth rate and/or polymer production. A clear-cut requirement of calcium for growth in microorganisms has rarely been demonstrated (Wyatt, 1961, 1964; Wyatt et al., 1962; Hunter, 1972). This is due to the fact that it is very difficult to reduce the concentration of free calcium below 1 μM. The concentration of the free calcium can be lowered by the addition of calcium-specific chelant (EGTA). Turakhia (1984) was able to grow Ps. aeruginosa in the presence of 0.006 M EGTA (free calcium in the media was approximately 10^{-10} M). His results (Appendix G) showed that either EGTA or free calcium affected the maximum specific growth rate of Ps. aeruginosa.

Bacterial EPS

The formation of extracellular polymer has long been recognized as an important process in the metabolism of many dispersed and immobilized bacteria. Traditionally, two types of extracellular polymer have been distinguished depending on the spatial association of the polymer with the cell (Brock, 1979). Extracellular polymer which remains in a rather compact layer attached to the cell is referred to as a capsule. Conversely, extracellular polymer which does not exhibit a close association with the cell and can exist as a rather dispersed accumulation is referred to as a slime layer. The capsule-slime component of biofilms is termed extracellular polymeric substances (EPS) because little is known about its composition.

EPS Characterization. Numerous microorganisms produce exopolysaccharides, i.e. polysaccharide found outside the cell wall, either attached to the cell in the form of capsules or secreted into the extracellular environment in the form of slime. Such polymers vary considerably in their chemical structures. There are many qualitative analyses of bacterial EPS, usually considered to be carbohydrate with acidic groups (Corpe et al., 1976; Fletcher and Floodgate, 1973), amino groups (Baier, 1975), and sometimes associated with proteins (Corpe et al., 1976). A variety of chemical structures is represented in the polysaccharides synthesized by bacteria (Sutherland, 1982). Some components such as D-glucose, D-mannose, D-galactose, and D-glucuronic acid occur very frequently; others such as L-rhamnose, L-fucose, D-mannuronic acid, and D-guluronic acid are slightly less common.

Ps. aeruginosa EPS. Pseudomonas aeruginosa was the test organism for this experimental program. The literature on the composition of slime produced by dispersed culture of Ps. aeruginosa is contradictory. Eagon (1956) reported that Ps. aeruginosa produces slime, which consists largely of mannans, but no uronic acid or amino sugars were detected. Later, Eagon (1962) showed that, in addition to mannose, which accounted for 50% of the material, the slime contained appreciable amounts of nucleic acid (mostly DNA), and small amounts of proteins. Linker and Jones (1964) showed the production, by a pathogenic Pseudomonas organism, of a polysaccharide very similar to alginic acid, a polyuronide usually obtained from sea weed. Both mannuronic and small amounts of guluronic acid appear to be present. Carlson and Mathews (1966) have reported that Ps. aeruginosa slime is a polymer composed of uronic acids. Brown et al. (1969) reported the slime produced by eight strains of Ps. aeruginosa (stationary phase) to be qualitatively the same. The slime was shown to be predominantly polysaccharide (mainly glucose with smaller amount of mannose) with some nucleic acids material and a small amount of protein.

The extracellular polymers have been shown to be involved in the selective accumulation of ions in many gram negative bacteria (Galanos et al., 1977; Leive, 1974). Buckmire (1983) observed preferential adsorption of Ca, K, P, and S (2-4 times greater than in growth medium) on individual cell and extracellular components, indicating the role of EPS (and possibly associated macromolecules) in the adsorption of ions. The lipopolysaccharide of gram-negative bacteria contains a number of potential cation-binding sites (Schindler and Osborn, 1979; Galanos et

al., 1977) having a high affinity for calcium and magnesium. Outside the cell, calcium can bind to carboxylate and sulfate groups of many polysaccharides, many of which are also linked to proteins (Levine and William, 1984).

Calcium and EPS Formation

Wilkinson and Stark (1956) observed that calcium, magnesium, and potassium stimulated polysaccharide production by *Enterobacter aerogenes*. Linker and Evans (1976) observed that the composition of *Pseudomonas aeruginosa* alginate was not influenced by different calcium levels in the medium. However, the composition of *Az. vinelandii* (Larsen and Haug, 1971) was affected by the calcium concentration in the medium and postulated that mannuronic acid residues were epimerised to guluronic residue by an extracellular enzyme dependent on calcium ion. Couperwhite and McCallum (1974) observed that the addition of EDTA to batch culture media affected the ratio of D-guluronic acid to D-mannuronic acid in the alginate produced by *Az. vinelandii*. Corpe (1964) observed increased polysaccharide production by *Chromobacterium violaceum* in the presence of calcium.

Calcium and Biofilms

Calcium has been implicated in direct or indirect bridging between adjacent cell surfaces. Fletcher (1980) considers that calcium may act as a cross-linking or charge screening agent for the ionic groups in the EPS. Turakhia et al. (1983) were able to detach a mixed microbial film in a turbulent flow system with EGTA (a calcium-specific chelant)

and postulated that calcium was essential to the structural integrity of the biofilm.

EDTA chelates divalent cations in the following preferential sequence:

$$Ca^{2+} > Mg^{2+} > Sr^{2+} > Ba^{2+}$$

However, disaggregation in EDTA might be connected with chelation of less strongly bound cations, as well as Ca^{2+}. In recent years, however, EDTA has been superseded in many studies involving calcium (Cooksey and Cooksey, 1980; Turakhia et al., 1983) by EGTA, which can bind calcium over 10^5 times (Reed and Bygrave, 1975) more effectively than it binds magnesium.

It is likely that calcium plays a more important role in adsorption than any other cation. Calcium has a higher coordination number (7 or 8) and the coordination geometry is irregular in both bond angle and bond length. In both regards, calcium is quite different from magnesium, which maintains six coordination in a closely regular octahedron. Because magnesium requires a certain specific geometry, it is weakened in its ability to bind irregular geometries of coordination sites of biological molecules. Magnesium does not cross-link structures readily, for cross-linking usually demands a high coordination number and irregular geometries, which are characteristics of calcium.

Biofilm Detachment

At any point in the development of a biofilm under turbulent flow conditions, external portions of biofilm are sheared away into the fluid flow.

Detachment phenomenon can be arbitrarily categorized as erosion or sloughing. Erosion refers to continuous removal of small portions of biofilm, which is highly dependent on fluid dynamic conditions. Under these circumstances, rate of detachment increases with increasing biofilm thickness and fluid shear stress at the biofilm-fluid interface (Trulear and Characklis, 1982). Sloughing refers to a random, massive removal of biofilm attributed to nutrient or oxygen depletion deep within the biofilm (Howell and Atkinson, 1976). Sloughing is more frequently witnessed with thicker, less dense film which develops under low shear conditions.

Detachment can also occur for reasons other than hydrodynamic forces. Bakke (1983) has observed a massive detachment when substrate (lactate) loading to the biofilm was instantaneously doubled. Turakhia et al. (1983) and Characklis (1980) have observed increased detachment (of mixed microbial film) upon addition of chelants (EGTA and EDTA respectively) suggesting the importance of calcium to the cohesiveness of the biofilm. Many other chemicals (e.g., chlorine, bromine chloride, bromo-chloro-dimethyhydantoin, surfactants) have also been used for detachment with varying success.

Most of the detachment work with chemicals has been monitored directly by measuring the changes in frictional resistance and/or heat transfer resistance. No significant work has quantified the amount of material remaining on the surface, identified the detached material, or quantified the amount of material detached.

Detachment of biofilm is the major objective of many anti-fouling additives. Very little is known regarding the kinetics and the extent

of detachment. Such kinetic expressions would be useful for modelling purposes and as a comparative criterion for evaluating anti-fouling treatments.

Organism

Pseudomonas aeruginosa

This organism has been studied extensively both in continuous flow stirred tank reactors (CFSTR), i.e., chemostats, and in annular biofilm reactors. Information on growth rate and EPS formation rates are known under defined experimental conditions in chemostat and biofilm environments (Robinson et al., 1984; Bakke et al., 1984). Pseudomonas aeruginosa is a common waterborne polymer-forming bacteria capable of causing severe infections in a compromised host (Woods et al., 1980; Costerton, 1979). The primary mode of growth of Ps. aeruginosa in nature and disease is in polymer-enclosed microcolonies attached to a variety of surfaces. The polymer-enclosed, attached mode of growth purportedly protects Ps. aeruginosa (and other biofilm organisms) from the bactericidal activity of bacteriophages and amoebae which are numerous in natural systems and from antibiotics and host defense mechanisms in diseased systems (Costerton, 1979). Ps. aeruginosa can be considered a classic biofilm organism and for this reason is the bacterial species used in this study.

Relevant characteristics describing Ps. aeruginosa are as follows.

a) gram stain: negative (Buchanan et al., 1974)

b) morphology: rod shaped, typically 0.5 - 0.8 μm

		by 1.5 - 3.0 μm (Buchanan et al., 1974)
c)	metabolism:	chemoorganotroph (Buchanan et al., 1974)
d)	respiration:	strict aerobe (Buchanan et al., 1974)
e)	motility:	polar monotrichous flagellation (Buchanan et al., 1974)
f)	polymer composition:	primarily mannuronic and glucuronic acids (Evans and Linker, 1973; Mian et al., 1978)

MATHEMATICAL DESCRIPTION OF THE SYSTEM

Cellular production and polymer formation by *Ps. aeruginosa* can be described mathematically using a mass balance approach. This section contains a mathematical model which describes biofilm processes, including accumulation and activity of bacteria immobilized in a biofilm and dispersed in the bulk phase. In this model the substrate carbon is partitioned into extracellular product and biomass carbon. For both of these processes, some substrate carbon is oxidized to carbon dioxide providing energy for synthesis of cells and EPS (Trulear, 1983).

The annular reactor (Figure 1) and the chemostat (Figure 2) were operated as continuous flow stirred tank reactors (CFSTR) in which bulk fluid concentration gradients do not exist. Accumulation of compounds in the bulk fluid can be described by a material balance of the general form:

$$\begin{matrix}\text{net}\\ \text{rate of}\\ \text{accumulation}\end{matrix} = \begin{matrix}\text{net}\\ \text{rate of}\\ \text{transport}\end{matrix} + \begin{matrix}\text{net}\\ \text{rate of}\\ \text{transformation}\end{matrix} \qquad (1)$$

Accumulation of attached biofilm components can be described by a constitutive equation of the same general form as Equation 1, but with no transport term.

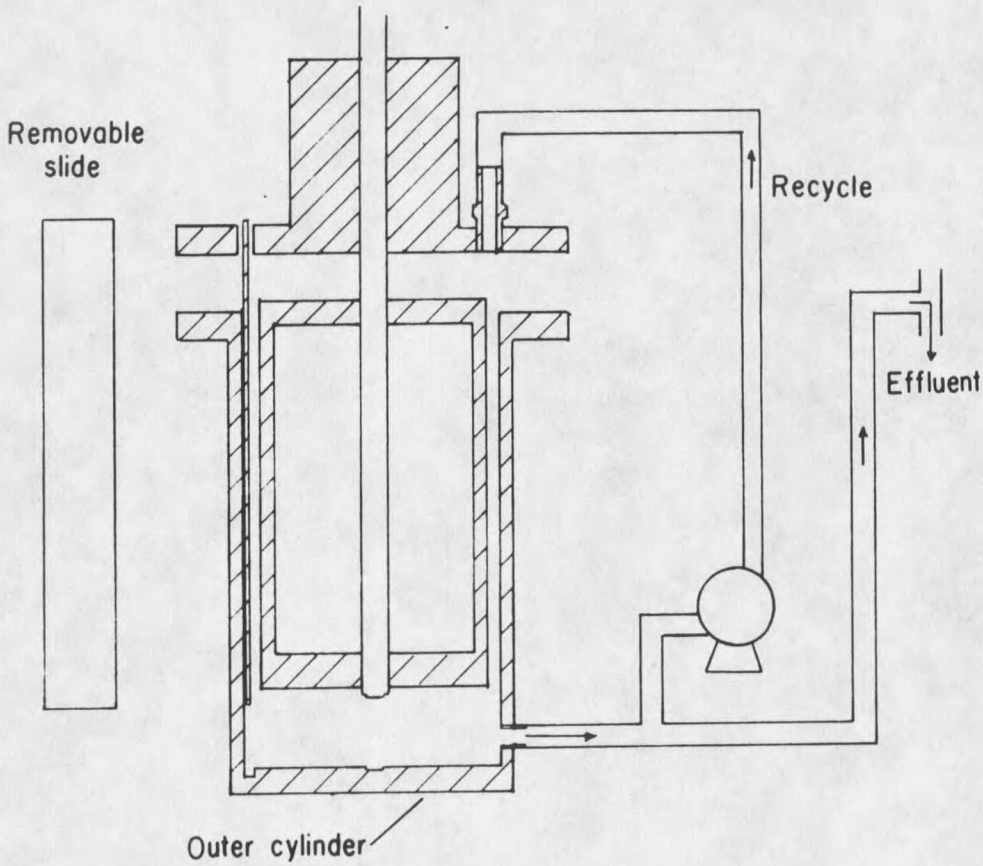

Figure 1. A simplified diagram of the annular reactor.

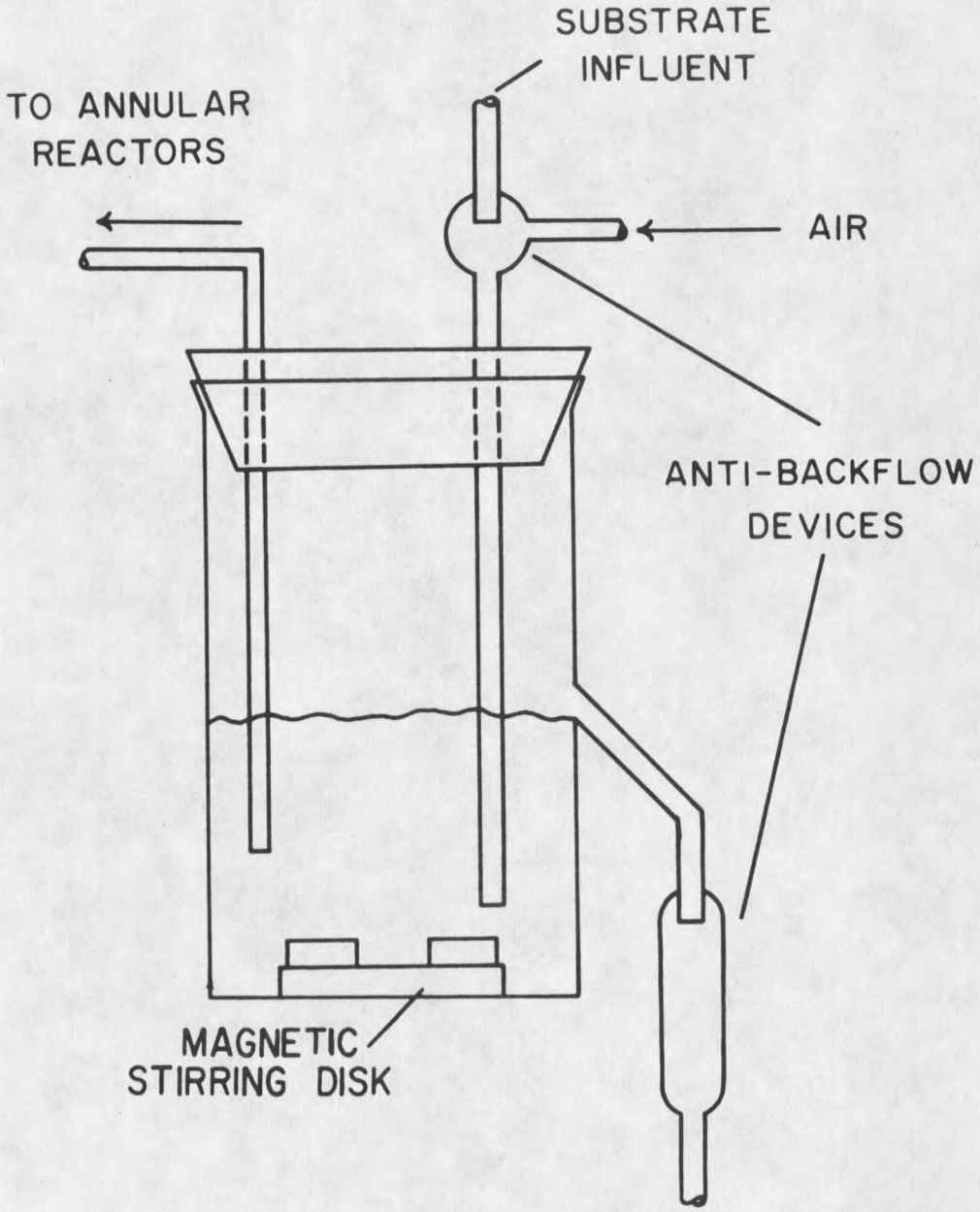

Figure 2. A simplified diagram of the chemostat.

Chemostat Equation

Cellular carbon. A mass balance across the chemostat for cellular carbon can be written as follows:

$$V\,dx/dt = F\,(x_i - x) + \mu\,x\,V \qquad (2)$$

net rate of cellular accumulation	net rate of cellular input by flow	rate of cellular production

where,

V =	volume of the system	(L^3)
x =	cellular carbon concentration	$(M_x L^{-3})$
t =	time	(t)
F =	volumetric flow rate of the reactor feed	$(L^3 t^{-1})$
x_i =	influent cellular carbon concentration	$(M_x L^{-3})$
μ =	specific cellular growth rate	(t^{-1})

The chemostat was operated at steady state and the influent feed was sterile ($x_i = 0$). Incorporating these conditions, Equation 2 can be simplified as follows:

$$F\,x = \mu\,x\,V \qquad (3)$$

Dividing both sides of equation by V and noting that F/V is equal to dilution rate, D, Equation 3 can be simplified to:

$$D = \mu \qquad (4)$$

According to Equation 4, the growth rate of the suspended cells in the chemostat can be maintained constant by controlling the dilution rate.

Annular Reactor Equations

The effect of calcium on cellular, polymer, and glucose carbon in the annular reactor (Figure 3) can be meaningfully analyzed using a mass balance approach.

Biofilm cellular carbon. A mass balance for the accumulation of cellular carbon in the biofilm can be written as follows:

$$A\, dx_b/dt = R_{xb} A + R_{dx} A \qquad (5)$$

$A\, dx_b/dt$	$R_{xb} A$	$R_{dx} A$
net rate of cellular carbon accumulation in the biofilm	rate of cellular reproduction in the biofilm	rate of cellular detachment from the biofilm

where,

A	=	surface area	(L^2)
x_b	=	cellular carbon areal density in the biofilm	$(M_x L^{-2})$
R_{xb}	=	cellular carbon reproduction rate in the biofilm	$(M_x L^{-2} t^{-1})$
R_{dx}	=	cellular carbon detachment rate from the biofilm	$(M_x L^{-2} t^{-1})$

Defining biofilm specific cellular growth rate, μ_b, as:

$$R_{xb} = \mu_b x_b \qquad (6)$$

where,

μ_b	=	specific cellular growth rate in the biofilm	(t^{-1})

The biofilm cellular carbon balance (Equation 5) can be written as:

$$A\, dx_b/dt = \mu_b x_b A - R_{dx} A \qquad (7)$$

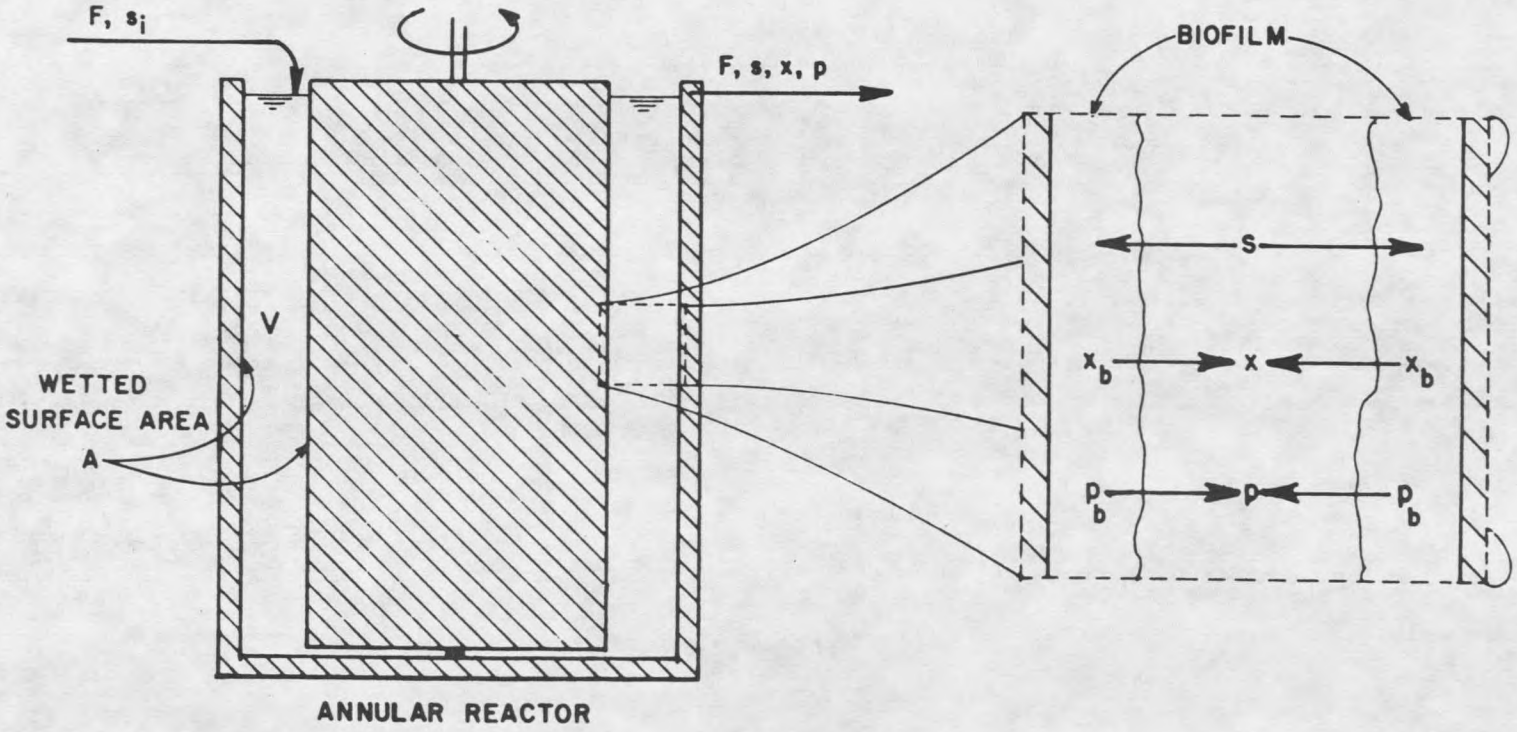

Figure 3. The annular reactor (AR) was operated as a continuous flow stirred tank reactor (CFSTR). The insert describes the local environment in the reactor. The mathematical model was based on this conceptual model.

Biofilm polymer carbon. A mass balance for the accumulation of polymer carbon can be written as follows:

$$A\, dp_b / dt = R_{pb} A - R_{dp} A \qquad (8)$$

net rate of polymer carbon accumulation in the biofilm	rate of polymer formation in the biofilm	rate of polymer detachment from the biofilm

where,

p_b = polymer carbon density in the biofilm $(M_p L^{-2})$

R_{pb} = polymer carbon formation rate in the biofilm $(M_p L^{-2} t^{-1})$

R_{dp} = polymer carbon detachment rate from the biofilm $(M_p L^{-2} t^{-1})$

Polymer formation may be related to organism growth rate and population density according to the Luedeking and Piret equation for product formation (Luedeking and Piret, 1959; Robinson et al., 1984; Bakke et al., 1984).

$$R_{pb} = k_b \mu_b x_b + k'_b x_b \qquad (9)$$

where,

k_b = growth-associated polymer formation rate coefficient in the biofilm $(M_p M_x^{-1})$

k'_b = nongrowth-associated polymer formation rate coefficient in the biofilm $(M_p M_x^{-1} t^{-1})$

The biofilm polymer carbon balance (Equation 8) can be written:

$$A \frac{dp_b}{dt} = (k_b \mu_b x_b + k'_b x_b) A - R_{dp} A \qquad (10)$$

Liquid cellular carbon. A mass balance across an AR on liquid cellular carbon can be written as follows:

$$V \frac{dx}{dt} = F (x_i - x) + R_{dx} A + \mu x V \qquad (11)$$

net rate of cellular carbon accumulation in the liquid	net rate of cellular input by flow	rate of cellular detachment from the biofilm	rate of cellular reproduction in the liquid

Influent cellular carbon concentration in this study was equal to zero. Furthermore, the AR was operated at a high dilution rate, $D = 6\ h^{-1}$, which is an order of magnitude greater than the maximum specific cellular growth rate. Cellular reproduction in the liquid phase is therefore negligible. Also, accumulation rate in the liquid phase is negligible (Trulear, 1983). Incorporating these conditions and dividing both sides of Equation (11) by V, the AR liquid cellular carbon balance can be written as:

$$R_{dx} = D \times V / A \qquad (12)$$

Liquid polymer carbon. A mass balance across the AR on the liquid polymer carbon can be written as follows:

$$V \frac{dp}{dt} = F (p_i - p) + R_{dp} A + r_p \times V \qquad (13)$$

net rate of polymer carbon accumulation in the liquid	net rate of polymer input by flow	rate of polymer detachment from the biofilm	rate of polymer formation in the liquid

Influent polymer carbon concentration in this study was equal to zero. Furthermore, due to the 10 minute hydraulic retention time the liquid phase polymer carbon formation and accumulation can be assumed to be negligible (Bakke et al., 1984). Incorporating these conditions and dividing both sides of Equation 13 by V, the AR liquid polymer carbon balance can be written as:

$$R_{dp} = D\ p\ V\ /\ A \tag{14}$$

Glucose carbon. A mass balance across an AR on glucose carbon can be written as follows:

$$V\frac{ds}{dt} = F\ (s_i - s) - \frac{R_{xb}\ A}{Y_{xb/s}} - \frac{R_{pb}\ A}{Y_{pb/s}} \tag{15}$$

net rate of glucose carbon accumulation in the liquid	net rate of glucose input by flow	rate of glucose removal for cellular reproduction in the biofilm	rate of glucose removal for polymer formation in the biofilm

where,

$Y_{xb/s}$ = yield coefficient of cellular carbon from substrate $(M_x M_s^{-1})$

$Y_{pb/s}$ = yield coefficient of polymer carbon from substrate $(M_p M_s^{-1})$.

Note that the glucose removal term for liquid phase reproduction and polymer formation have not been included in the substrate balance since they were assumed to be negligible in the preceding sections.

Oxygen. A mass balance across an AR on oxygen can be written as follows:

$$\frac{VdO_2}{dt} = F(O_{2i} - O_2) + N_oA - \frac{R_{xb}A}{Y_{xb/o}} - \frac{R_{pb}A}{Y_{pb/o}} \quad (16)$$

net rate of oxygen accumulation in the liquid	net rate of oxygen input by flow	net rate of oxygen transfer into the reactor	net rate of oxygen removal for cellular reproduction in the biofilm	net rate of oxygen removal for polymer formation in the biofilm

where,

O_2	=	effluent oxygen concentration	(M_oL^{-3})
O_{2i}	=	influent oxygen concentration	(M_oL^{-3})
N_o	=	flux of oxygen into the annular reactor	$(M_oL^{-2}t^{-1})$
$Y_{pb/o}$	=	yield coefficient of polymer carbon from oxygen	$(M_pM_o^{-1})$
$Y_{xb/o}$	=	yield coefficient of cellular carbon from oxygen	$(M_xM_o^{-1})$

The diffusion flux can be estimated as (Appendix F):

$$N_o = \frac{k_c\ (O_2^* - O_2)\ V}{A} \quad (17)$$

where,

k_c	=	mass transfer coefficient	(t^{-1})
O_2^*	=	saturated oxygen concentration	(M_oL^{-3})

The water input to the annular reactor was saturated ($O_{2i} = O_2^*$). Incorporating these conditions, Equation (16) can be written as:

$$\frac{dO_2}{dt} = (D + k_c)\ (O_{2i} - O_2) - \frac{R_{xb}\ A}{(V\ Y_{xb/o})} - \frac{R_{pb}\ A}{(V\ Y_{pb/o})}$$

Note that the oxygen removal term for liquid phase reproduction and polymer formation have not been included in the oxygen balance since they were assumed to be negligible in the preceding sections.

EXPERIMENTAL APPARATUS AND METHODS

Annular reactor (AR) and tubular reactor (TR) systems were used for this research. The TR was only used for mixed culture biofilms. However, all the experiments in AR were conducted with *Ps. aeruginosa* biofilms. A chemostat was used to supply the AR with *Ps. aeruginosa* inoculum. Batch growth experiments were conducted in BOD Respirometer.

Experimental Apparatus

BOD Respirometer

A BOD respirometer is an apparatus to continuously monitor oxygen uptake due to growth and reproduction of microorganisms. The respirometer (Oceanography International Corporation, College Station, TX) continuously replaces oxygen utilized by a manometer triggered electrolysis reaction.

It consists of a sample bottle and an electrolysis cell. A schematic representation of the cell and some of the associated components is shown in Figure 4. When electrolyte in the cell is in contact with the switch electrode, oxygen is not produced at the oxygen electrode. The CO_2 produced as a metabolic end product is removed from the air space by KOH pellets. This results in a slight vacuum in the air space. This causes a rise of electrolyte in the inner tube of the cell and a fall in electrolyte in annular space below the switch electrode. When the contact with the switch is broken, oxygen gas is

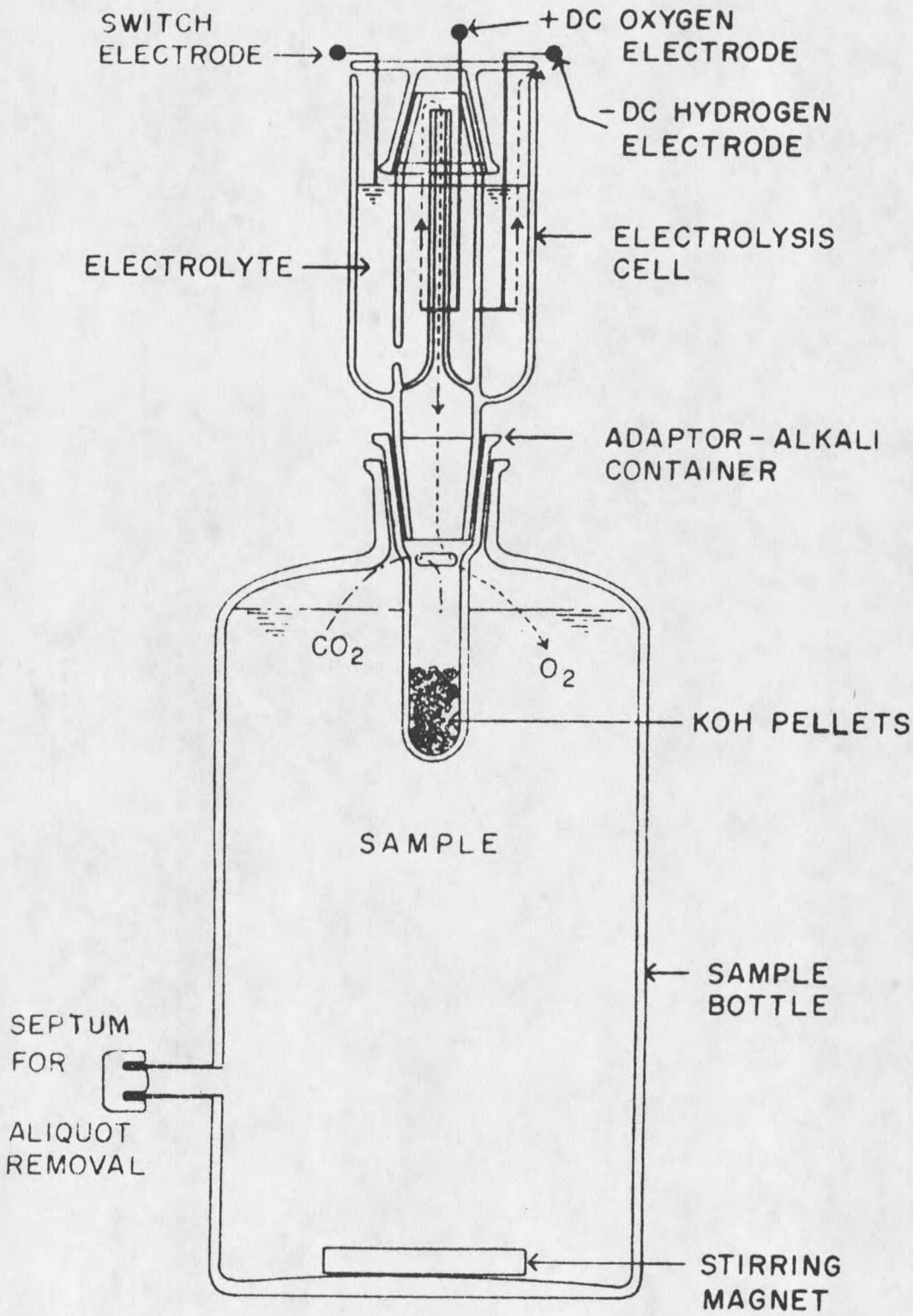

Figure 4. A schematic diagram of BOD respirometer.

generated to fill the partial vacuum until the pressure deficit has been satisfied. At such time the electrolyte again makes contact with the switch electrode. The time during which the electrolysis cell was generating oxygen to the sample was monitored electronically (Faraday's Law) and displayed as oxygen uptake.

Chemostat System

Chemostat. A chemostat is a constant volume, continuously stirred tank reactor for microbial growth. The purpose of the chemostat in this study was to serve as a continuous source of microorganisms (at a constant growth rate and uniform physiological state) for the annular reactor in which experiments were conducted. The chemostat consists of Berzelius Pyrex beaker with side arm and a rubber stopper (Figure 2). Anti-backflow cylinders on the influent and effluent lines were used to prevent contamination of the substrate feed solution and the reactor solution due to backflow of microorganisms. Table 1 presents the relevant characteristics and dimensions of chemostat.

Table 1. Relevant Characteristics and Dimensions of Chemostat.

Liquid volume	=	4.5E-4 m^3
Operating height	=	8.5E-2 m
Diameter	=	8.8E-2 m
Dilution rate	=	2.4E-1 h^{-1}
Substrate solution volumetric flow rate	=	1.8E-4 m^3 h^{-1}
Mean residence time	=	4.2 h

Substrate feed. Substrate solution was continuously fed to the chemostat using a multi-channel peristaltic pump (Minarik Electric Company, Los Angeles, CA, Model SL14P). The growth medium consisted of glucose as a sole source of carbon and energy. Table 2 shows the composition of the growth medium which was prepared with distilled water and sterilized by autoclaving (121°C for 40 minutes).

Table 2. Composition of Growth Medium for Chemostat and Annular Reactor.

Constituent	Influent Concentration ($g\ m^{-3}$) Chemostat	AR
Glucose	10.0	10.0
NH_4Cl	3.6	3.6
$MgSO_4\ 7H_2O$	1.0	1.0
Na_2HPO_4 (Buffer)	568.0	213.0
KH_2PO_4 (Buffer)	544.4	204.5
Calcium	--	#
Micronutrients	*	*
pH (pH units)	6.8	6.8

* For composition of the micronutrients see Table 3.

Calcium was an experimental parameter. Hence, it is not included in this table.

NOTE: For glucose concentration other than 10 $g\ m^{-3}$ the concentration of the nutrient and micronutrients were adjusted proportionally. Medium prepared with distilled water.

The influent concentration was calculated after combination with dilution water. Chemostat influent glucose concentration was 10 $mg\ l^{-1}$ (Experiments 1 - 2) and 100 $mg\ l^{-1}$ (Experiments 3 - 7).

Table 3. Composition of Micronutrients Calculated for a Glucose Concentration of 1000 g m^{-3}.

Constituent	Concentration g m^{-3}
$(HOCOCH_2)_3N$	20.00
$(NH_4)_6\ Mo_7O_{24}\ \ 4H_2O$	0.05
$FeSO_4\ \ 7H_2O$	5.60
$ZnSO_4\ \ 7H_2O$	5.00
$MnSO_4\ \ H_2O$	0.40
$CuSO_4\ \ 5H_2O$	0.10
$Na_2B_4O_7\ \ 10H_2O$	0.05

NOTE: For glucose concentration other than 1000 g m^{-3}, the concentration of micronutrients was adjusted proportionally.

Air supply. Chemostat contents were continuously aerated with filtered laboratory air fed into the reactor through the anti-backflow device.

Microbial inoculum. The *Ps. aeruginosa* strain used for the pure culture studies was obtained from Professor Nels Nelson, Department of Microbiology, Montana State University, Bozeman, Montana. *Ps. aeruginosa* was stored initially in a refrigerator on Trypticase glucose agar extract (TGEA) plates and replated 2 to 3 weeks to maintain viability. Later the organism was stored at approximately -10°C in a 15% glycerol suspending medium. Bacto Pseudomonas agar media was used for identification of *Pseudomonas aeruginosa*.

Annular Reactor System

Annular reactors. The annular reactors (AR) were constructed of acrylic plastic and consist of two concentric cylinders, a stationary outer cylinder and a rotating inner cylinder. Figure 1 illustrates details of the reactor. Rotational velocity was controlled by a fractional horsepower gear motor (Model No. NSH11D3 with series 200 speed controller, Bodine Electric Co., Chicago, IL) and continuously monitored by a tachometer/torque transducer unit mounted on the shaft between the rotating cylinder and the motor drive pulley assembly (Bridger Scientific, Inc., Bozeman, MT). Each annular reactor contained four removable slides which were used for biofilm sampling and/or biofilm mass measurements. These slides formed an integral fit with the inside wall of the outer cylinder. The reactor was completely mixed (Trulear, 1983) by virtue of the recirculating action of a peristaltic pump (Cole-Palmer Instrument Co., Chicago, IL, model No. WZ1R057) which was used to pump the AR liquid solution from the bottom to the top of each AR at volumetric flow rate approximately ten times faster than the overall volumetric flow rate through each AR. Table 4 presents relevant characteristics and dimensions of the AR. Advantages of the annular configuration include the following:

- Because of complete mixing, no concentration gradient exists in the bulk fluid phase, which simplifies sampling and mathematical analysis.
- Fluid shear stress at the wall can be varied independently of reactor mean residence time.

- High surface area to volume ratio.

Table 4. Relevant Characteristics and Dimensions of the Annular Reactor.

Reactor	
Liquid volume	6.00E-4 m^3
Total wetted surface area	1.49E-1 m^2
Inner cylinder wetted surface area	7.30E-2 m^2
Outer cylinder wetted surface area	7.60E-2 m^2
Diameter of the inner cylinder	1.02E-1 m
Diameter of the outer cylinder	1.14E-1 m
Width of the annular gap	6.00E-5 m
Wetted height of the inner cylinder	1.77E-1 m
Wetted height of the outer cylinder	1.84E-1 m
Total volumetric flow rate	3.60E-3 m^3 h^{-1}
Mean residence time	1.67E-1 h
Rotational speed	250 rpm
Removable slides	
Wetted surface area	2.94E-3 m^3
Width	1.60E-2 m
Height	1.84E-1 m
Area used for biofilm sampling	2.54E-3 m^3

Dilution water. Distilled water was used as dilution water for the annular reactors. The flow rate of the dilution water was controlled at 60 ml min^{-1} using a variable speed peristaltic pump (Cole-Palmer Instrument Company, Chicago, IL, model No. 7533-00). The flow rate of the dilution water was monitored with an in-line flow meter (Gilmont Instruments Inc., Great Neck, NY, size No. 13). The dilution water filtered through a 0.2 μm filter (Gelman Sciences, Inc., Ann Arbor, MI, product No. 12117) before entering the AR.

Dilution water treatment. Dilution water treatment consisted of passage through a filtration cascade (5.0 and 0.45 μm filters, Gelman Sciences, Inc., Ann Arbor, MI, products No. 12585 and 12581 respectively). The calcium content of the dilution water was controlled by the addition of $CaCO_3$-HCl stock solution. The pH of the resulting mixture was controlled using a pH controller (New Brunswick Scientific Co., Inc., New Brunswick, NJ, model No. M1055-7000). Figure 5 shows a simplified flow diagram of the annular reactor system.

Substrate feed. Sterile substrate solution was continuously fed to the AR using a multichannel peristaltic pump (Minarik Electric Company, Los Angeles, CA, model No. SL14P). Table 2 shows the composition of the substrate solution. Additional buffering capacity was provided to the AR with Tris-HCL buffer (10 mM; pH 7) during treatment with chelant to maintain pH at a constant value.

Tubular Reactor System

Tubular reactor. The tubular reactor (TR) is a chemostat with an external recycle loop as indicated in Figure 6. The external recycle loop consisted of 1.45 cm I.D., Al-6X stainless steel heat exchange tubing with a wall thickness of 0.07 cm. The influent flow rate, F, (0.09 l min^{-1}) was smaller than the recycle flow rate, F_R, (9.1 l min^{-1}). At this relatively high recycle rate, the entire system behaves as a continuous stirred tank reactor. The temperature inside the reactor was maintained at 25°C using a concentric tube heat exchanger installed in the recycle loop.

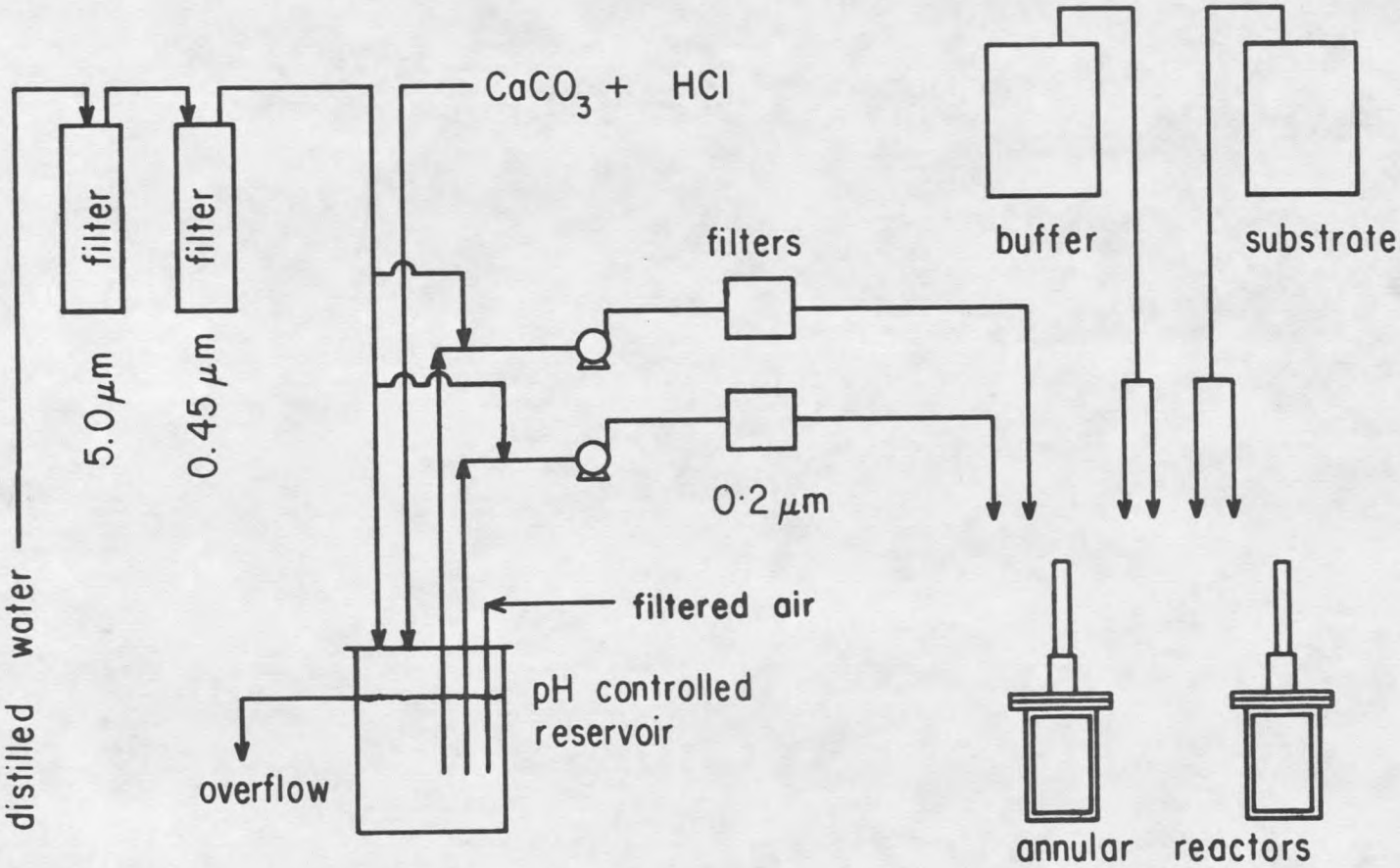

Figure 5. Flow diagram of the annular reactor system.

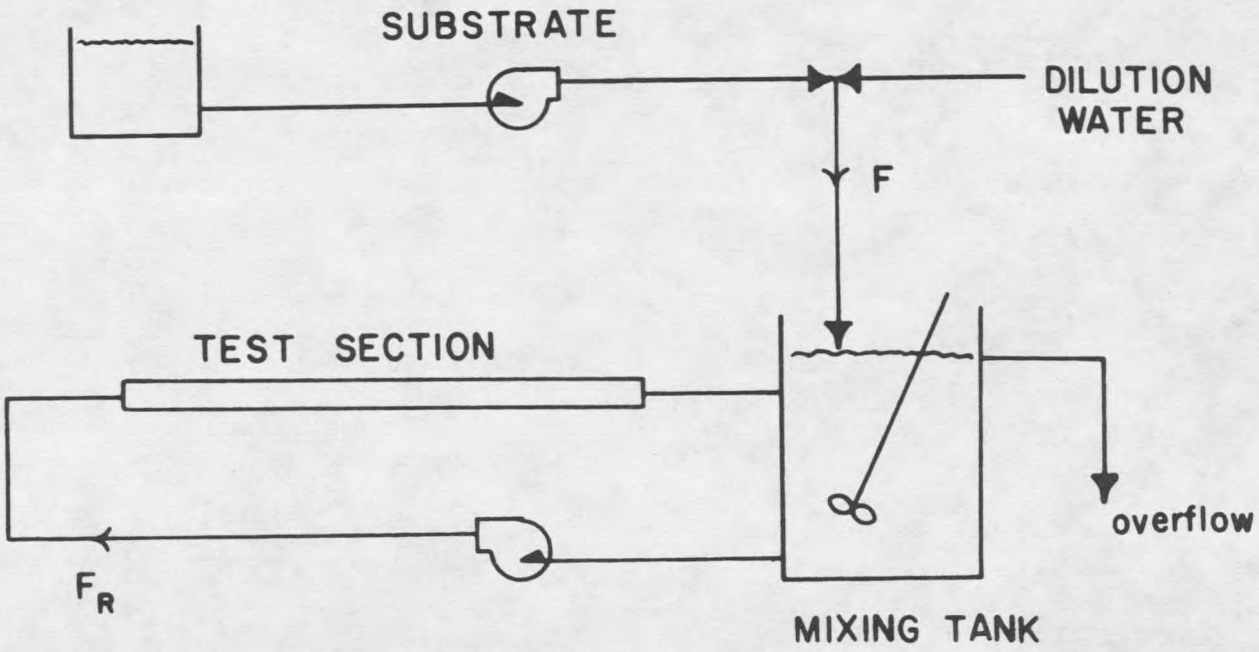

Figure 6. Simplified flow diagram of the tubular reactor.

Dilution water and substrate feed. Treated dilution water was continuously fed into the TR using reduced tap water line pressure (AW Cash Valve Mfg. Corp., Decatur, IL, type A-315 Pressure Regulator). The dilution flow rate was controlled using a needle valve (Whitney Co., Oakland, CA, model No. ORM2) and monitored with an in-line flow meter (Gilmont Instrument Inc., Great Neck, NY, size No. 13). Sterile growth medium was continuously fed to the TR by gravity flow. Flow rate was controlled with a Dial-A-Flow valve (Sorenson Research Co., Salt Lake City, UT, catalog No. DAF-30) and monitored with an in-line flow meter (Gilmont Instrument Inc., Great Neck, NY, size No. 11). Table 5 shows the composition of the substrate solution used.

Table 5. Growth Medium Composition for Tubular Reactor Experiments.

Constituent	Concentration $g\ m^{-3}$
Glucose	10.0
NH_4Cl	3.6
$MgSO_4\ 7H_2O$	1.0
KH_2PO_4	3.0
K_2HPO_4	18.0

NOTE: For glucose concentration other than 10 $g\ m^{-3}$ the concentration of the nutrients were adjusted proportionally. pH of the medium was 7.5.

Dilution water treatment. Bozeman City tap water was the source of the dilution water. Dilution water treatment consisted of passage

through a carbon adsorption column for the removal of residual chlorine and soluble organics followed by filtration through a cascade of filter (5.0 and 0.8 μm; Gelman Sciences, Inc., Ann Arbor, MI, products No. 12585 and 12623 respectively) for the removal of particulate and suspended cellular materials.

Microbial inoculum. The bacterial inocula for the experiments were prepared from a single batch of secondary aerobic sewage sludge from the treatment plant in Bozeman, MT. The sludge was divided into 10 ml aliquots, frozen in 15% glycerol with liquid nitrogen, and stored at -10°C until needed.

Experimental Procedure

Cleaning and Sterilization

Standard cleaning and sterilization procedures were established for each experimental system to ensure uniform conditions for experimental start-up.

BOD respirometer. The respirometer cleaning and sterilization procedure was as follows:

1. Following an experiment, the sample bottles were sterilized by autoclaving.
2. The sample bottles were soaked in a warm soap solution for a minimum of 5 minutes.
3. The sample bottles were scrubbed with a soft bristle brush, rinsed thoroughly, and dried.

4. Preceding the experiment, the growth medium (Table 6) was prepared, the sample bottles were filled with 1000 ml of growth medium.
5. Teflon coated, magnetic stirring bars were placed in the sample bottles.
6. Silicone grease was applied to the ground glass surfaces on the sample bottles. The adaptor-alkali container was placed on the sample bottle.
7. The sample bottles were autoclaved (121°C for 25 minutes).
8. The sample bottles were allowed to cool overnight in the incubator of the respirometer prior to initiating the experiment.

Table 6. Composition of Batch Growth Medium for BOD Respirometer Experiments.

Constituent	Concentration $g\ m^{-3}$
Glucose	1000
NH_4Cl	360
$MgSO_4\ 7H_2O$	100
Na_2HPO_4 (Buffer)	568
KH_2PO_4 (Buffer)	544
Calcium	#
Micronutrients	*
pH (pH units)	6.8

* For composition of the micronutrients see Table 3.

Calcium was an experimental parameter. Hence it is not included in this table.

Chemostat system. The chemostat system cleaning and sterilization procedure was as follows:

1. Following an experiment, the chemostat was sterilized by autoclaving.
2. The chemostat was disassembled and soaked in a warm soap solution for a minimum of 5 minutes.
3. The surface of the chemostat was scrubbed with a soft bristle brush and rinsed thoroughly.
4. The chemostat was assembled.
5. Preceding the experiment, the batch growth medium was prepared, the chemostat was filled with 300 ml of batch growth medium (1 g l^{-1} glucose). The chemostat and the substrate solution feed lines were autoclaved.
6. The substrate feed stock solution was prepared and autoclaved (121°C for 40 minutes).
7. The substrate feed lines were connected to chemostat and the solution was allowed to cool prior to initiating the experiment.

Annular reactor system. The AR system cleaning and sterilization was as follows:

1. Following an experiment, the AR was operated in a batch mode for 10 minutes. Fifteen milliliter of bleach (Purex) was added to the reactor.
2. The reactor was disassembled and soaked in a warm soap solution for a minimum of 5 minutes.

3. The surface of the AR was scrubbed with a soft bristle brush and rinsed.
4. The reactor was assembled.
5. Preceding an experiment, the dilution water 0.2 μm filter capsule, substrate feed lines, and buffer feed lines were autoclaved.
6. The dilution water feed lines were connected to the pH controlling reservoir. Twenty-five milliliter of bleach was added into the cascade filters and the flow of dilution water was started.
7. The AR's were filled with 10% bleach in distilled water and operated in a batch mode for 1 hour.
8. The sterile capsule filter was connected to the AR and the flow of dilution water was started.
9. The substrate and buffer stock solutions were prepared and autoclaved.
10. A minimum of 10-12 h (overnight) was allowed for residual chlorine to be flushed out from the annular reactors.
11. After 12 h, the substrate and buffer feed lines were connected to the AR's.
12. The experimental start-up procedure was initiated.

Tubular reactor system. The TR system cleaning and sterilization was as follows:

1. Following an experiment, twenty milliliters of bleach was added to the reactor and the TR was operated in the batch mode for 10 minutes.

2. The reactor was disassembled and cleaned with a soft bristle brush.
3. The reactor was assembled.
4. Before starting the experiment, stock solutions of glucose and buffer were prepared.
5. The dilution water and substrate feed lines were connected to the TR.
6. The TR was filled with the medium, and the flow rate in the recycle loop was adjusted.

Experimental Start-Up

BOD respirometer. The respirometer start-up procedure was as follows:

1. The sample bottles were inoculated with 1 ml of batch culture of *Ps. aeruginosa* through the septum on the bottles.
2. The electrolysis cell was filled with 2N H_2SO_4 to within 0.4 cm of the switch electrode.
3. The outer ground glass surface of the electrolysis cell was greased with silicone grease.
4. A sterile glass wool filter was placed in the stem of the electrolysis cell.
5. Six grams of KOH pellets were added to the alkali-container.
6. The electrolysis cell was placed on the alkali-container.
7. The current of the electrolysis cell was adjusted at 200 milliamps.

Chemostat. The experiment was started by inoculating the chemostat with 1 ml of batch culture of *Ps. aeruginosa*. The chemostat was operated in a batch mode for 10-12 h. This usually resulted in a concentrated suspension of organisms in the chemostat. Substrate solution flow was then started at the desired dilution rate. The chemostat was operated in the continuous flow mode for at least six residence time prior to use in AR to allow the reactor to reach steady state.

Annular reactors. Two parallel annular reactors were used for this study. The experiment was started by pumping organisms from a steady state chemostat culture of *Ps. aeruginosa* (chemostat dilution rate 0.24 h^{-1}) into the AR's for a period of 20-24 h (Experiments 1 & 2; 6 x 10^6 cells ml^{-1}) and for 8-10 h (Experiments 3-7; 10^8 cells ml^{-1}). This provided a defined microbial inoculum for the attachment experiments. Organism flow rates were maintained at 0.55 ± 0.05 ml min^{-1}. Substrate solution and dilution water were fed to the AR throughout the experiment. Additional buffering capacity was provided with Tris-HCl buffer (pH 7) during treatment with chelant to maintain pH at a constant value. EGTA or EDTA was added to the AR using step input and the concentration was kept constant for 1 hour. Two hours (twelve residence time) before chelant addition, the flow of calcium to the AR was stopped. Hence, the chelant demand in the liquid phase was negligible.

Tubular reactor. The experiment was started by inoculating the TR with a mixed microbial population. The TR was allowed to operate in

the batch mode for 10-12 h. This usually resulted in a concentrated suspension of organisms in the TR. The recirculating pump was then started. The dilution water, substrate, and the buffer flow was also started. A biofilm was allowed to form over a period of several days before EGTA was added to the system. Additional buffering capacity was provided with Tris-HCl buffer (pH 7.5) during treatment with EGTA to maintain pH constant.

Sampling

Liquid samples. Liquid samples from AR, TR, and the chemostat were directly collected from the effluent, prepared, and stored as follows:

a)	glucose	- filtered (Nuclepore Corp., Pleasanton, CA, No. 111107, average pore size 0.45 μm), samples were frozen until analysis
b)	suspended solids	- 25-100 ml samples were filtered (Nuclepore Corp., Pleasanton, CA, No. 111107, average pore size 0.45 μm), dried, and weighed
c)	acridine orange direct count (AODC)	- 4 ml samples were fixed in an direct equal volume of 4% sterile formalin, homogenized (Du Pont Co., Instrument Products Newton, CT, Sorvall Omni-Mixer), and refrigerated until analysis by the method of Hobbie et al. (1977)

d) carbon - filtered (Nuclepore Corp., Pleasanton, CA, No. 111107, average pore size 0.45 μm, 5 x 5 ml) and unfiltered samples (5 x 2 ml) were frozen until analysis.

Biofilm samples. Biofilm samples were obtained from the AR removable slides. Biofilm was scraped from the slide using a rubber policeman into 30-35 ml carbon-free distilled water. The resulting solution was homogenized (Du Pont Co., Instrument Products, Newton, CT, Sorvall Omni-Mixer) and subsamples were prepared and stored as follows:

a) acridine orange direct count (AODC) - 2-4 ml samples were fixed in 4 ml of sterile 4% formalin, and refrigerated until analysis by the method of Hobbie et al. (1977)

b) carbon samples - 5 x 1 ml samples were frozen until analysis

c) mass density - 15-25 ml samples were filtered (Nuclepore Corp., Pleasanton, CA, No. 11107, average pore size 0.45 μm), dried, and weighed.

Analytical Methods

The hierarchy of analytical procedures performed on biofilm or reactor liquid are summarized in Figure 7.

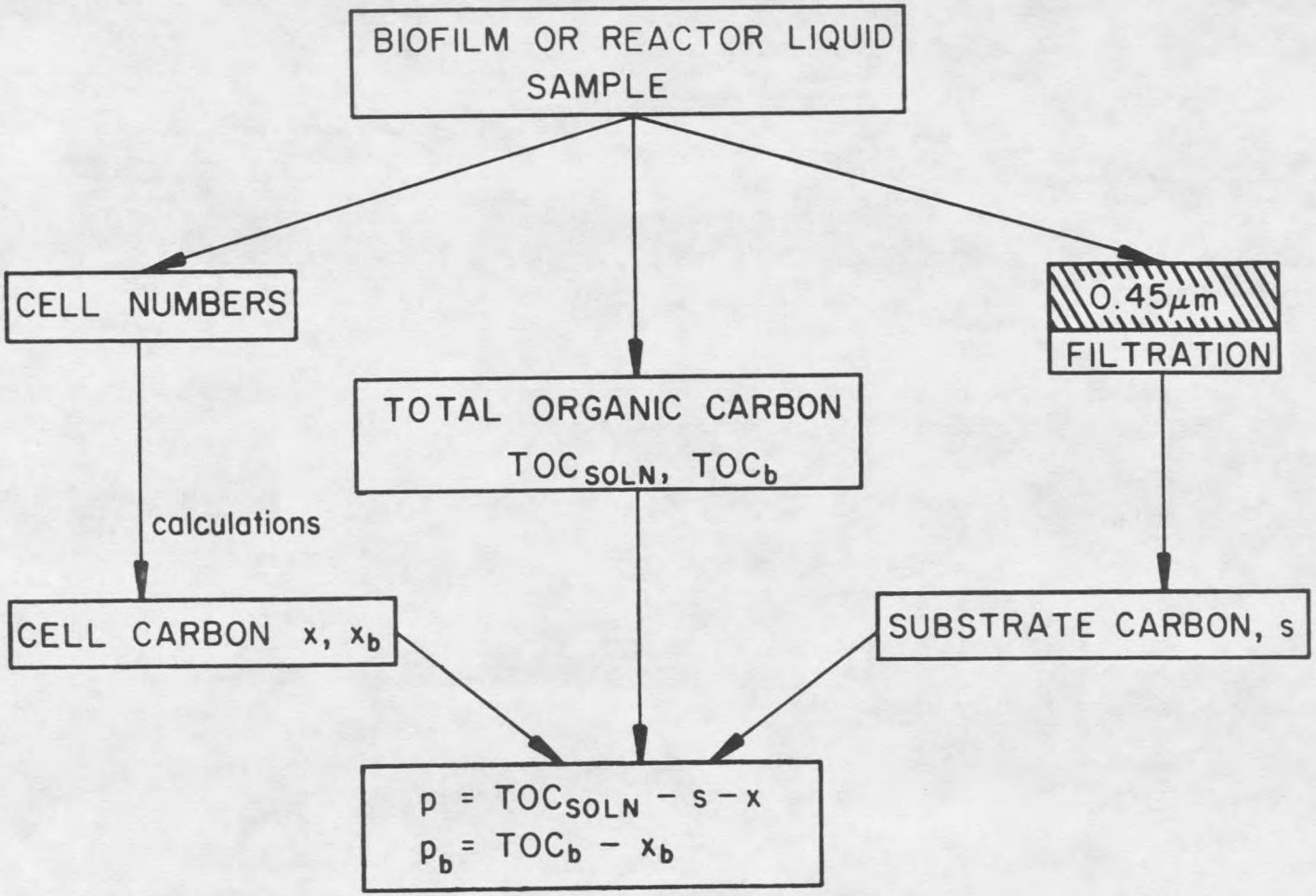

Figure 7. Hierarchy of analytical procedures.

Suspended solids. Suspended solids concentration was determined by filtering 20-100 ml of reactor effluent through predried (103°C for 1 hour), preweighed, Nuclepore membranes (Nuclepore Corp., Pleasanton, CA, No. 11107, average pore size 0.45 μm). After filtration, the filter was dried at 103°C for 1 hour and weighed (Mettler Instruments Corp., Hightstown, NJ, Type H20 Digital Balance).

Acridine orange direct count. Total number of cells in the effluent or the biofilm sample was determined by enumerating cells stained with acridine orange using epifluorescence microscopy (Leitz Wetzlar, Rochleigh, NJ, Ortholux II Universal Microscope) according to the method of Hobbie et al. (1977).

Carbon measurements. Carbon was used as the basis for the material balance relations which were used in this study. The carbon-containing components were as follows: glucose carbon, liquid phase cellular carbon, liquid phase polymer carbon, biofilm cellular carbon, and biofilm polymer carbon.

Glucose carbon concentration. Glucose carbon concentration, s, was determined by measuring glucose concentration enzymatically using a modified version (Trulear, 1983) of Sigma 510 Glucose Analysis Procedure (Sigma Chemical Co., St. Louis, MO). The measured glucose concentration was multiplied by 0.4 g glucose carbon (g glucose)$^{-1}$ to determine glucose carbon concentration.

Liquid phase cellular carbon concentration. The concentration of the liquid phase cellular carbon concentration, x, was calculated by

multiplying the acridine orange cell count and the average volume of the cell by the following quantities: 1.07 g cell cm^{-3} (Doetsch et al., 1973; Bakken and Olson, 1983), 0.22 dry cell weight (wet cell weight)$^{-1}$ (Luria, 1960; Bakken and Olson, 1983), and 0.5 g cell carbon (g cell dry weight)$^{-1}$ (Doetsch et al., 1973; Luria, 1960).

Liquid phase polymer concentration. The concentration of liquid phase polymer carbon, p, was calculated by measuring the total organic carbon (TOC) of a reactor liquid sample, TOC_{soln}, and performing the following calculation:

$$p = TOC_{soln} - s - x$$

TOC was determined using the ampule analysis module of the Oceanography International Carbon Analyzer (Oceanography International Corp., College Station, TX, Total Carbon System, Cat. No. 0524B).

Biofilm cellular carbon density. The density of biofilm cellular carbon, x_b, was determined by enumerating the total number of cells per unit area using acridine orange cell count and performing calculations analogous to those presented for x.

Biofilm polymer carbon density. The density of biofilm polymer carbon, p_b, was determined by measuring the TOC of a known volume of biofilm suspension, TOC_b, and performing the following calculation:

$$p_b = TOC_b - x_b$$

Total carbohydrate. Total carbohydrate on filtered and/or unfiltered effluent sample was determined using the phenol reaction

method of Hanson and Phillips (1981). These values were reported as glucose equivalents.

Total solids removed. Total amount of solids removed was determined by graphically integrating the curve describing the progression of effluent suspended solids during chelant addition.

Dry biofilm mass. Dry biofilm mass was determined by filtering 15-25 ml of biofilm suspension through predried (103°C), preweighed, Nuclepore membranes (Nuclepore Corp., Pleasanton, CA, No. 11107, average pore size 0.45 μm). After filtration, the filter was dried at 103°C for 1 hour and weighed (Mettler Instruments Corp., Hightstown, NJ, Type H20 Digital Balance).

Total calcium. Total calcium in the influent and effluent samples was determined by EDTA titration. Total calcium in the dry biofilm sample was determined by the Chemistry Station-Analytical Lab (Montana State University) using atomic adsorption.

Free calcium. Free calcium was determined with calcium activity electrode (Orion Research, Inc., Cambridge, MA, CA No. 93-20-00).

C, H, and N analysis. Carbon, hydrogen, and nitrogen content of the lyophilized biofilm samples were determined using a Carlo-Erba elemental analyzer (Chemical Engineering Department, Montana State University, Bozeman).

Dissolved oxygen. Dissolved oxygen in the influent and effluent was measured using a YSI model-54 oxygen meter (Yellow Springs Instrument Co., Inc.).

RESULTS

Comprehensive listings of raw data for all annular reactor, tubular reactor, and BOD respirometer experiments are listed in Appendices A through E. The annular reactor was used for all studies involving *Ps. aeruginosa* biofilms. The tubular reactor was used only for mixed culture biofilms. The BOD respirometer was used for batch growth of *Ps. aeruginosa*. Cellular, polymer, and substrate data are reported as carbon equivalents. Substrate, glucose, was the sole carbon and energy source and the experiments were operated under substrate-limiting conditions. The annular reactor was operated at three different calcium concentrations: 0.4 (no added calcium), 25, and 50 mg l^{-1}. Calcium concentration refers to total calcium and not free calcium, unless otherwise indicated.

Influence of Calcium on Biofilm Formation

The effect of calcium on cellular reproduction and polymer formation was measured by varying influent calcium concentration and measuring the changes in the following:

1. biofilm cellular carbon areal density, x_b
2. biofilm polymer carbon areal density, p_b
3. biofilm mass
4. immobilized calcium
5. cellular carbon concentration, x

6. polymer carbon concentration, p

7. glucose carbon concentration, s

8. oxygen concentration, O_2

The effect of calcium on transformation or process rate was determined from the above measurements using the material balances described earlier. Table 7 presents a summary of experimental conditions for all AR experiments.

Table 7. Summary of Experimental Conditions of Annular Reactor Experiments.

Expt #	AR #	D (h^{-1})	s_i (mg l^{-1})	Calcium (mg l^{-1}) Total	Free
1	7	6	4.00	9.0	ND
	8	6	3.84	9.0	ND
2	7	6	4.16	9.0	ND
	8	6	3.84	9.0	ND
3	7	6	6.56	0.4	0.04
	8	6	6.40	25.0	18.50
4	7	6	4.83	0.4	0.04
	8	6	4.70	50.0	44.00
5	7	6	6.16	25.0	18.50
	8	6	6.00	25.0	18.50
6	7	6	6.32	50.0	44.00
	8	6	6.04	50.0	44.00
7	7	6	6.40	0.4	0.04

ND = not determined.

Effect of Calcium on Accumulation Rates

Biofilm Mass

The progression of biofilm mass for three different calcium concentrations in the dilution water is presented in Figure 8. The results indicate that the presence of calcium in the dilution water increases the rate of biofilm accumulation. However, there was no detectable difference in biofilm mass at 48 h for all calcium concentrations. The extent of biofilm accumulation at the end of six days as a function of calcium in the dilution water is presented in Figure 9. Accumulation was highest for experiments with 50 mg l^{-1} calcium. The results indicate that calcium influences the rate and extent of biofilm accumulation. The results suggest that calcium can be used for controlling biofilm accumulation.

Biofilm Cellular Carbon

The progression of biofilm cellular carbon for three different calcium concentrations in the dilution water is presented in Figure 10. The addition of calcium in the dilution water increases the accumulation of biofilm cellular carbon. The extent of biofilm cellular accumulation (at the end of six days) increases with increasing calcium concentration in the dilution water (Figure 11). The results suggest that calcium can be used to attach more cells on a given surface.

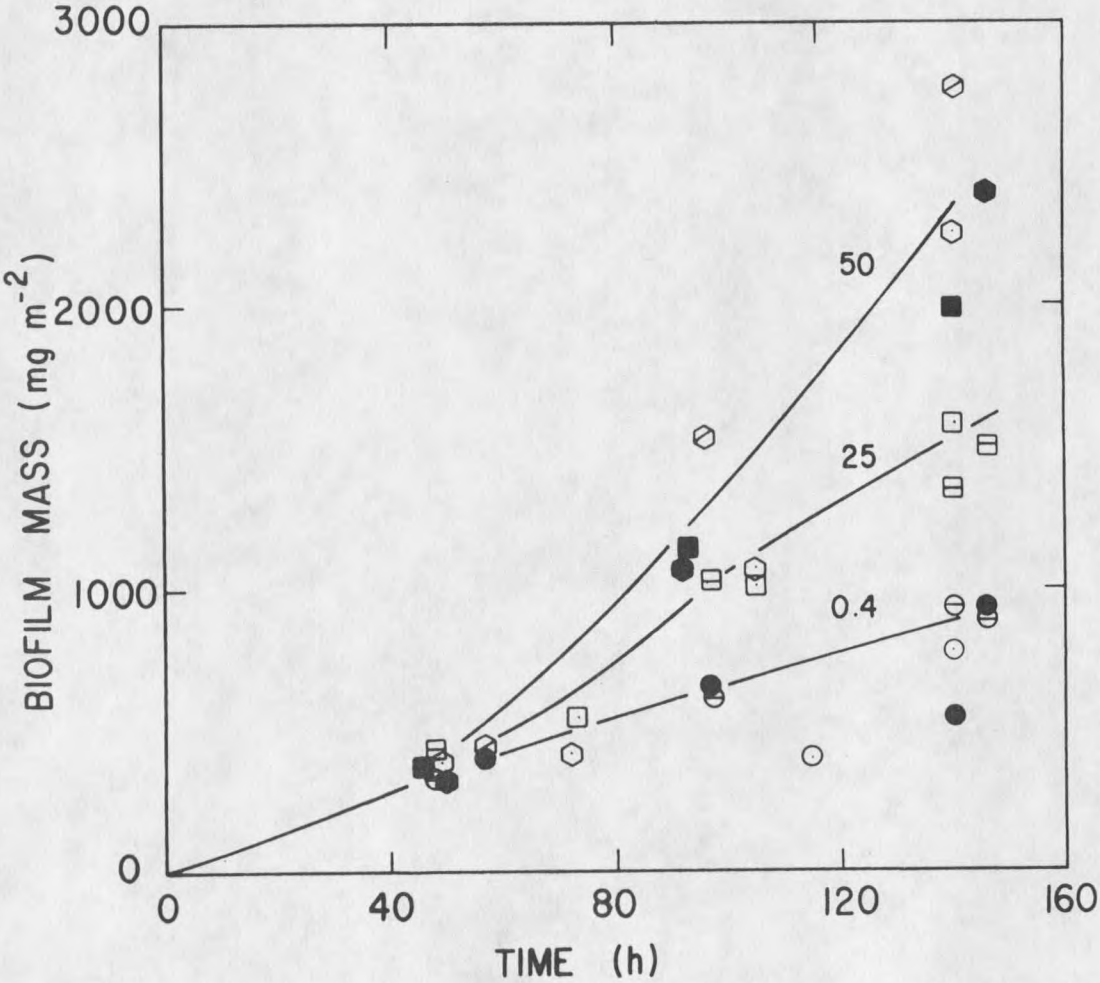

Figure 8. Progression of biofilm mass as a function of time for three different calcium concentrations. Lines drawn by observation. (⊘,○,● 50 mg l^{-1}; ⊟,□,■ 25 mg l^{-1}; and ⊖,○,● 0.4 mg l^{-1}).

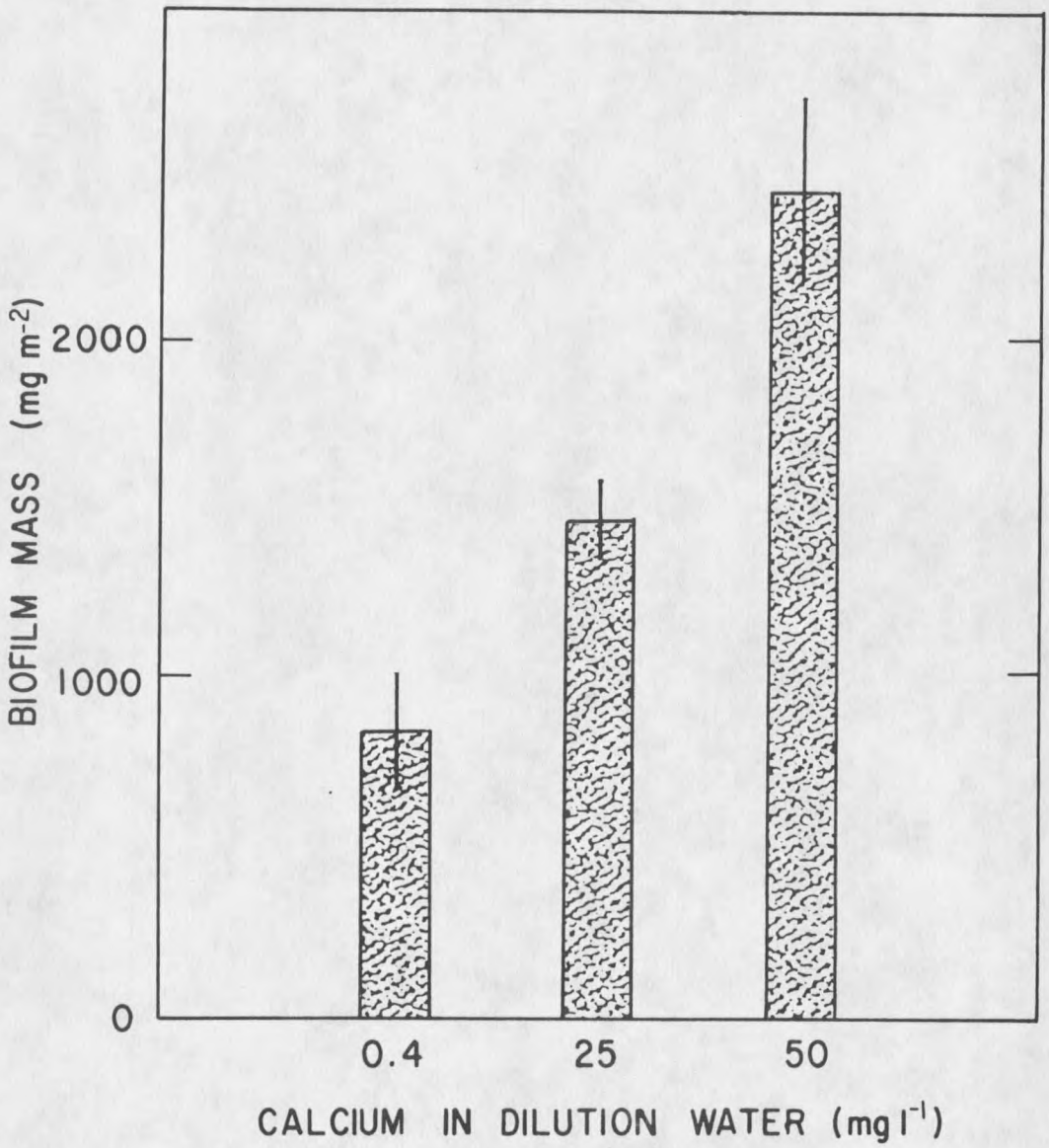

Figure 9. Change in biofilm mass (140 h) as a function of calcium in the dilution water. Error bars represent standard deviation of measurements of all experiments with same calcium concentration in the dilution water.

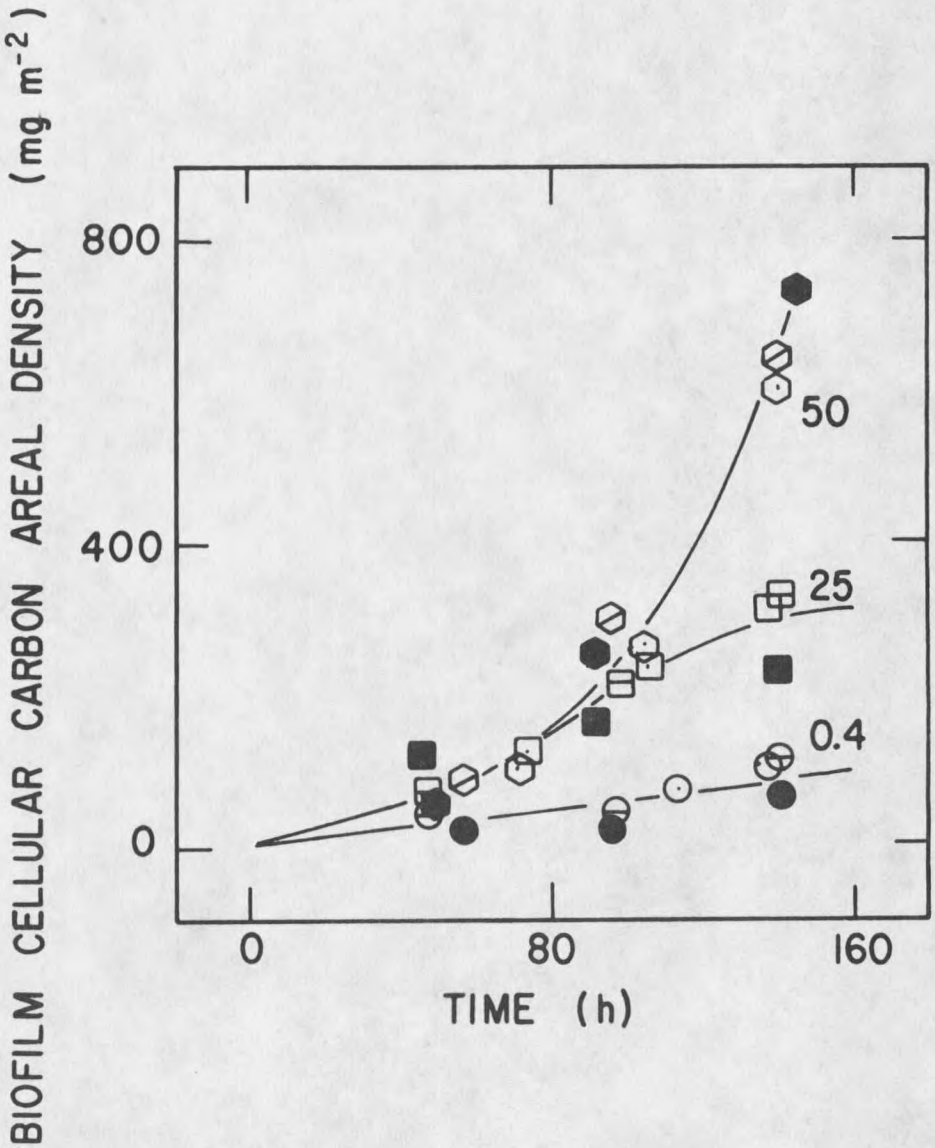

Figure 10. Progression of biofilm cellular carbon as a function of time for three different calcium concentrations. Curves represent time smoothed data. Parameters for time smoothed data were obtained using BMDP3R - nonlinear regression. (⊘,○,● 50 mg l^{-1}; ⊟,□,■ 25 mg l^{-1}; and ⊖,○,● 0.4 mg l^{-1}).

Biofilm Polymer Carbon

The amount of extracellular polymer accumulated within the reactor at the end of the experimental period (six days) was not influenced by calcium concentrations in the dilution water (Figure 11). There was no significant difference in biofilm polymer carbon (between experiments) at any time during biofilm development.

Biofilm Calcium

Calcium concentration in the biofilm increases with increasing calcium in the dilution water (Figure 12). Twelve residence times before sampling biofilm for calcium analysis, the flow of $CaCO_3$ + HCl stock solution was stopped. Hence, there was no added calcium in the dilution water during the sampling period.

Fixed and Volatile Biomass

Fixed and volatile contents of the biofilm (140-146 h) at different calcium concentrations are presented in Table 8. The data indicate that fixed and volatile biomass under different calcium concentrations remained the same.

The fixed mass remaining after ignition generally represents the inorganic component of the biofilm and may include potassium, calcium, magnesium, sodium, iron, and trace amounts of cobalt, copper, molybdenum, and zinc. These elements are known to be required for metabolism.

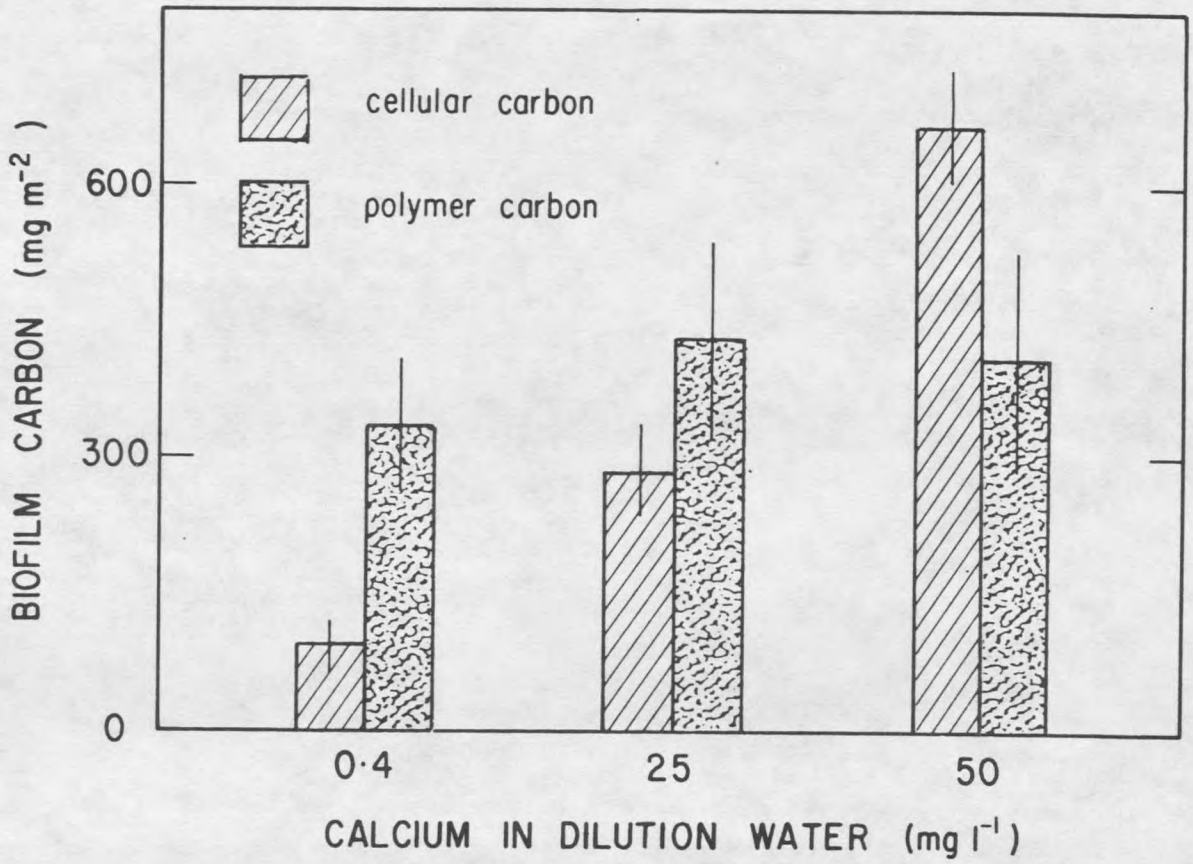

Figure 11. Change in biofilm cellular and polymer carbon (140 h) as a function of calcium in the dilution water. Error bars represent standard deviation of measurements of all experiments with same calcium concentration in the dilution water.

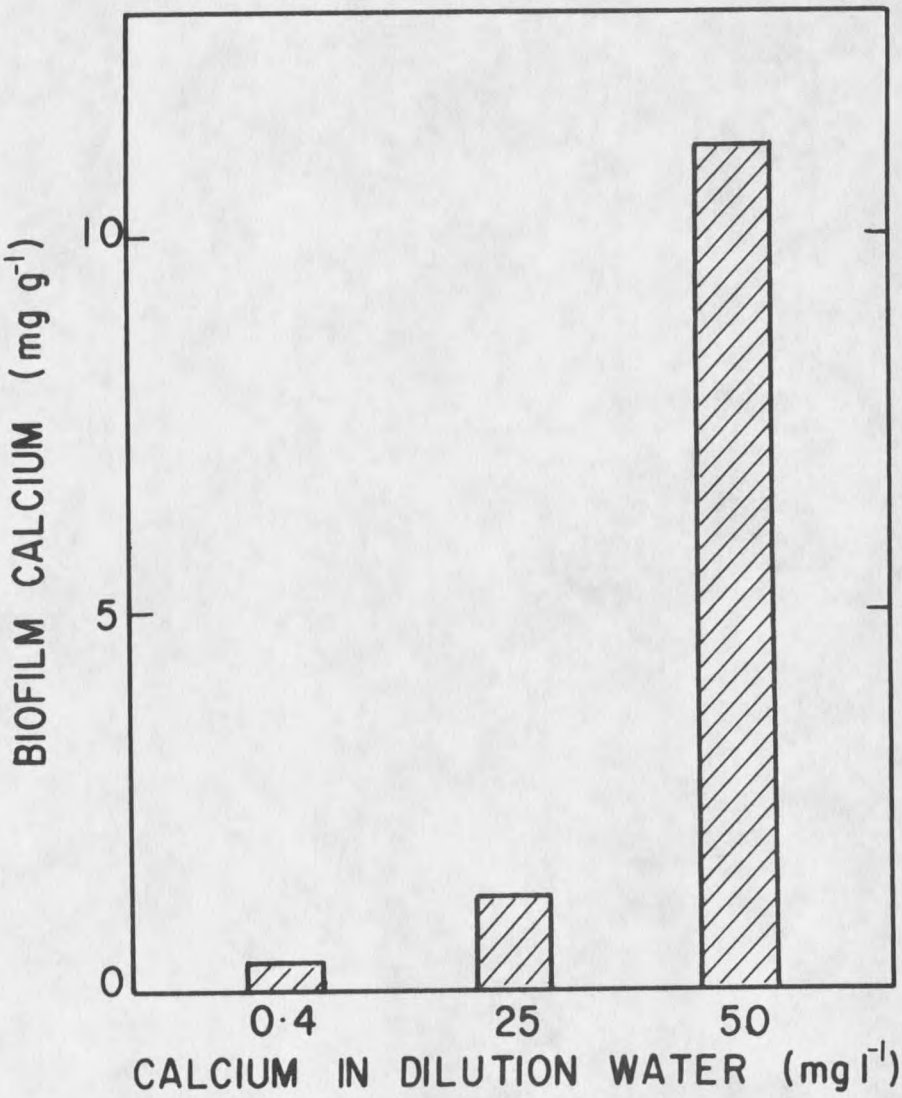

Figure 12. Change in biofilm calcium as a function of calcium in the dilution water.

Table 8. Composition of Biofilm (Dry Weight Basis).

Expt #	Calcium $mg\ l^{-1}$	C %	H %	N %	Fixed Solids %	Volatile Solids %
5	25.0	48.0	7.0	12.3	13.4	86.6
6	50.0	48.6	6.9	13.1	13.5	86.5
6*	50.0	47.8	6.9	12.8	12.8	87.2
7	0.4	47.5	6.9	12.4	13.6	86.4

* Analysis of biofilm left on the surface after EGTA addition.

Biofilm Elemental Analysis

Carbon, nitrogen, and hydrogen contents of the lyophilized biofilm samples under different calcium concentrations were determined using the Carlo-Erba elemental analyzer (Table 8). The data indicate that the overall biofilm elemental composition under different calcium concentrations remained the same.

The results obtained are consistent with C, H, and N content of microbial cells reported in the literature, i.e., approximately 50% carbon, 20% oxygen, 10-15% nitrogen, and 8-10% hydrogen on a dry weight basis (Grady and Lim, 1980).

Effluent Glucose Concentration

Biofilm metabolic activity can be monitored indirectly by measuring changes in effluent substrate (glucose) concentration. Figure 13 is a typical experimental progression of effluent glucose (carbon equivalents). At time zero, the effluent glucose concentration equals

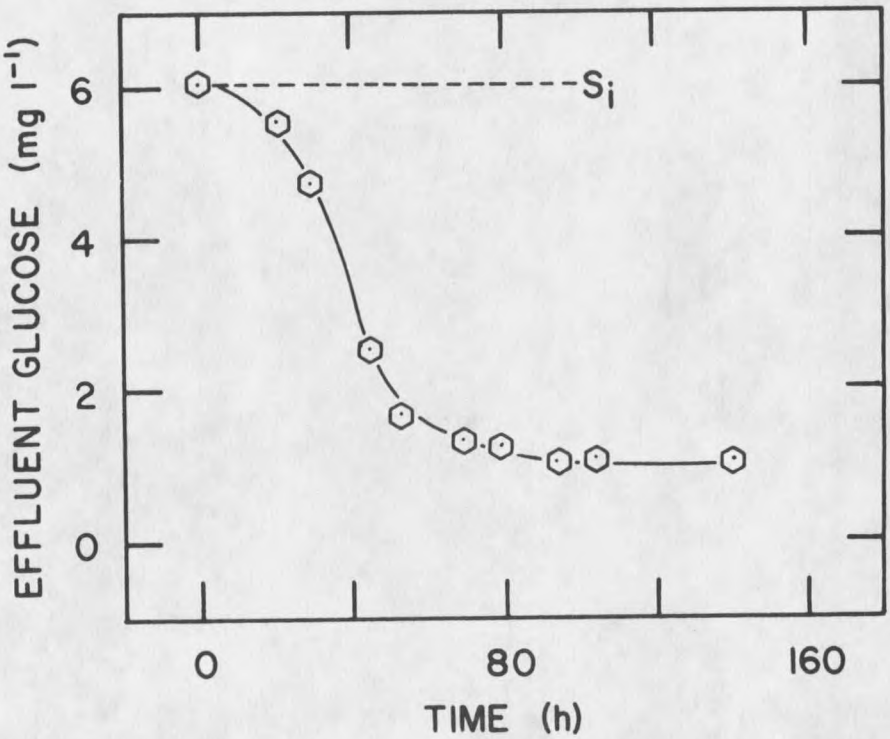

Figure 13. Change in effluent glucose (carbon equivalents) as a function of time. Curve represents time smoothed data (Experiment 6, AR #8).

the influent concentration. As the biofilm accumulates, there is a rapid decrease in effluent glucose concentration. After 50 h, no significant changes in effluent glucose concentration occur. The glucose is removed to support cellular metabolism in the biofilm. Effluent glucose data from AR experiments are presented in Appendix D.

Effluent Oxygen Concentration

Metabolic activity in the biofilm can also be monitored by measuring the changes in effluent oxygen concentration. Figure 14 shows a typical progression of effluent oxygen concentration. The oxygen removed from the bulk fluid serves as the electron acceptor for glucose oxidation within the biofilm. Effluent oxygen data from AR experiments are presented in Appendix D.

Effect of Calcium on Process Rates

Specific Substrate Removal Rate

Specific activity of cells within the biofilm can be monitored indirectly by specific substrate removal rate (substrate removed per cell per unit time). Equation 15 accounts for glucose utilization in the annular reactor. This equation can be used to calculate the specific substrate removal rate.

$$V \frac{ds}{dt} = F (s_i - s) - \frac{R_{xb} A}{Y_{xb/s}} - \frac{R_{pb} A}{Y_{pb/s}} \qquad (15)$$

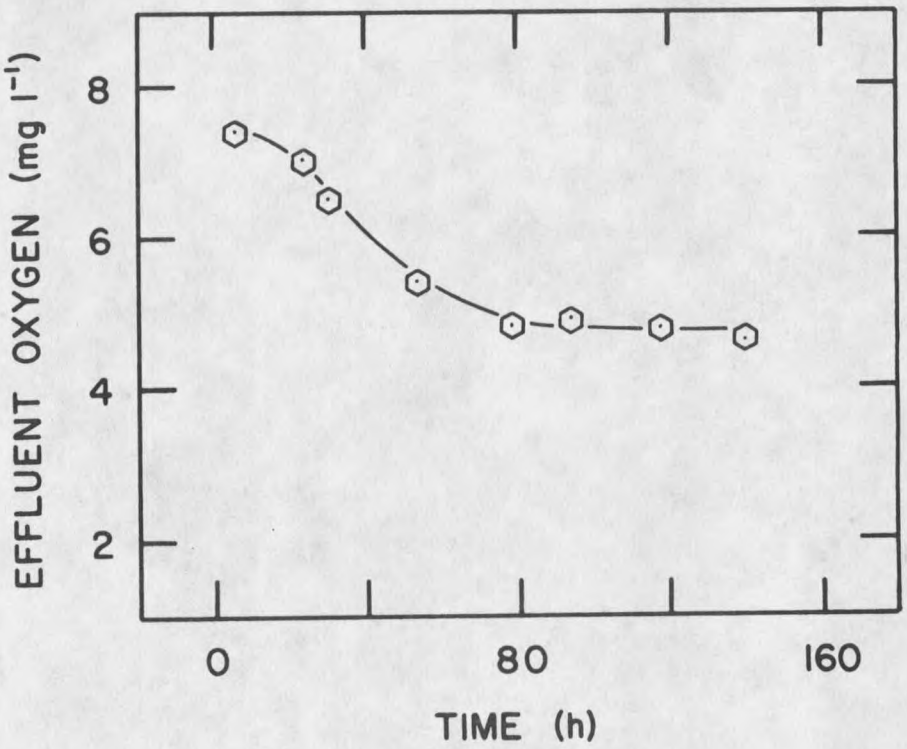

Figure 14. Change in effluent oxygen concentration as a function of time. Line drawn by observation (Experiment 6; AR#8).

Accumulation rate of substrate in the annular reactor was negligible ($ds/dt = 0$) during the sampling period (48-146 h). Incorporating this condition and substituting for R_{xb} and R_{pb}, Equation 15 can be written as:

$$\frac{D(s_i-s)V}{x_b A} = \mu_b \left(\frac{1}{Y_{xb/s}} + \frac{k_b}{Y_{pb/s}} \right) + \frac{k'_b}{Y_{pb/s}} \tag{19}$$

Specific substrate removal rate, q_s, is defined as the left hand side of Equation 19:

$$q_s = \frac{D(s_i - s)V}{x_b A} \tag{20}$$

The specific substrate removal rate, when compared at a specific experimental run time, was highest for biofilm developed under 0.4 mg l^{-1} calcium in the dilution water (Figure 15). This difference in specific substrate removal rate was due to less accumulated biofilm cellular mass in the low (0.4 mg l^{-1}) calcium experiment. As a result, more substrate was available per cell. There was no significant difference in specific substrate removal for biofilm developed under 25 and 50 mg l^{-1} calcium in the dilution water.

Specific Oxygen Removal Rate

Equation (18) accounts for oxygen utilization in the annular reactor. This equation was rearranged to calculate specific oxygen removal rate:

$$\frac{(D+k_c)(O_{2i}-O_2)V}{x_b A} = \mu_b \left(\frac{1}{Y_{xb/o}} + \frac{k_b}{Y_{pb/o}} \right) + \frac{k'_b}{Y_{pb/o}} \tag{21}$$

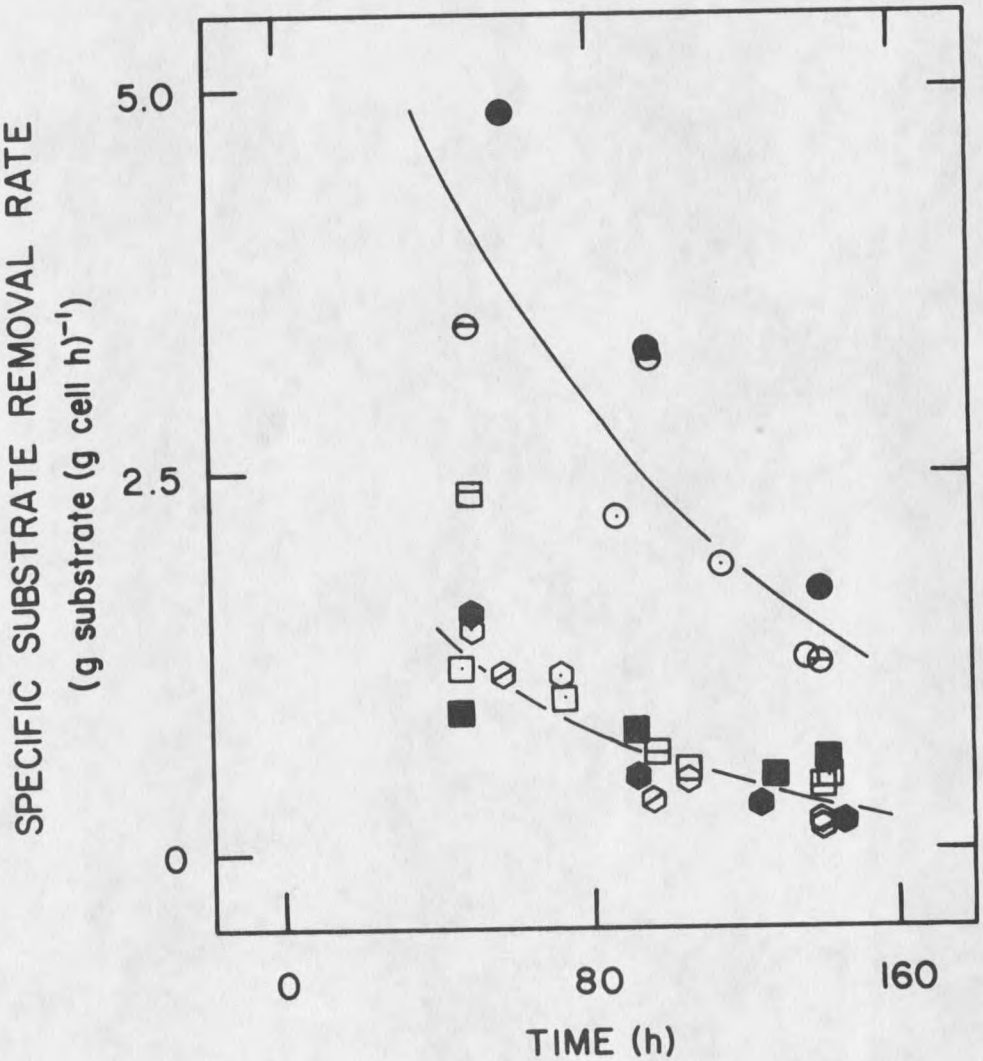

Figure 15. Change in specific substrate removal rate as a function of time with calcium in the dilution water as a parameter. Curves represent time smoothed data. (⊘,○,● 50 mg l^{-1}; ⊟,□,■ 25 mg l^{-1}; and ⊖,○,● 0.4 mg l^{-1}).

The specific oxygen removal rate, q_o, is defined as the left hand side of Equation 21:

$$q_o = \frac{(D + k_c)(O_{2i} - O_2)\ V}{x_b\ A} \tag{22}$$

Specific oxygen removal rate was highest for the biofilm developed under 0.4 mg l^{-1} calcium in the dilution water (Figure 16). Again, there was less attached cellular mass in the low calcium experiment which may account for higher specific oxygen removal rate. There was no significant difference in the specific oxygen removal rate for biofilm developed under 25 and 50 mg l^{-1} calcium in the dilution water.

Specific Cellular Growth Rate in the Biofilm

The specific cellular growth rate in the biofilm was calculated by dividing cellular carbon reproduction rate in the biofilm (R_{xb}) by biofilm cellular carbon concentration (x_b). During the initial period of biofilm accumulation, the cells are growing near their maximum growth rate (Figure 17). As reactor substrate concentration decreases (with increasing time), the specific cellular growth rate decreases as expected.

Specific Cellular Detachment Rate

The specific cellular detachment rate was calculated by dividing cellular carbon detachment rate (R_{dx}) by biofilm cellular carbon (x_b). The specific cellular detachment rate also decreases with time (Figure 18). At the end of the experimental period, the specific cellular

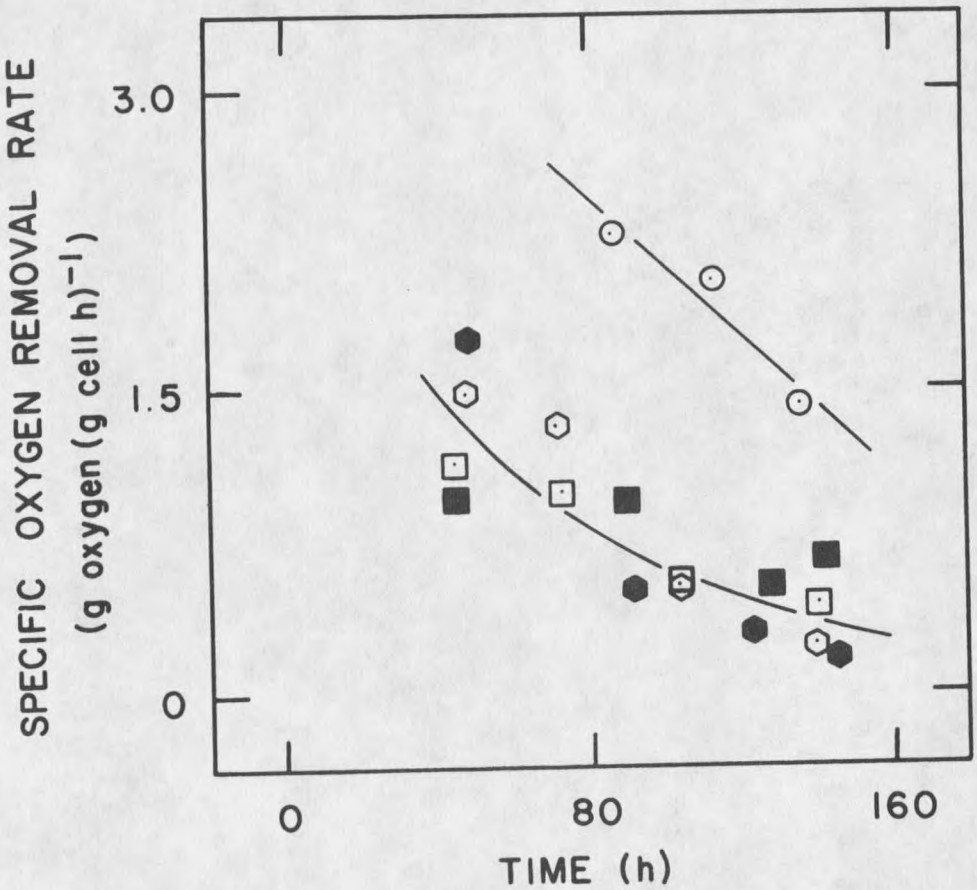

Figure 16. Change in specific oxygen removal rate as a function of time with calcium in the dilution water as a parameter. Curves represent time smoothed data. (○,● 50 mg l^{-1}; □,■ 25 mg l^{-1}; and ○ 0.4 mg l^{-1}).

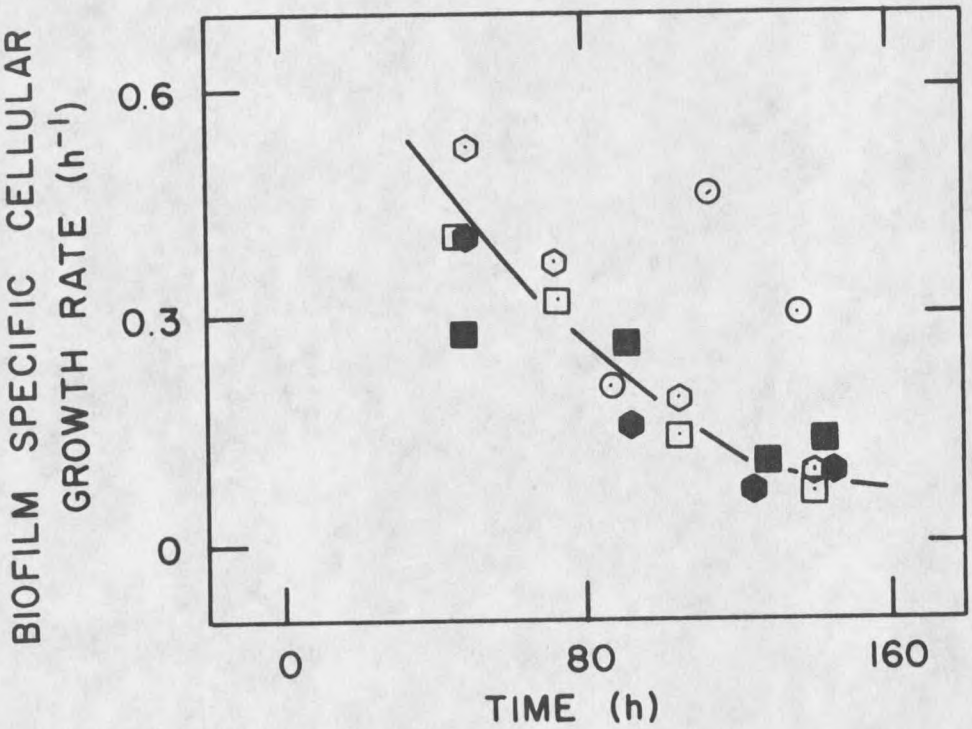

Figure 17. Change in biofilm specific cellular growth rate as a function of time. Line drawn by observation. (⊙,● 50 mg l^{-1}; ⊡,■ 25 mg l^{-1}; and ⊙ 0.4 mg l^{-1} calcium).

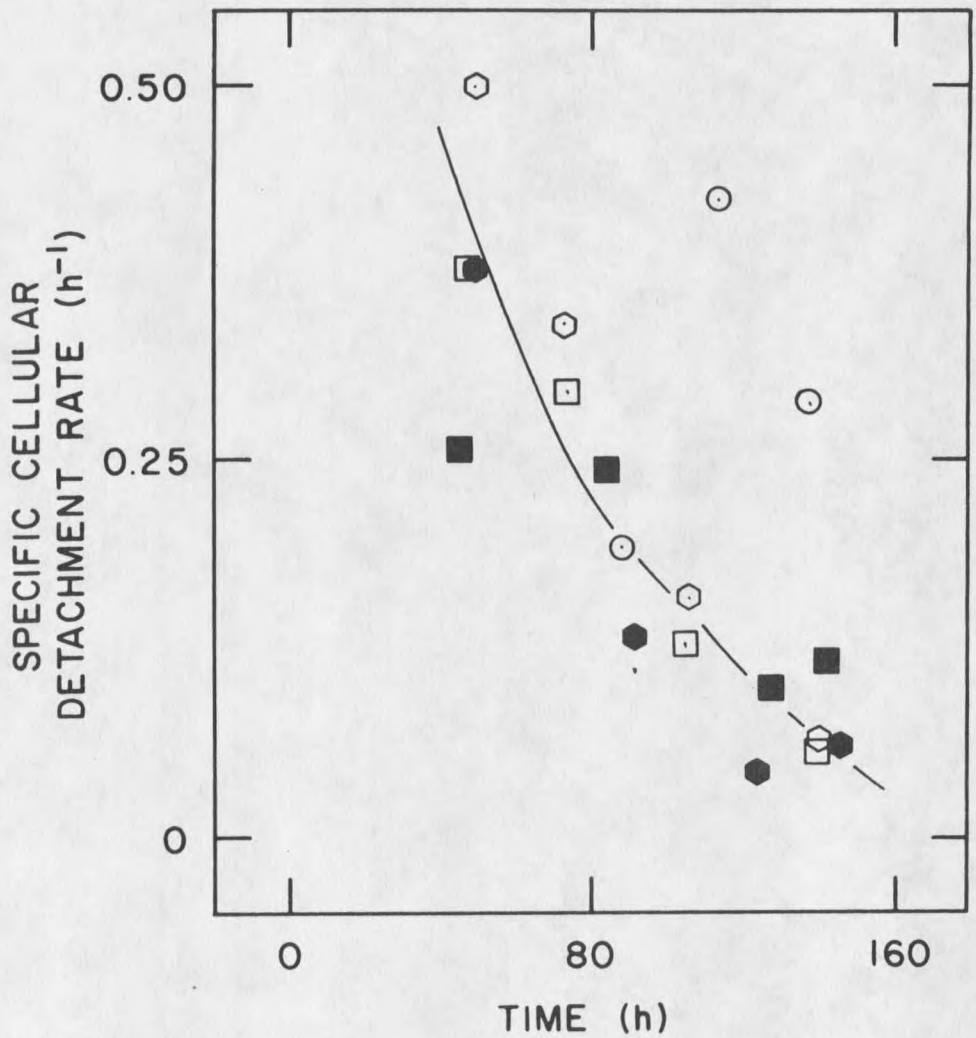

Figure 18. Change in biofilm specific cellular detachment rate as a function of time. Line drawn by observation. (○,● 50 mg l^{-1}; □,■ 25 mg l^{-1}; and ⊙ 0.4 mg l^{-1} calcium).

detachment rate approaches specific cellular growth rate and the system approaches steady state.

Specific Polymer Production Rate

Specific polymer production rate was calculated by dividing polymer carbon formation rate (R_{pb}) by biofilm cellular carbon concentration (x_b). Specific polymer production rate decreases with time because substrate concentration decreases (Figure 19).

Specific Polymer Detachment Rate

Specific polymer detachment rate was calculated by dividing polymer carbon detachment rate (R_{dp}) by biofilm polymer carbon concentration (p_b). Specific polymer detachment rate decreases with time and appears to reach a steady state after 80 h (Figure 20).

Effect of Chelant on Biofilm

This section describes experiments wherein buffered EGTA and/or EDTA was used to detach *Ps. aeruginosa* and mixed culture biofilms. Results of detachment experiments with mixed culture biofilms were published in *Applied and Environmental Microbiology*, December 1983. Experimental conditions and summaries of the experimental results from AR and TR are given in Tables 9 and 10, respectively. Raw data from AR and TR experimental studies with the addition of chelant are presented in Appendices B and C.

Twelve residences time (AR experiments) before the addition of EGTA, the flow of $CaCO_3$ + HCl stock solution was stopped. Hence, there

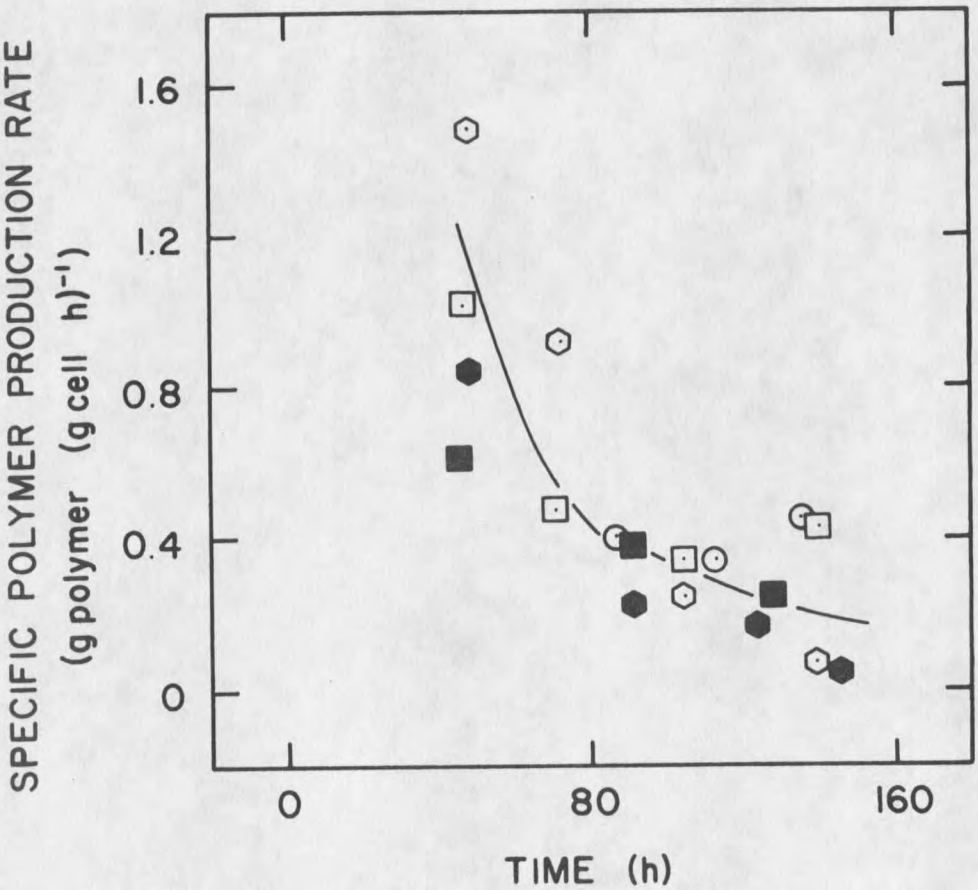

Figure 19. Change in biofilm specific polymer production rate as a function of time. Line drawn by observation. (⊙,● 50 mg l^{-1}; □,■ 25 mg l^{-1}; and ⊙ 0.4 mg l^{-1} calcium).

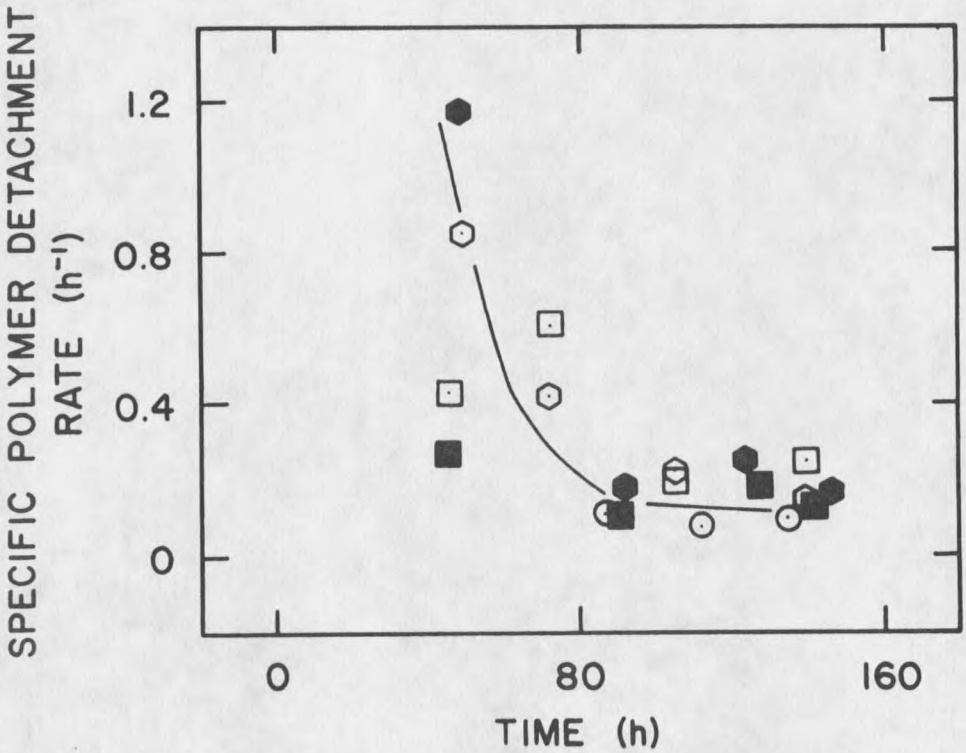

Figure 20. Change in biofilm specific polymer detachment rate as a function of time. Line drawn by observation. (⬡,● 50 mg l^{-1}; ⊡,■ 25 mg l^{-1}; and ○ 0.4 mg l^{-1} calcium).

Table 9. Summary of Annular Reactor Detachment Experiments.

Expt #	AR #	s_i mg l^{-1}	Total calcium during biofilm accumulation* mg l^{-1}	Chelant (EGTA) added mM	Biofilm mass mg m^{-2}	Biomass detached mg m^{-2}
1	7	4.00	9.00	0.00	ND	0.0**
	8	3.84	9.00	0.25	ND	86.5
2	7	4.16	9.00	0.00	ND	0.0**
	8	3.84	9.00	0.50	ND	260.0
3	7	6.56	0.40	1.00	919.5	116.3
	8	6.40	25.00	1.00	1353.2	362.2
4	7	4.83	0.40	1.00@	937.5	90.1
	8	4.70	50.00	1.00	2772.53	313.0
6	7	6.32	50.00	1.00	2403.8	318.7

ND = not determined.
@ Chelant was EDTA.
* There was no added calcium in the dilution water during chelant addition.
** Control experiments; no additional removal of biomass from the surface.

For experiments 1 & 2, the biofilm was allowed to accumulate for four and five days, respectively, before chelant was added.

For experiments 3, 4, & 6, chelant was added to the AR after six days of accumulation.

Time of EGTA/EDTA addition was 60 min.

Table 10. Experimental Conditions and Summary of Tubular Reactor Results.

	Experiment #1	Experiment #2
Dilution rate (h^{-1})	0.50	0.50
Influent (mg l^{-1}) substrate	17.60	17.60
Volume (l)	10.49	7.80
Surface area (m^2)	0.80	0.77
Tris (mM)	10.00	10.00
EGTA (mM)	1.00	1.00
Total biomass (mg) detached in one hour	325	865

Time of EGTA addition was 120 min.

was no added calcium in the dilution water during detachment studies. One hour (two hours in case of TR experiments) before the addition of EGTA or EDTA, sufficient Tris-HCl was added to the system to give a final concentration of 10 mM Tris and the dilution water was also buffered with 10 mM Tris. Cessation of calcium feed and buffer addition did not perturb the system since no significant changes in the analytical characteristics of the effluent were detected (AR #7; Experiments 1 & 2).

The experiment consists of adding a known concentration of EGTA or EDTA (step input) to the bioreactor and monitoring the changes in the following quantities in the effluent:

suspended solids

suspended cells

glucose

total carbohydrate

Experimental progressions are presented in which time zero is defined as time at which EDTA or EGTA was added.

Suspended Solids

The effect of EGTA and/or EDTA on the biofilm was monitored by measuring changes in effluent suspended solids. The response of a biofouled annular reactor to the addition of a known concentration of EGTA (1.0 and 0.5 mM, respectively) is presented in Figures 21 and 22. The addition of EGTA resulted in the detachment of a portion of the biofilm as reflected by an increase in effluent suspended solids. Similar results were obtained with all other AR experiments with *Ps*.

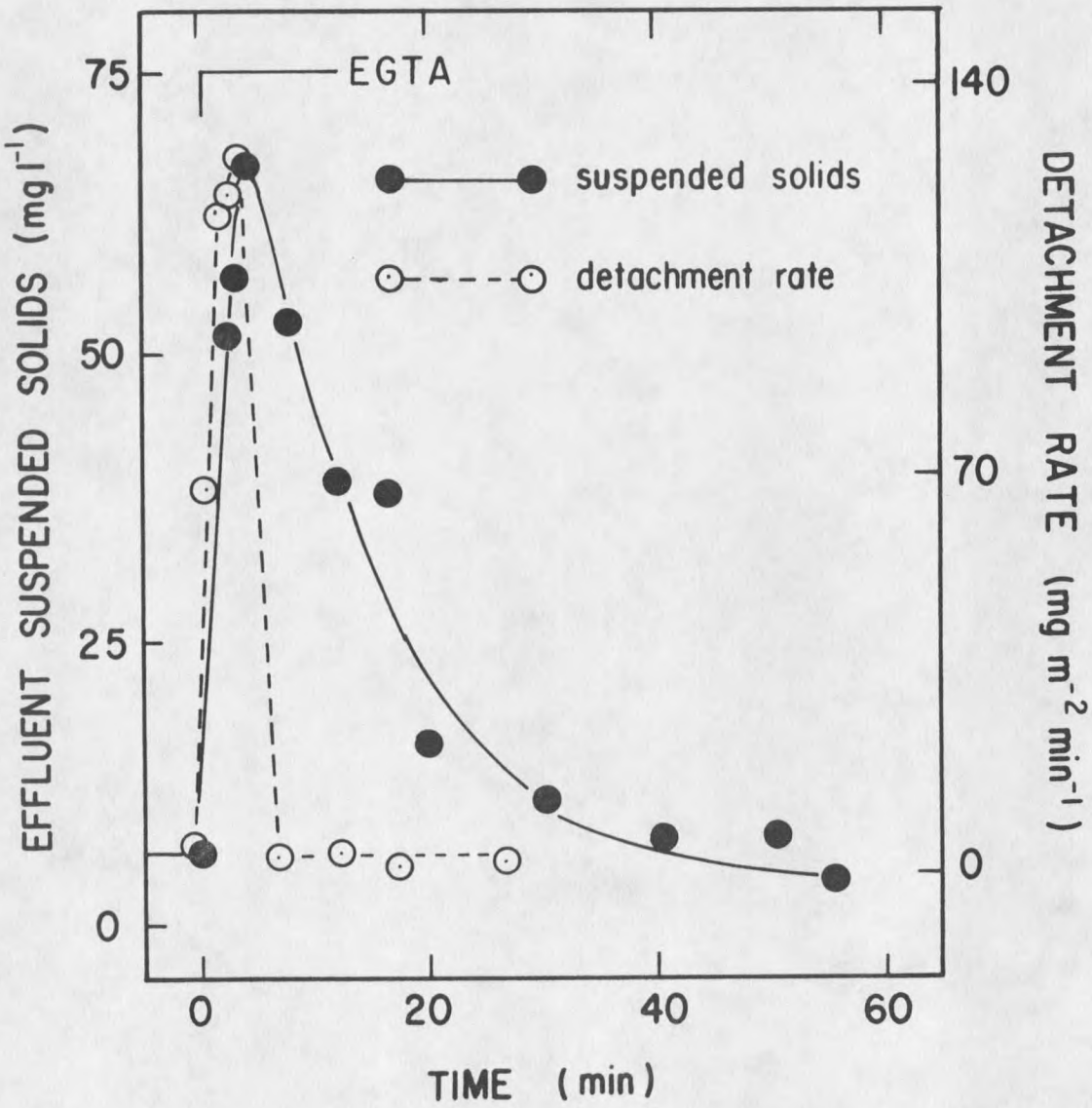

Figure 21. Response of a biofouled annular reactor (Experiment 6) to the addition of 1 mM EGTA. Lines drawn by observation.

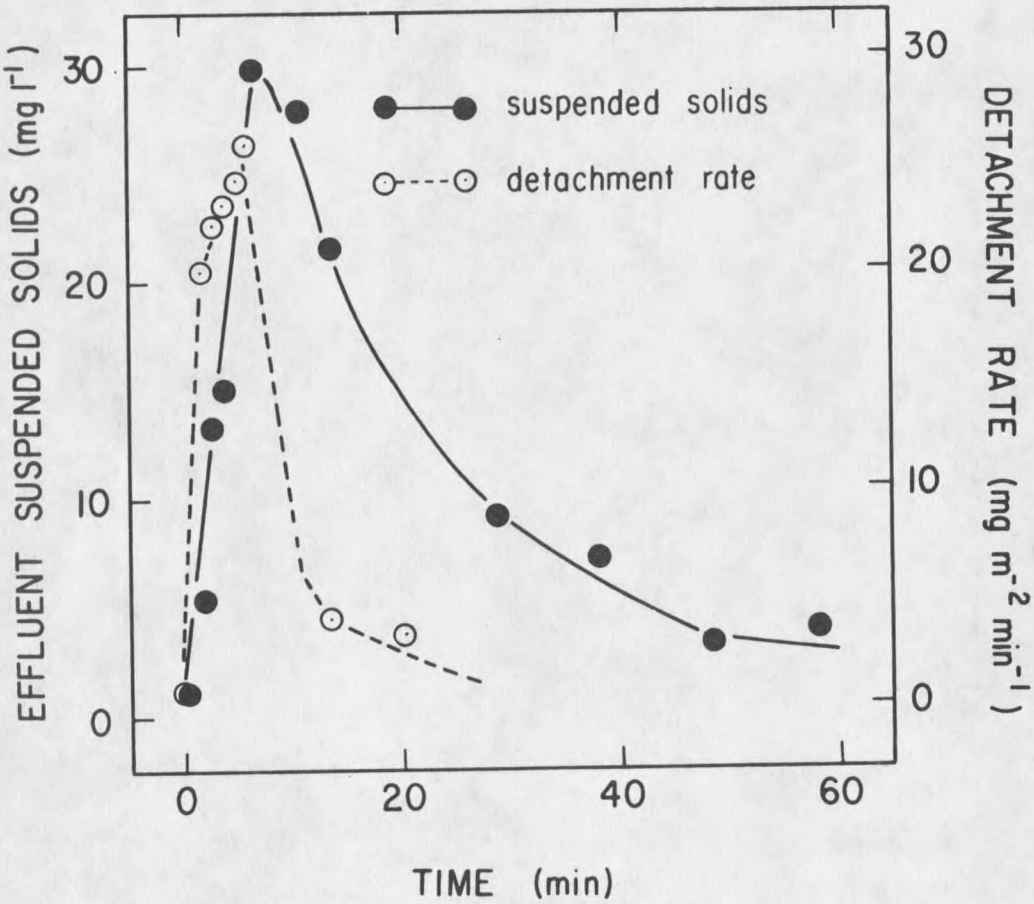

Figure 22. Response of a biofouled annular reactor (Experiment 2; AR #8) to the addition of 0.5 mM EGTA. Lines drawn by observation.

aeruginosa biofilms. These results suggest that free calcium (or calcium-associated ligands of lower affinity than that of calcium for EGTA) is essential to the structural integrity of the Ps. aeruginosa biofilms.

EGTA was also added to the tubular reactor containing a mixed culture biofilm. The addition of EGTA resulted in the removal of mixed culture biofilm as reflected by the increase in suspended solids in the effluent (Figure 23). Similar results (Figure 24) were also obtained in a second experiment, where the biofilm mass was tenfold greater than in the first experiment. Thus, calcium is also essential to the structural integrity of mixed culture biofilms.

A contiguous portion of the mixed culture biofilm from the tubular reactor was scraped from the surface and suspended in the growth media. Disaggregation of the biofloc was observed under a phase contrast microscope when EGTA was added.

Detachment Rate

A material balance approach was used to determine biofilm detachment rate from the surface. A mass balance (for suspended solids) across the reactor is as follows:

$$\underbrace{\frac{V\,dx_T}{dt}}_{\text{net rate of accumulation in the reactor}} = \underbrace{-F\,x_T}_{\text{net rate of output by flow}} + \underbrace{R_D\,A}_{\text{net rate of detachment}} \qquad (23)$$

where,

V = volume of the system (L^3)

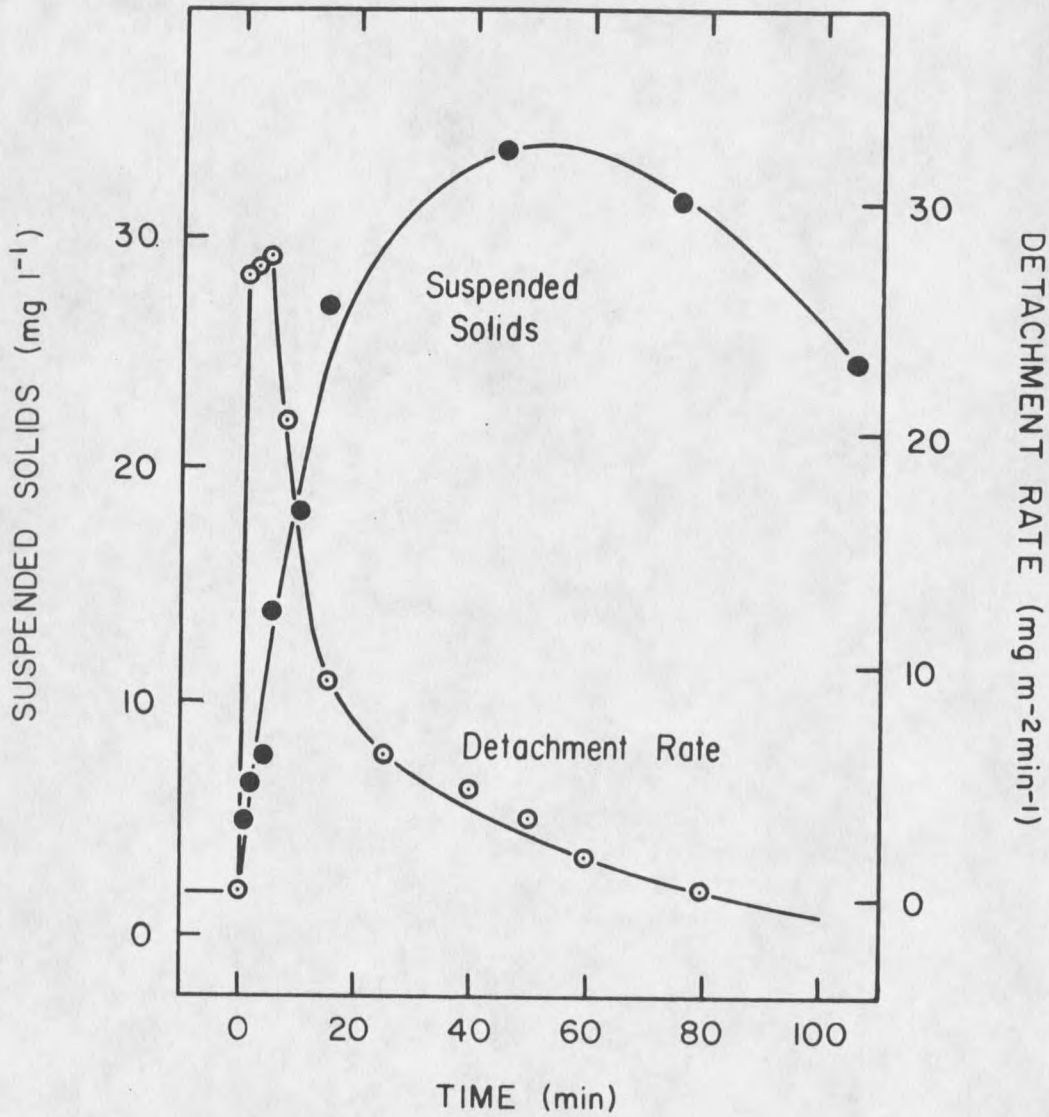

Figure 23. Response of a biofouled tubular reactor (Experiment #1) to the addition of 1 mM EGTA. Lines drawn by observation.

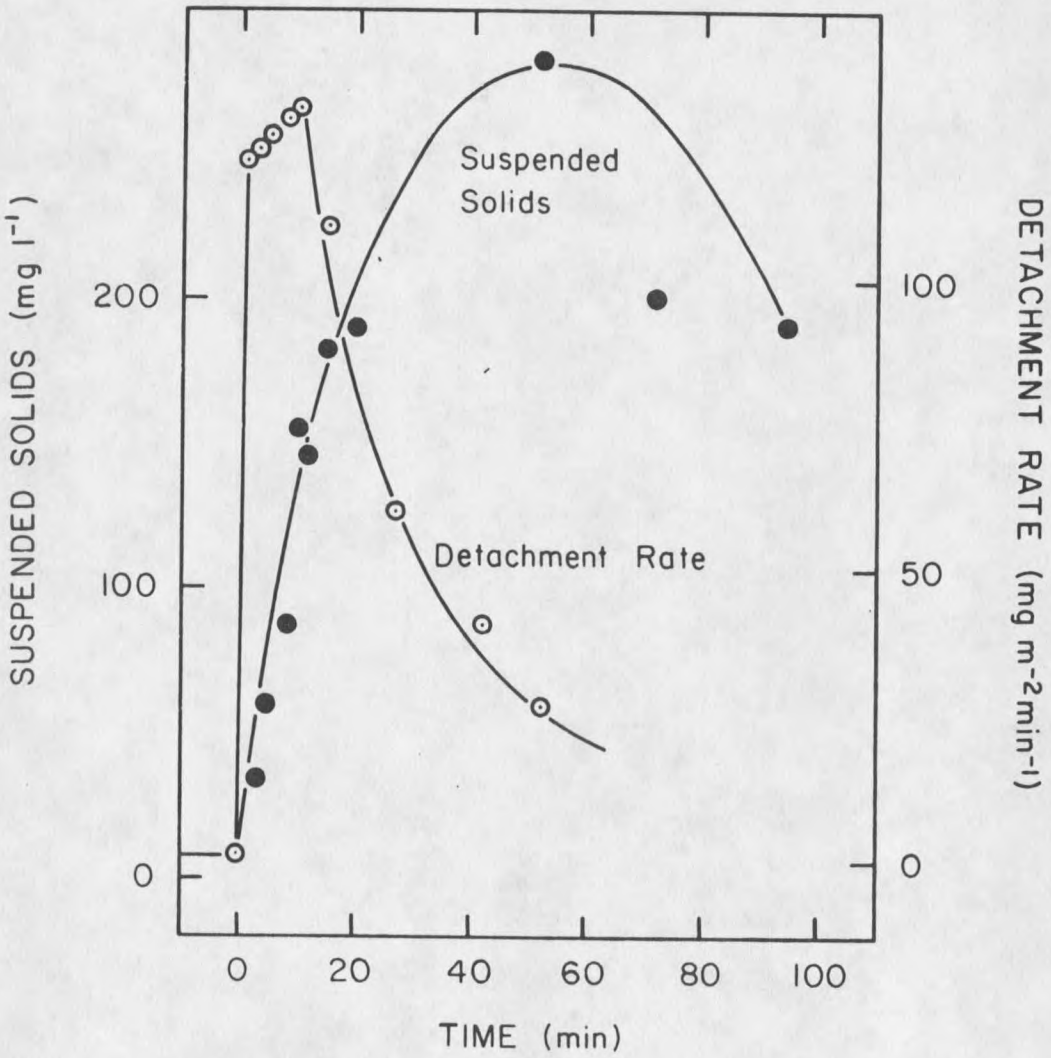

Figure 24. Response of a biofouled tubular reactor (Experiment #2) to the addition of 1 mM EGTA. Lines drawn by observation.

A	=	surface area	(L^2)
x_T	=	suspended biomass concentration	(ML^{-3})
t	=	time	(t)
R_D	=	net detachment rate	$(ML^{-2}t^{-1})$
F	=	influent flow rate	(L^3t^{-1})

The detachment rate can be calculated by rearranging Equation 23 as follows:

$$R_D = (V\, dx_T/dt = F\, x_T) / A \qquad (24)$$

The detachment rate, R_D, in these experiments (AR's and TR's) was calculated using Equation 24.

The addition of chelant resulted in the removal of Ps. aeruginosa and mixed culture biofilm in the first 5-10 minutes (Figures 21-24).

Suspended Cells and Polymers

The suspended biomass resulting from detachment was composed of cellular and polymer biomass. The addition of EGTA to annular reactors containing Ps. aeruginosa biofilm resulted in partial removal of cellular and polymer components of the biofilm as measured by the increase in their respective constituents (Figures 25 and 26) in the effluent. Total carbohydrate was used to estimate the extracellular polymer content in the effluent. Similar results were obtained with all Ps. aeruginosa biofilms (AR experiments) and mixed culture biofilms (TR experiments).

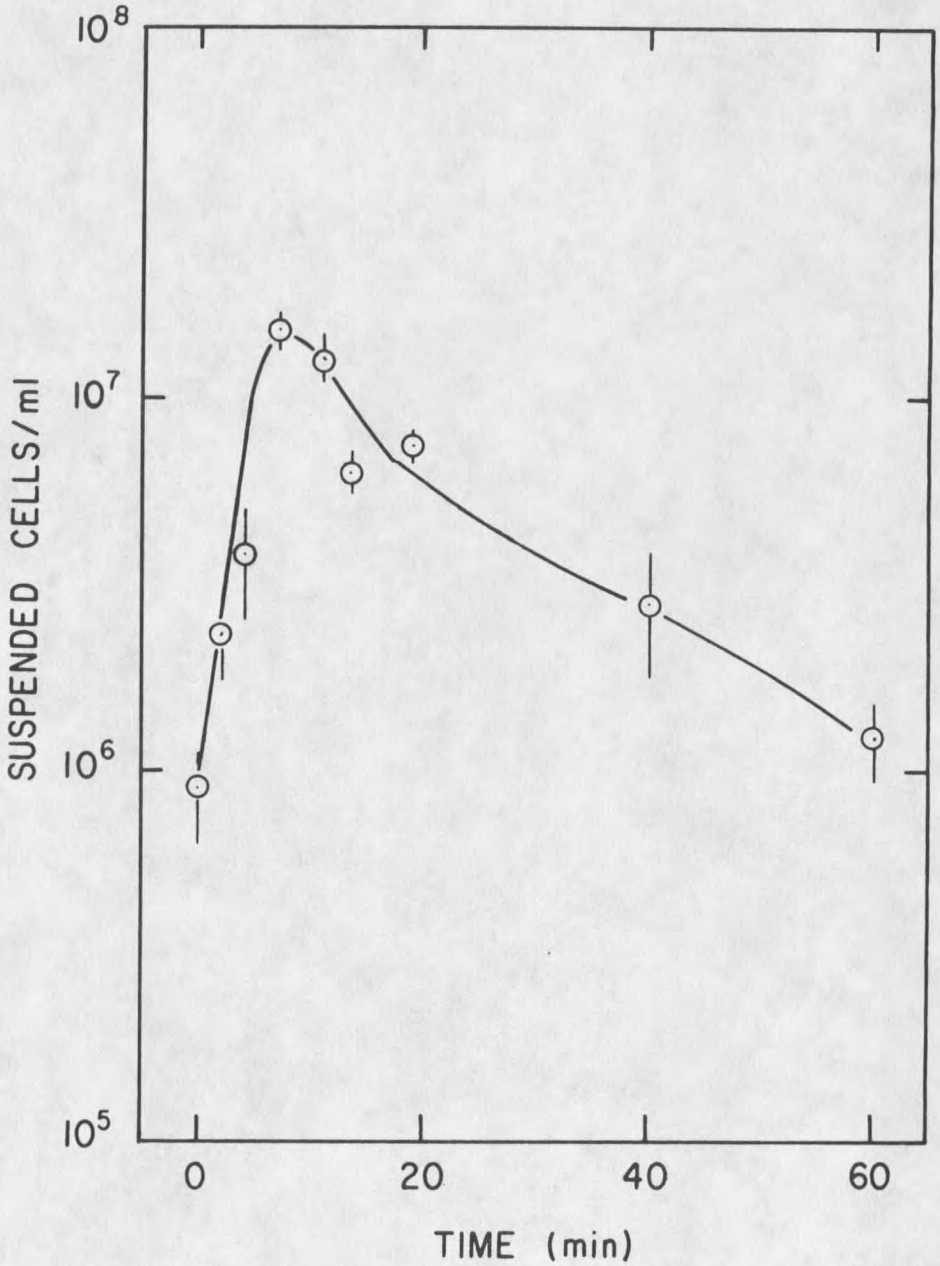

Figure 25. Change in suspended cell concentration in the effluent of the annular reactor (Experiment 2; AR #8) after EGTA (1 mM) addition. Line drawn by observation. Error bars represent standard deviation of measurements of the same sample.

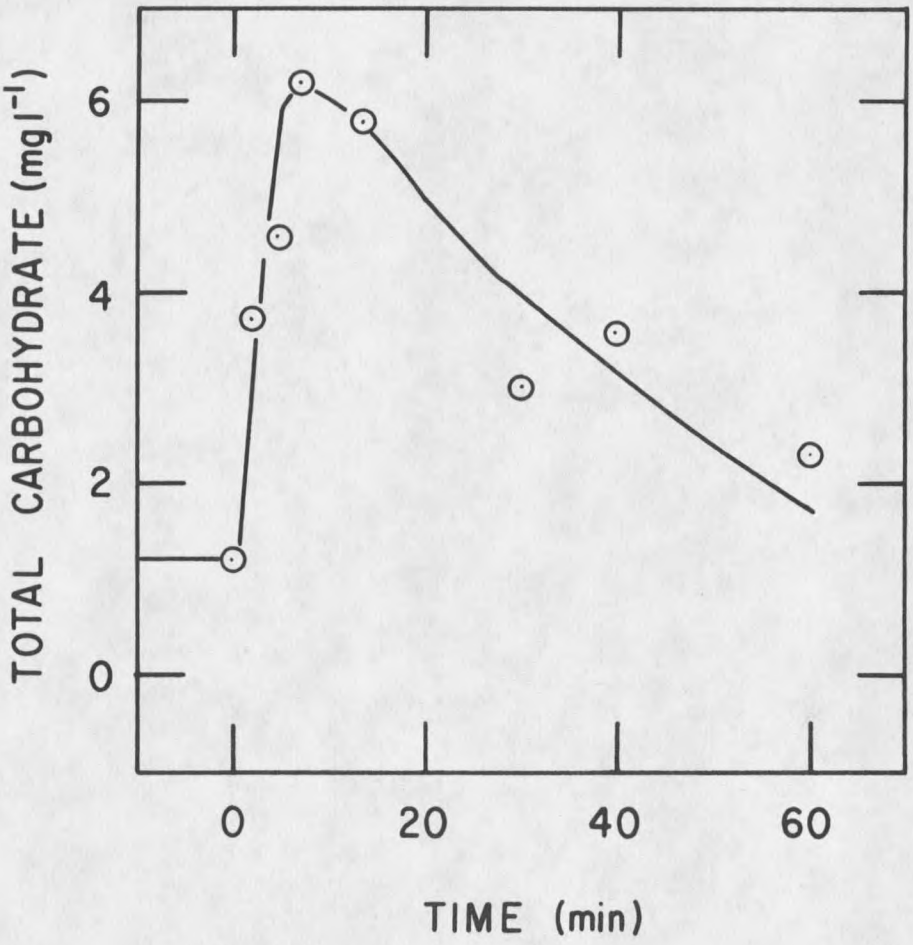

Figure 26. Change in total carbohydrate (as glucose equivalents) in the effluent of the annular reactor (Experiment 2; AR #8) as a result of EGTA (1 mM) addition. Line drawn by observation.

The calculated suspended cell mass in the effluent was consistently much smaller than the suspended solids mass (Figure 27), which suggests that the detached biofilm mass was comprised of material other than bacterial cells. This is consistent with the findings of Trulear (1983) who showed that biofilm is largely extracellular polymer substance (EPS). The results of these and other (Costerton et al., 1978) experiments show that EPS is largely carbohydrate in nature (Figures 26 and 28).

Microbial Activity

The effect of chelant (EGTA or EDTA) on microbial activity was monitored by measuring the changes in effluent glucose concentration, an *in situ* measure of microbial activity. There was no significant change in effluent glucose concentration as a result of chelant (EGTA and EDTA) addition (AR experiments) indicating that chelant did not affect overall microbial substrate utilization (Table 11). Thus, microbial activity was presumably unaffected. There was also no change in the effluent glucose concentration as a result of EGTA addition to mixed culture biofilms (Appendix B).

Total Biofilm Detached

The total amount of biomass detached as a result of chelant addition was determined by integrating the curve (e.g., Figures 21-24) describing the progression of effluent suspended solids. The amount of biofilm detached in the various experiments are reported in Tables 9 and 10. There was no significant difference in the amount of biofilm

Table 11. Change in Effluent Glucose Carbon Concentration as a Result of Chelant Addition (AR Experiment 4).

Time after chelant addition (min)	Effluent glucose carbon (mg l^{-1})	
	AR #7*	AR #8**
0	0.58	0.64
15	0.70	--
20	--	0.64
30	0.80	--
40	0.80	--
50	--	0.67
60	0.80	0.67

*EDTA (1.0 mM).

**EGTA (1.0 mM).

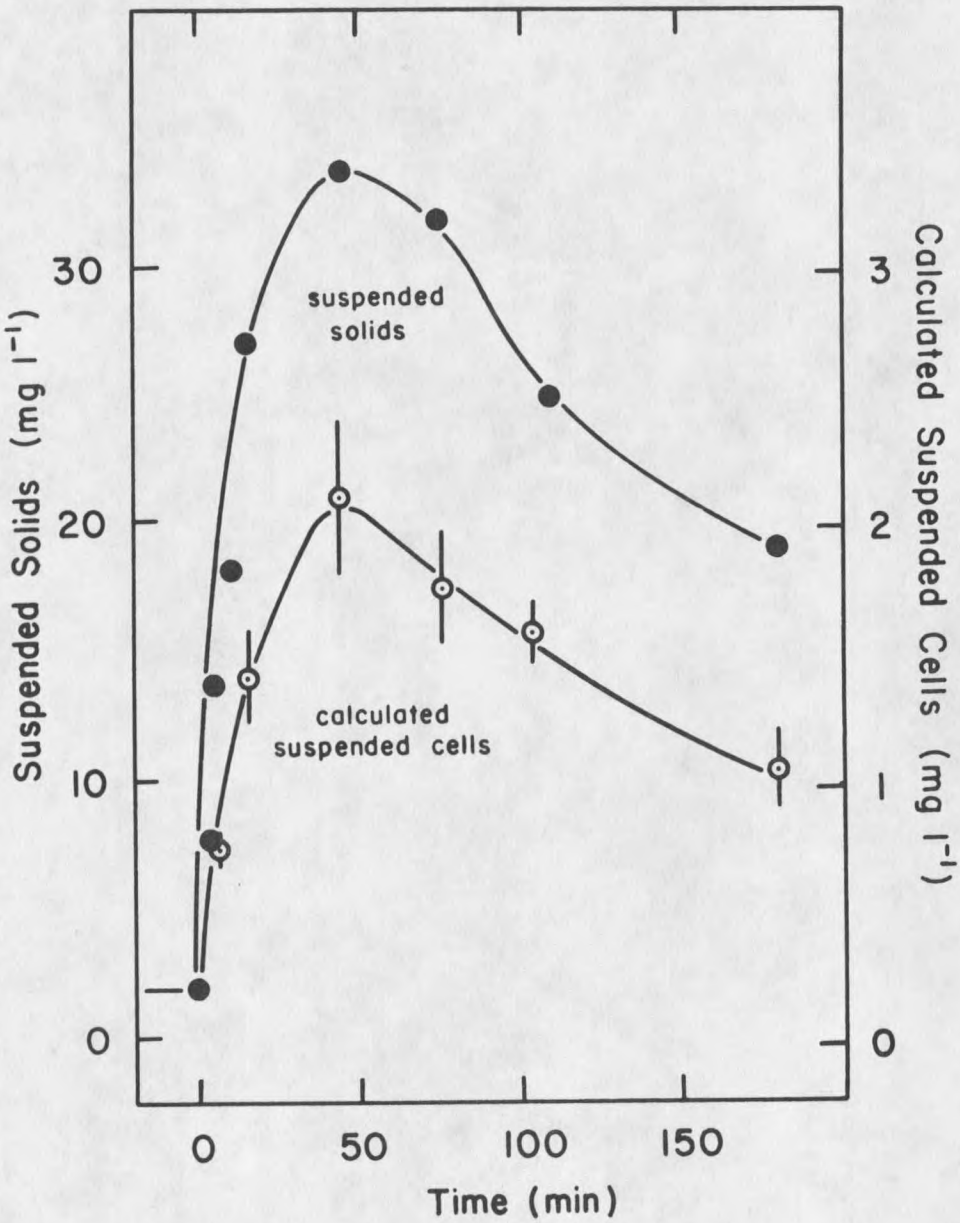

Figure 27. Change in suspended solids and suspended cell mass in the effluent due to the addition of 1 mM EGTA. Lines drawn by observation. Error bars based on standard deviation from epifluorescent cell counts.

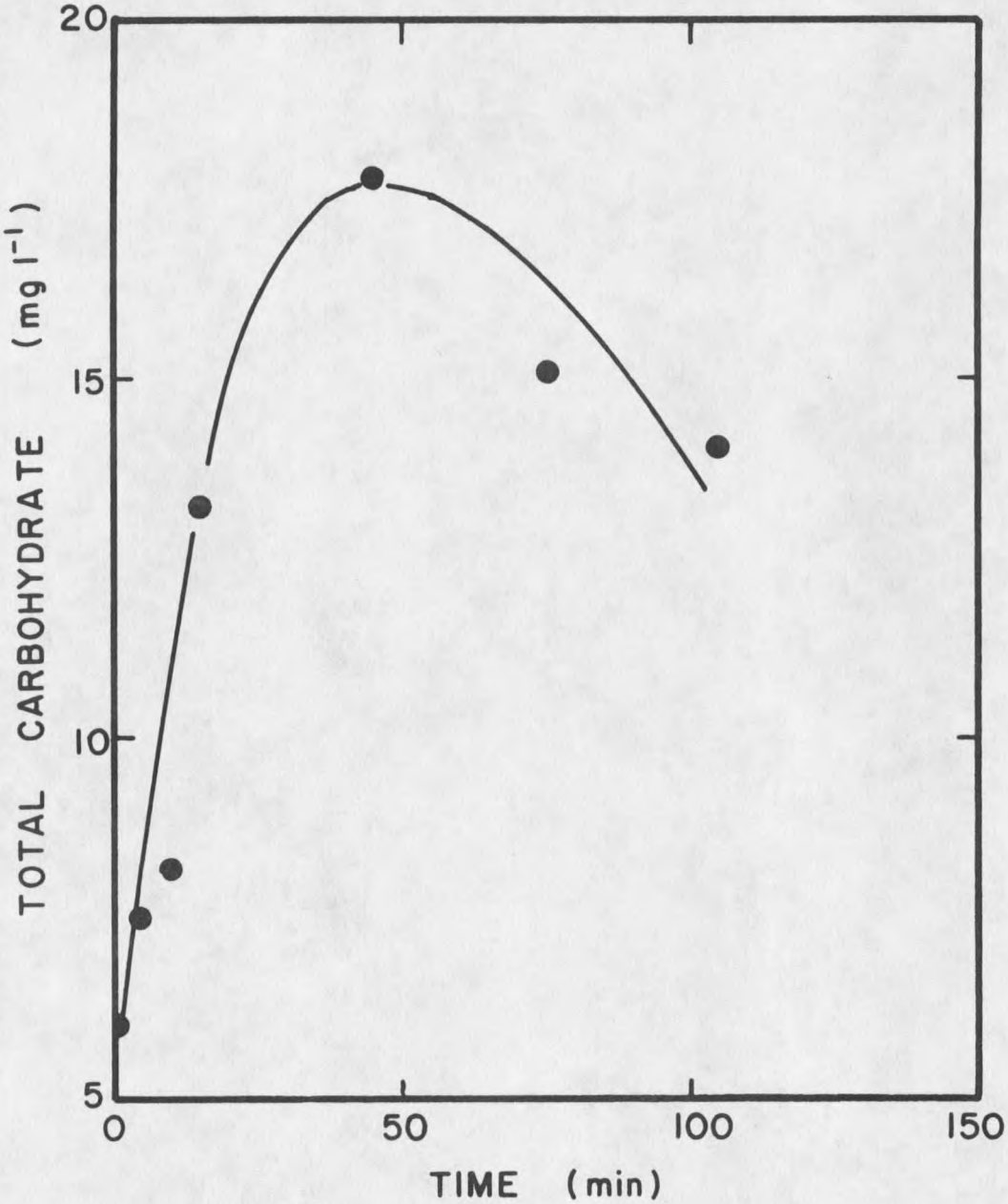

Figure 28. Change in total carbohydrate (as glucose equivalents) in the effluent of tubular reactor (Experiment #1) after the addition of 1 mM EGTA. Line drawn by observation.

removed when either EGTA or EDTA was added to the Ps. aeruginosa biofilm developed in low calcium (0.4 mg l^{-1}) conditions.

The amount of mixed culture biofilm removed in the second experiment was significantly higher than the first experiment largely because the biofilm in the second experiment was allowed to form over a much longer period.

Biofilm Calcium

The change in biofilm calcium concentration before and after the addition of EGTA and/or EDTA (Table 12) indicates a significant decrease in calcium concentration in the Ps. aeruginosa biofilm occurs as a result of chelant addition.

Table 12. Biofilm Calcium Before and After Chelant (EGTA) Addition.

Expt #	AR #	Calcium in dilution water mg l^{-1}	Biofilm calcium (μg g^{-1})	
			Before chelant addition	After chelant addition
3	7	0.4	ND	55
3	8	25.0	1250	110
4	7	0.4*	388	117
4	8	50.0	11200	800

ND = not detectable.

* Chelant was EDTA.

Batch Growth Experiments

The effect of calcium on maximum specific growth rate of *Ps. aeruginosa* was determined by measuring the oxygen uptake in batch (suspended) cultures using BOD respirometer. The BOD respirometer monitors oxygen uptake in three different batch cultures simultaneously. Two different calcium concentrations, 3.2 (no added calcium) and 25 mg l^{-1}, were tested. Raw data from batch growth experiments are presented in Appendix E. Experimental conditions and summaries of experimental results are given in Table 13.

Table 13. Experimental Conditions and Summary of Batch Growth Experimental Results.

Expt #	Unit #	s_i mg l^{-1}	Total calcium mg l^{-1}	Free calcium mg l^{-1}	μ_m h^{-1}	$Y_{s/o}$ $gC(gO_2)^{-1}$
1	1	80	25.0	ND	0.386±0.004	0.80
	2	80	3.2	ND	0.318±0.003	1.00
	3	80	3.2	ND	0.334±0.004	0.89
2	1	400	25.0	12.50	0.432±0.003	ND
	2	400	3.2	0.02	0.325±0.001	ND
	3	400	3.2	0.02	0.329±0.001	ND
3	1	400	25.0	12.50	0.349±0.002	0.89
	2	400	25.0	12.50	0.364±0.003	0.89
	3	400	3.2	0.02	0.308±0.002	0.89

ND = not determined.

The experiments were initiated by inoculating the sample bottles with a batch culture of *Ps. aeruginosa*. Calcium was added to the sample bottles using sterile disposable syringes from a sterile $CaCO_3$ +

HCl stock solution. The sample bottles were continuously stirred to facilitate the transfer of oxygen to the liquid. The temperature of the system was maintained at 24°C.

Microbial growth and reproduction was monitored by measuring cumulative oxygen uptake. The progression of oxygen uptake (Figures 29-31) is frequently referred to as "bacterial growth curve." The cumulative oxygen uptake is a logistic function of time. Microbial growth and reproduction proceeds exponentially until glucose reaches a growth-limiting concentration. At that point, the reaction (i.e., microbial growth) decelerates. A plateau in oxygen uptake will be reached when all the substrate is exhausted. This "plateau" is analogous to reaction completion. The experiments were terminated when a plateau in oxygen consumption was reached.

Maximum Specific Growth Rate

The maximum specific growth rate, μ_m, can be calculated by plotting the oxygen uptake data on semi-logarithmic coordinates. The linear scope of the semi-log plot (Figure 32) is the maximum specific growth rate. The maximum specific growth rates of *Ps. aeruginosa* for all the experiments are listed in Table 12. The maximum specific growth rate of *Ps. aeruginosa* in the presence of 25 mg l^{-1} calcium was approximately 16% higher than that in the presence of 3.2 mg l^{-1} (no added calcium). However, the reproducibility in μ_m, at a given calcium concentration, between experiments was poor. A t-test (Zar, 1984) was used to test the hypothesis that there is no significant difference in μ_m between two different calcium concentrations within experiments.

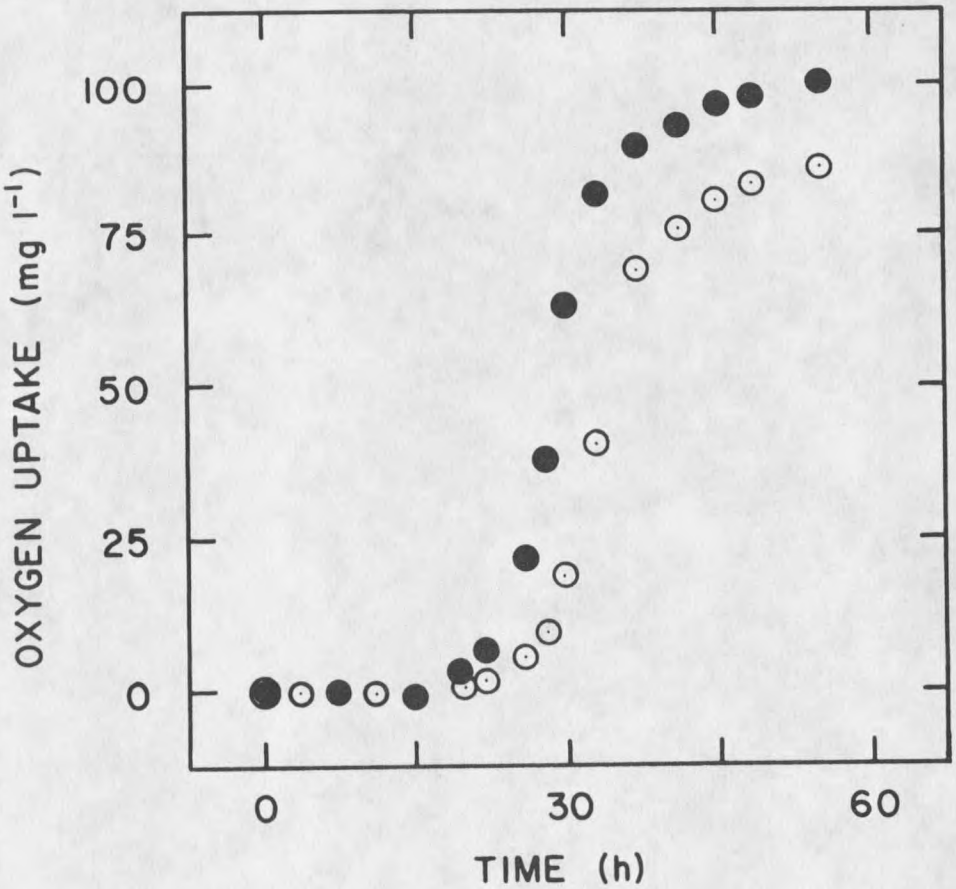

Figure 29. Change in oxygen uptake as a function of time for two different calcium concentrations (Batch Experiment #1). (● 25 mg l^{-1}; ○ 3.2 mg l^{-1}) ⊙ represents the average value of oxygen uptake from two different experimental units.

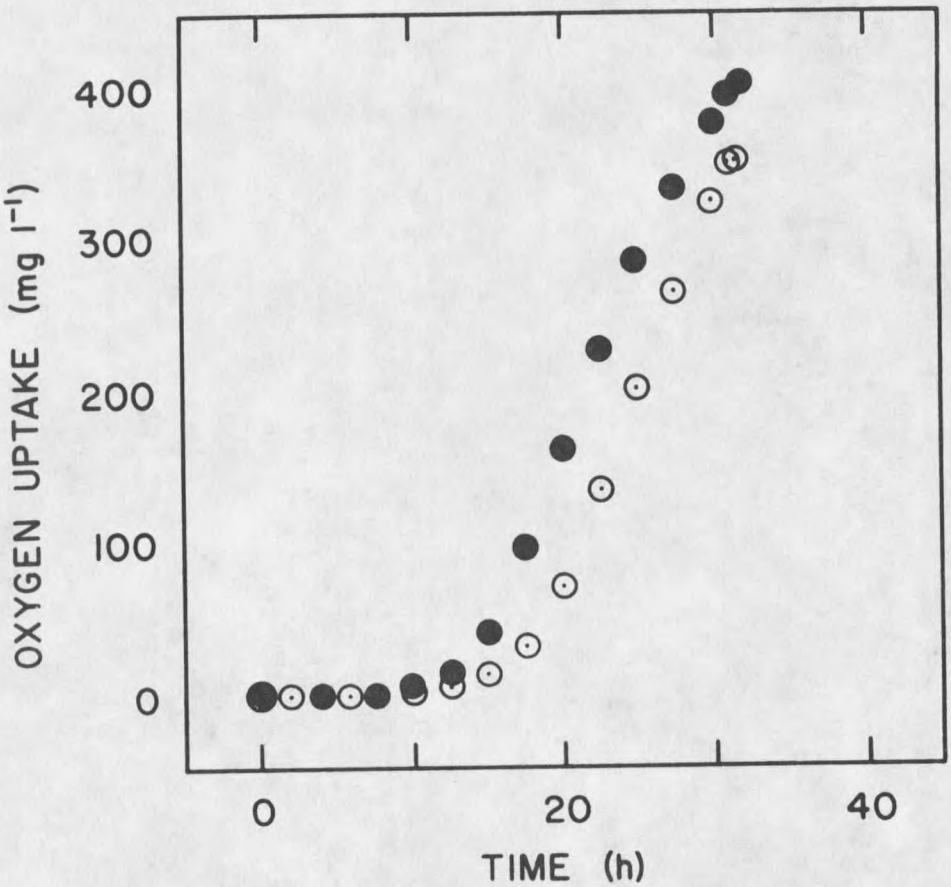

Figure 30. Change in oxygen uptake as a function of time for two different calcium concentrations (Batch Experiment #2). (● 25 mg l^{-1}; ○ 3.2 mg l^{-1}) ⊙ represents the average value of oxygen uptake from two different experimental units.

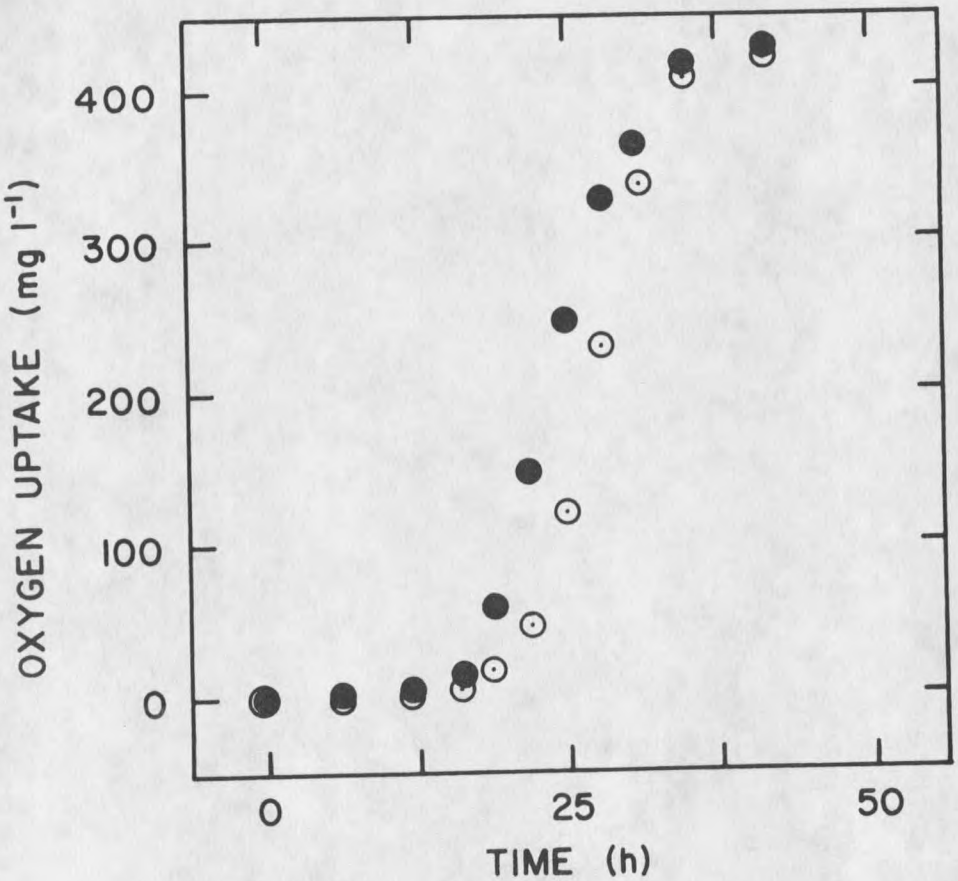

Figure 31. Change in oxygen uptake as a function of time for two different calcium concentrations (Batch Experiment #3). (● 25 mg l^{-1}; ⊙ 3.2 mg l^{-1}) ● represents the average value of oxygen uptake from two different experimental units.

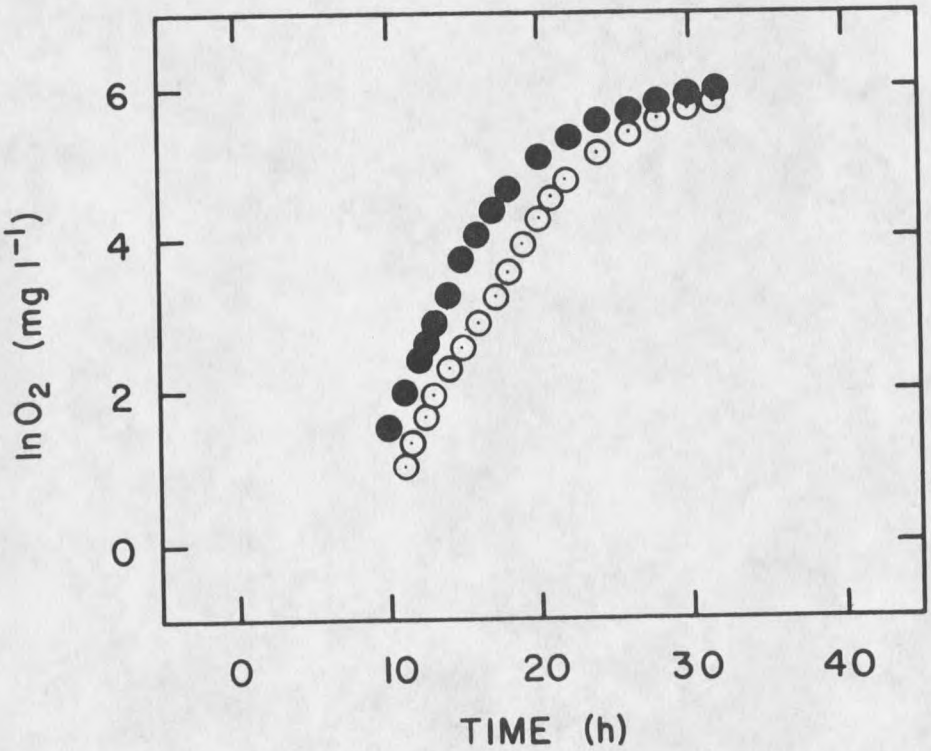

Figure 32. Change in oxygen uptake as a function of time on a semi-log coordinate for different calcium concentrations (Batch Experiment #1). (● 25 mg l^{-1}; ○ 3.2 mg l^{-1}) ⊙ represents the average value of oxygen uptake from two different experimental units.

There was a significant difference (at 95% confidence level) in μ_m between 3.2 and 25 mg l^{-1} calcium concentrations for all experiments. So, calcium concentration affects μ_m in this concentration range.

Stoichiometric Coefficient

The conversion of glucose to biomass can be described by the following stoichiometric equation:

$$24C_6H_{12}O_6 + 59O_2 + 17NH_3 \dashrightarrow 17C_5H_7NO_2 + 59CO_2 + 110H_2O \qquad (25)$$

Equation 25 represents the stoichiometric equation (Busch, 1971) for removal of glucose by a mixed microbial population in a batch reactor which is initially substrate-saturated. The reaction is "complete" when all the substrate is exhausted. The elemental formula $C_5H_7NO_2$ represents the biomass composition for the particular reaction environment. According to Equation 25, one gram of oxygen is required for biochemical conversion of 0.91 g glucose (carbon equivalents) into biomass by the mixed population.

The oxygen uptake data (by Ps. aeruginosa) can be used to calculate the stoichiometric ratio, $Y_{s/o}$, between glucose carbon and oxygen. The stoichiometric-limiting nutrient (glucose) provides a convenient, reproducible end point or final state of microbial reaction process in batch cultures. The plateau in oxygen uptake serves as a marker for the termination of substrate removal.

The stoichiometric ratio, $Y_{s/o}$, can be calculated by dividing input glucose carbon concentration by cumulative oxygen uptake at plateau. $Y_{s/o}$ for various experiments are listed in Table 12. The

results suggest the stoichiometric ratio between glucose and oxygen was not affected by calcium concentration in the medium. The average value for $Y_{s/o}$ was 0.89±0.06 g glucose carbon (g oxygen)$^{-1}$. Thus, $Y_{s/o}$ for Ps. aeruginosa is not significantly different from that obtained by Busch (1971) for mixed populations.

The results suggest that minimum energy required for biochemical conversion of glucose to biomass is independent of calcium concentrations in the medium. However, the rate of biochemical transformation can be influenced by calcium concentrations in the medium.

DISCUSSION

This section discusses the experimental results with specific relevance to biofilm development and compares the findings with other published results.

Elementary Composition of Microorganisms

The chemical composition of the *Ps. aeruginosa* biofilms is compared to biofouling deposits obtained from power plant condensers, laboratory mixed culture biofilms, and suspended cell cultures in Table 14. The data suggest the following:

1. The carbon content of the suspended and immobilized microorganisms obtained under controlled laboratory condition is approximately fifty percent.
2. The composition of the deposit obtained from power plant condenser tubes is low in carbon, probably the result of mineral precipitation and/or inorganic particulates accumulated in the deposit over a long period of time.

It is customary in fermentation and wastewater treatment engineering to express the complex and integrated mixture of intracellular organic molecules in microbial cells by an elemental formula. Various formulae have been proposed to represent the organic composition of microbial cells. One of the oldest and most widely accepted formulae on an ash free basis is $C_5H_7NO_2$ or $CH_{1.4}N_{0.2}O_{0.4}$ (Grady and Lim, 1980),

Table 14. Chemical Composition of Various Biofilms and Suspended Cultures.

	% of Dry Weight					
	C	H	N	Fixed Solids	Volatile Solids	References
Ps. aeruginosa biofilm	53.1	6.1	12.4	13.3	86.7	This study
Mixed culture biofilm	42.8	-	10.0	20.0	80.0	Characklis, 1980
Power plant condenser	6.4-13.8	-	0.51-3.0	-	-	Characklis, 1980
S. cervisiae	45.0	6.8	9.0	8.6	91.4	Wang et al., 1976
Pseudomonas $C_{12}B$	45.6	6.7	12.7	3.0	97.0	Wang et al., 1976
C. utilis	46.9	7.2	10.2	7.0	93.0	Herbert, 1976
Kl. aerogenes	48.9	7.1	12.3	3.6	96.4	Herbert, 1976
Power plant condenser	18.5	2.5	3.1	-	-	*
Simulated test heat exchanger	5.1	1.3	0.7	83.6	16.4	*

* Analysis of samples obtained from titanium tubes carrying Hudson River water at New York Power Authority plant site (1985).

Table 15. Elemental Composition of Biofilm (Ash Free Basis).

Expt #	Calcium mg l^{-1}	C %	H %	N %	O[@] %	Elemental formula for biomass
5	25.0	55.46	8.07	14.20	22.25	$CH_{1.75}N_{0.22}O_{0.30}$
6	50.0	55.28	7.82	14.86	22.03	$CH_{1.70}N_{0.23}O_{0.30}$
6*	50.0	55.31	7.95	14.85	21.88	$CH_{1.72}N_{0.23}O_{0.30}$
7	0.4	54.99	7.97	14.33	22.70	$CH_{1.74}N_{0.22}O_{0.31}$
Average		55.26	7.95	14.56	22.23	$CH_{1.73}N_{0.23}O_{0.30}$

* Analysis of biofilm left on the surface after EGTA addition.

[@] By difference.

Table 16. Elemental Composition for Biomass of Various Sources.

Organism	% of ash free weight				Elemental formula	References
	C	H	N	O		
C. utilis	50.4	7.7	5.8	36.1	$CH_{1.83}N_{0.10}O_{0.54}$	Herbert, 1976
C. utilis	46.9	7.3	10.8	35.1	$CH_{1.87}N_{0.20}O_{0.56}$	Herbert, 1976
C. utilis	50.4	7.7	11.0	31.0	$CH_{1.83}N_{0.19}O_{0.46}$	Herbert, 1976
C. utilis	46.9	7.3	11.0	34.9	$CH_{1.87}N_{0.20}O_{0.56}$	Herbert, 1976
Kl. aerogenes	50.6	7.4	13.0	29.0	$CH_{1.75}N_{0.22}O_{0.43}$	Herbert, 1976
Kl. aerogenes	50.0	7.2	14.1	28.7	$CH_{1.73}N_{0.24}O_{0.43}$	Herbert, 1976
Kl. aerogenes	50.7	7.4	10.1	31.8	$CH_{1.75}N_{0.17}O_{0.47}$	Herbert, 1976
Kl. aerogenes	50.0	7.2	14.1	28.7	$CH_{1.73}N_{0.24}O_{0.43}$	Herbert, 1976
S. cerevisiae	49.3	6.7	9.8	34.2	$CH_{1.64}N_{0.16}O_{0.52}$	Harrison, 1967
S. cerevisiae	47.7	7.3	9.4	35.6	$CH_{1.83}N_{0.17}O_{0.56}$	Kok and Roels, 1980
S. cerevisiae	49.3	7.4	9.8	33.5	$CH_{1.81}N_{0.17}O_{0.51}$	Wang et al., 1976
P. denitrificans	48.4	7.3	11.4	32.9	$CH_{1.81}N_{0.20}O_{0.51}$	Stouthamer, 1977
P. denitrificans	51.0	6.4	11.3	31.3	$CH_{1.51}N_{0.19}O_{0.46}$	Shimizu et al., 1978
E. coli	48.1	7.1	13.4	31.4	$CH_{1.77}N_{0.24}O_{0.49}$	Bauer and Ziv, 1976
Pseudomonas $C_{12}B$	47.0	7.8	12.6	32.6	$CH_{2.00}N_{0.23}O_{0.52}$	Mayberry et al., 1968
A. aerogenes	45.9	7.0	13.4	33.7	$CH_{1.83}N_{0.25}O_{0.55}$	Mayberry et al., 1968
Ps. aeruginosa	55.3	7.9	14.6	22.2	$CH_{1.73}N_{0.23}O_{0.30}$	This study

but many others have been reported (Table 16). The carbon, hydrogen, and nitrogen content (ash free basis) of the Ps. aeruginosa biofilm obtained from the annular reactor is reported in Table 15. The overall elemental composition of the biofilm developed under different calcium concentrations is the same. The average composition of Pseudomonas aeruginosa biofilm can be represented by the elemental formula $CH_{1.7}N_{0.2}O_{0.3}$.

The elemental formulae for the Ps. aeruginosa biofilm and relevant suspended cultures vary considerably as reported in Table 16. One of the difficulties in assessing the composition of the microbial cellular mass is the definition of biomass. In most published results and in this study, biomass includes cellular mass plus any polymeric products that are intimately associated with the cells, such as extracellular polysaccharides in the capsule or slime layer. In this research glucose was the sole carbon and energy source and the limiting nutrient. Changes in limiting nutrient, carbon source, or microbial species may affect the relative amounts of extra- and intracellular components thus significantly influencing the overall elemental composition of the biomass.

Biofilm Calcium

Biofilm calcium increases with increasing calcium concentration in the dilution water (Figure 12). The biofilm calcium reported in Figure 12 does not discriminate between intracellular calcium and calcium immobilized within the extracellular matrix. Calcium is not generally accumulated in the cytoplasm by "normal" growing cells and appears to

be exclusively extracellular (Belliveau and Lanyi, 1978; Silver, 1978; Wacker and William, 1968). Campbell (1983) reported that the concentration of total calcium in the cytoplasm is usually in the range of 1-10 mmole per liter of cell water. Harvey et al. (1984) reported that the concentration of calcium in the extracellular matrix of an anaerobic biofilm was approximately 100 times greater than in the cell. The maximum concentration of intracellular calcium in the biofilm cells developed under 50, 25 and 0.4 $mg \cdot l^{-1}$ calcium was estimated to be 0.95, 0.78 and 0.45 mg calcium per gram of dry biofilm mass, respectively. The estimated values of intracellular calcium were significantly smaller than the values of biofilm calcium reported in Figure 12 for all calcium concentrations. Hence, a major portion of biofilm calcium reported in this study (Figure 12) can be assumed to represent calcium immobilized in the extracellular polymer matrix.

The extracellular polymers are involved in selective accumulation of ions in many gram-negative bacteria (Galanos et al., 1977; Leive, 1974; Buckmire, 1983). The lipopolysaccharide of gram-negative bacteria contains a number of potential cation binding sites (Schindler and Osborn, 1979, Galanos et al., 1977) having a high affinity for calcium and magnesium. Sukenik et al. (1985) examined a flocculated algal culture using energy dispersive X-ray analysis and reported the presence of calcium and phosphorous in the flocculated culture. Stahl et al. (1983) reported that the presence of calcium in the medium causes flocculation in yeast.

Bacterial extracellular polymers are also of considerable importance in the adsorption/retention of certain heavy metals by

activated sludge. The polymers are important to the heavy metal uptake capacity of activated sludge. Brown and Lester (1979) have shown that the extracellular polymers of several species of gram-negative bacteria in activated sludge are involved in the adsorption of exogenous heavy metal ions from solution (Brown and Lester, 1979). Aiking et al. (1984) reported that Klebsiella aerogenes NCTC 418 growing in the presence of cadmium in a continuous culture accumulated cadmium up to 5.8% of the bacterial dry weight.

A similar result was obtained with six days old Ps. aeruginosa biofilm (this study) when cadmium was added at a rate of 0.05 mg l^{-1} to the annular reactor for 24 h. After 24 h, the Ps. aeruginosa biofilm contained 3.0 mg cadmium per gram of dry biofilm mass and the concentration of cadmium in the wet biomass was approximately 13000 times greater than that in the dilution water. There was no change in effluent glucose carbon concentration (0.6 mg l^{-1}) as a result of cadmium addition so that cadmium did not affect overall microbial activity.

Specific Substrate Removal Rate

Equation 19 predicts a linear relationship between specific substrate removal rate, q_s, and specific cellular growth rate in the biofilm, μ_b (Figure 33). The y-intercept of the best-fit line is 0.165 (SE = 0.175) and the slope equalled 3.04 (SE = 0.63). Robinson et al. (1984) also obtained a linear relationship between specific substrate removal rate and specific cellular growth, μ, of Ps. aeruginosa in suspended cultures (chemostat data). A t-test was performed on the

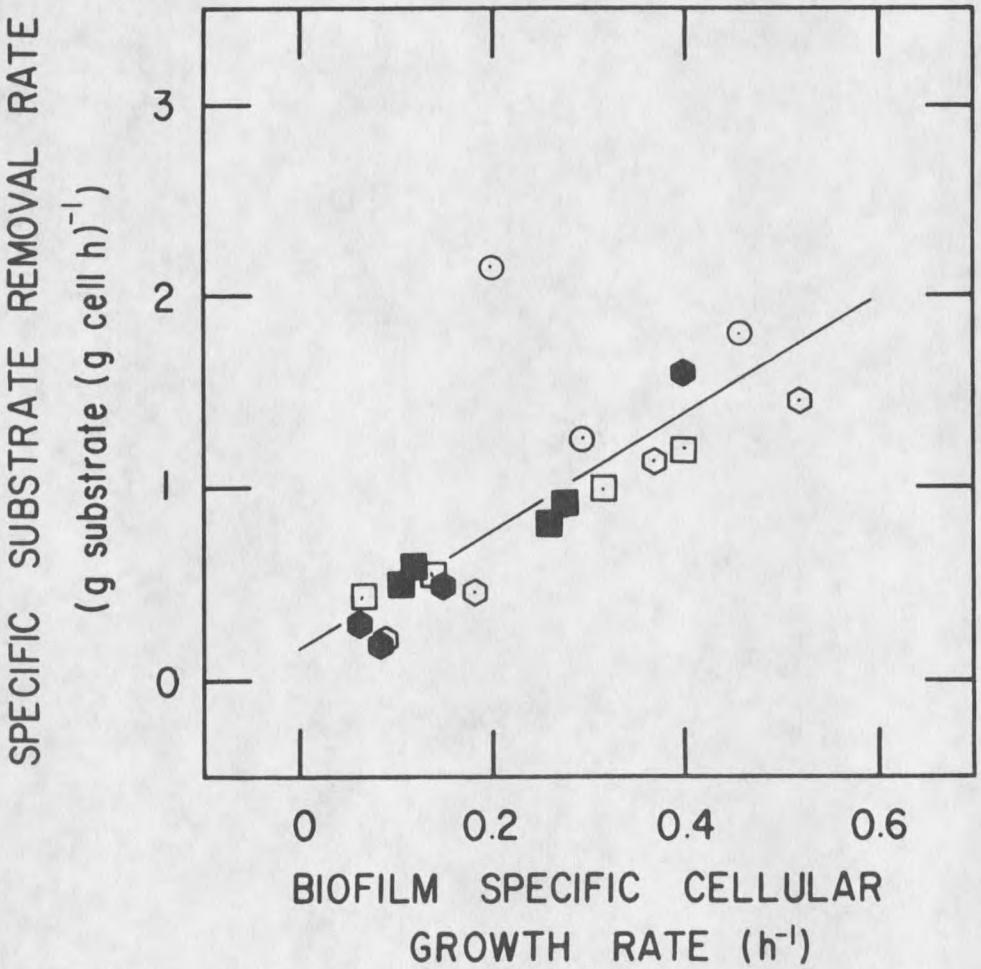

Figure 33. Change in specific substrate removal rate as a function of biofilm specific cellular growth rate. The straight line represents the best-fit described by Equation 19. (⊙,● 50 mg l^{-1}; □,■ 25 mg l^{-1}; and ○ 0.4 mg l^{-1} calcium).

data to statistically determine the correlation between the biofilm data at different calcium concentrations and the chemostat (suspended culture) data reported by Robinson et al. (1984). At the five percent level of statistical significance, there was no difference between the chemostat data and the biofilm data from this study. Similar results were also reported by Bakke et al. (1984) for Ps. aeruginosa biofilm in the annular reactor at 200 rpm.

Results from this study at different calcium concentrations and results reported by Bakke et al. (1984) suggest that metabolic activity of Ps. aeruginosa in biofilms is not significantly different than that in suspended cultures. Hence, the specific cellular growth rate of Ps. aeruginosa in biofilms and/or suspended cultures can be estimated by monitoring the changes in specific substrate removal rate if the biofilm cell concentration is known. One important restriction requires that no significant diffusional resistance exist in the biofilm, which was the case in this study. Another concern requires that the substratum surface not release any toxic components which influence metabolism. In this study, acrylic plastic was the substratum. Also, the soluble substrate should not adsorb to any great extent.

Specific Oxygen Removal Rate

As in the case of specific substrate removal rate, the specific oxygen removal rate, q_o (Equation 21) is also a linear function of specific cellular growth rate in the biofilm, μ_b (Figure 34). The y-intercept of the best-fit line is 0.186 (SE = 0.189) and the slope is 3.25 (SE = 0.69). Thus, the specific cellular growth rate of

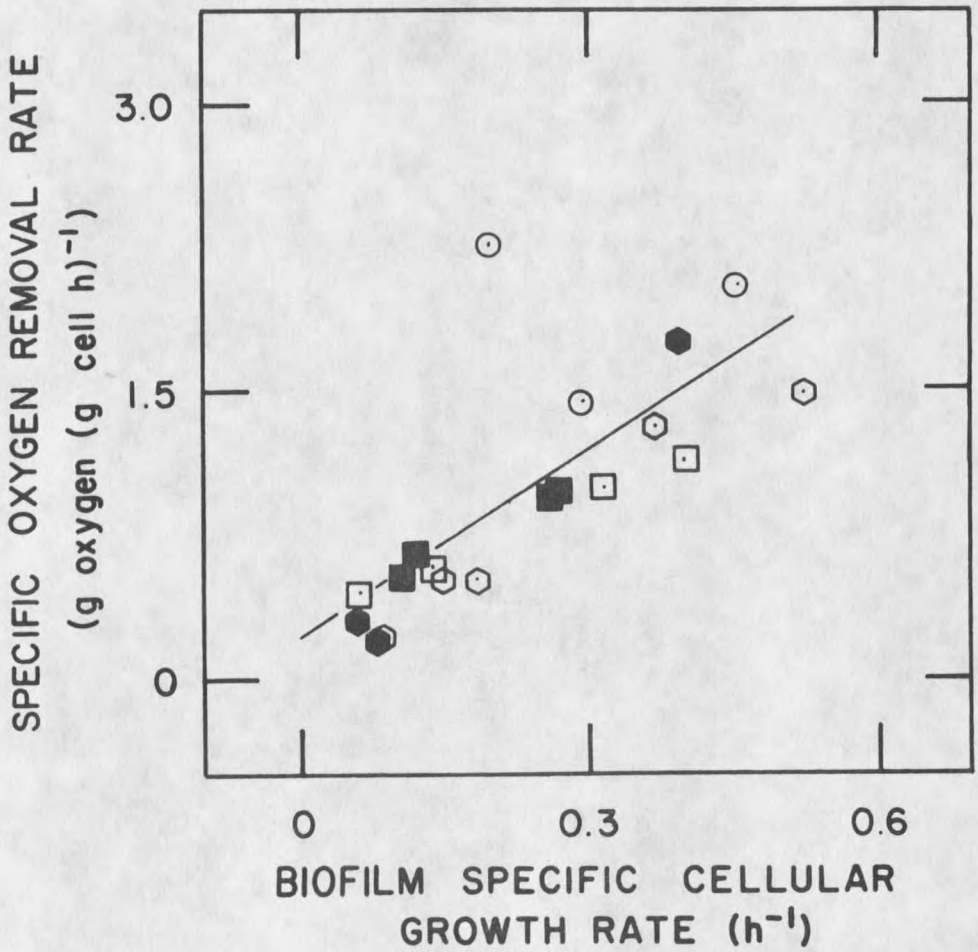

Figure 34. Change in specific oxygen removal rate as a function of biofilm specific cellular growth rate. The straight line represents the best-fit described by Equation 21. (○,● 50 mg l^{-1}; □,■ 25 mg l^{-1}; and ⊙ 0.4 mg l^{-1} calcium).

immobilized Ps. aeruginosa can also be estimated by measuring changes in specific oxygen removal rate.

Specific Cellular Growth Rate

The specific cellular growth rate of Ps. aeruginosa in the biofilm was calculated by dividing biofilm cellular carbon reproduction rate, R_{xb}, by the biofilm cellular carbon concentration, x_b (Figure 17). The result indicates that specific cellular growth rate of Ps. aeruginosa in the biofilm decreases with time, which is not surprising since the same amount of substrate is being consumed by an increasing number of cells.

Trulear (1983) reported that specific cellular growth rate of Ps. aeruginosa in suspended culture is related to substrate concentration and can be described by the Monod (1949) equation:

$$\mu = \frac{\mu_m \; s}{K_s + s} \tag{26}$$

where,

μ_m = maximum specific cellular growth rate (t^{-1})

K_s = saturation constant (ML^{-3})

Trulear (1983) calculated μ_m and K_s for Ps. aeruginosa from suspended culture data using a linearized form of Equation 26 (Lineweaver-Burk equation). The maximum specific growth rate, μ_m, was reported (Trulear, 1983) to be 0.4 h^{-1} (SE = 0.02) and saturation constant, K_s, was 2.03 mg l^{-1} (SE = 0.78). In Figure 35, the biofilm specific cellular growth rate, μ_b, is presented as a function of reactor

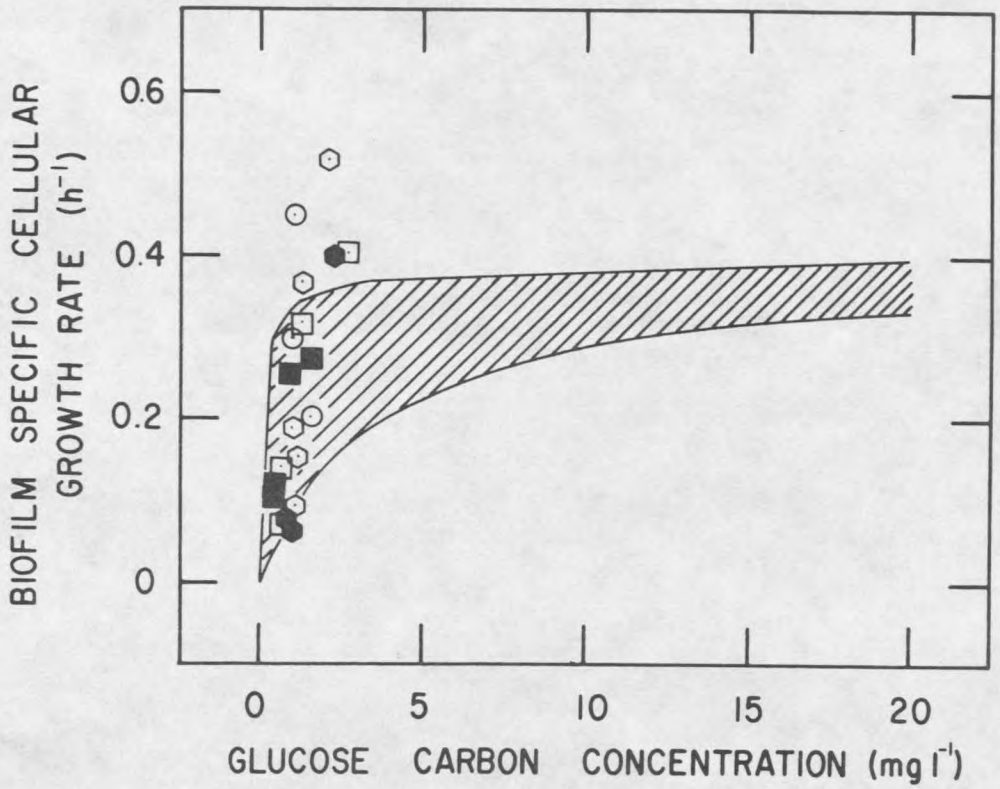

Figure 35. Plot of biofilm specific cellular growth rate as a function of glucose carbon concentration. The shaded portion represents the 95 percent confidence interval of the Monod equation based on parameters (μ_m and K_s) estimated by Trulear (1983) for Ps. aeruginosa in suspended culture. (○,●50 mg l^{-1}; □,■ 25 mg l^{-1}; and ⊙ 0.4 mg l^{-1} calcium).

substrate concentration, s. The shaded portion in Figure 35 represents the 95 percent confidence interval of the Monod equation based on growth parameters μ_m and K_s estimated by Trulear (1983) for Ps. aeruginosa in suspended culture. Thus, the cellular growth rate in the biofilm, within the narrow range of substrate concentration tested, can be estimated by growth parameters reported by Trulear (1983) for suspended culture. Trulear (1983) reported that cellular reproduction by Ps. aeruginosa in the biofilm can be described by the growth parameters (μ_m and K_s) estimated from suspended culture. The biofilm data outside the shaded region were obtained during the initial period (48-70 h) of the experiments in this study. The specific cellular growth rate of Ps. aeruginosa in the biofilm calculated for this initial period was greater than or equal to the maximum specific cellular growth rate of Ps. aeruginosa reported in the literature (Jenkins, 1980; Trulear, 1983). During this initial period, however, accurate measurement of biofilm cellular carbon concentration is difficult because there is less than 80 mg cellular carbon m^{-2} on the surface. Alternatively, it is possible that cells on the surface during the initial period are more "active" due to the high substrate flux into the system.

Calcium is required for growth of many, and probably all, bacterial species (Shooter and Wyatt, 1955; Shankar and Bard, 1952; Campbell, 1983, Weinberg, 1977). Calcium is known to be required for stability and/or maximal activity of several enzymes in both eucaryotes and procaryotes (Campbell, 1983). Results from this study indicate that the maximum specific growth rate, μ_m, for Ps. aeruginosa

(suspended culture) in the presence of 25 mg l^{-1} calcium was approximately 16% higher than with calcium at 3.2 mg l^{-1}. Hence, higher biofilm cellular accumulation in the presence of 25 and 50 mg l^{-1} calcium in the dilution water, as compared to 0.4 mg l^{-1} calcium, may be partly due to the difference in maximum specific cellular growth rate of Ps. aeruginosa in the biofilm. Results from a separate study (Appendix G) also indicate that EGTA or free calcium affected the maximum specific growth rate of Ps. aeruginosa (Table 17). Most reports on calcium requirement for cellular growth compare the cell crop in the absence of calcium to cell crop in the presence of calcium by measuring the differences in light absorbance of the cellular suspension at a predetermined time. There is little or no information on the effect of calcium on maximum specific cellular growth rate in published reports, especially in open or continuous flow systems. The mechanism by which calcium affects the specific growth rate is not known and needs further investigation.

Table 17. Effect of EGTA (or Free Calcium) on Maximum Specific Growth Rate of Pseudomonas aeruginosa.

EGTA added molar	Log (free calcium) molar	μ_m h^{-1}
0.000	-5.82*	0.3925 ± 0.0064
0.002	-8.77	0.2831 ± 0.0077
0.004	-9.15	0.2621 ± 0.0034
0.006	-9.35	0.2572 ± 0.0057

Total calcium in the medium 2 mg l^{-1}.
*Measured with specific ion electrode.

Cellular Detachment Rate

The progression of biofilm cellular carbon for three different calcium concentrations in the dilution water is presented in Figure 10. Cellular carbon accumulation is the net result of two different processes, (a) growth and reproduction at the surface and (b) cellular detachment from the surface. Results reported in the previous section suggest that calcium affects the maximum specific growth rate of *Ps. aeruginosa*.

This section describes the effect of calcium on cellular detachment rate. In Figure 36, the ratio of specific cellular detachment rate to specific cellular reproduction rate is plotted as a function of time for three different calcium concentrations in the dilution water. This ratio represents the fraction of cells produced at the surface which detach. At steady state, specific cellular detachment rate equals specific cellular reproduction rate and the ratio will be unity. The data indicate that a major portion (greater than 92%) of the attached cells growing under 0.4 and 25 mg l^{-1} calcium are detaching and the system is approaching a steady state. The cellular carbon accumulation rate (dx_b/dt) at 0.4 and 25 mg l^{-1} calcium also seems to be approaching zero state (Figure 10). A lesser fraction of cells at 50 mg l^{-1} calcium detach (as little as 72%). This might be due to the fact that (a) cellular accumulation rate (within the experimental period) at 50 mg l^{-1} was increasing exponentially with time (Figure 10) and (b) specific cellular growth rate was significantly greater than specific cellular detachment rate. Thus, cells accumulating at

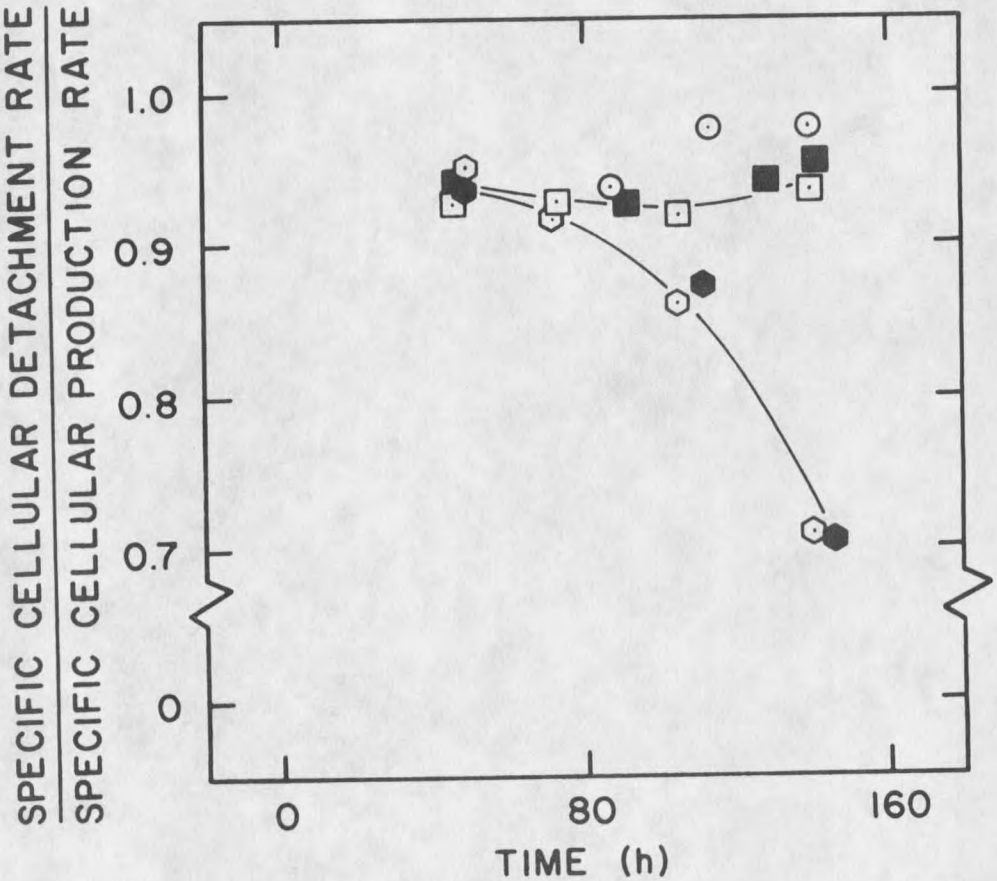

Figure 36. Ratio of specific cellular detachment rate to specific cellular production rate as a function of time. Lines drawn by observation. (○,● 50 mg l^{-1}; □,■ 25 mg l^{-1}; and ⊙ 0.4 mg l^{-1} calcium).

50 mg l^{-1} calcium tend to stay or "stick" to a greater extent. Thus, cellular detachment appears to be influenced by calcium concentration and may be controlling the biofilm accumulation rate. Understanding biofilm detachment is, therefore, not only necessary to predict biofilm behavior, but may serve as a means to control biofilm activity or accumulation.

Biofilm detachment can also be imposed through changes in the biofilm environment. Immediate detachment of Ps. aeruginosa and mixed culture biofilm was observed when the free calcium in the biofilm (this study) was altered by chelant addition. Detachment was presumably caused by removal of calcium important in the biofilm structure.

Specific Polymer Production Rate

Specific polymer production rate is a linear function of specific cellular growth rate in the biofilm (Figure 37) as described by Equation 9. The growth associated polymer rate coefficient, k_b, is 2.07 mg polymer carbon/mg glucose carbon (SE = 0.39), and the non-growth associated polymer coefficient, k'_b, is -0.02 mg polymer carbon/mg glucose carbon/h (SE = 0.11). The non-growth associated polymer formation coefficient, k'_b, can be assumed to be negligible as compared to the growth associated polymer coefficient, k_b.

Robinson et al. (1984) reported that polymer production by Ps. aeruginosa in a suspended culture was growth and non-growth associated. The growth associated polymer coefficient (0.27 mg polymer carbon/mg glucose carbon) for Ps. aeruginosa in suspended culture reported by Robinson et al. (1986) was much smaller than that obtained for

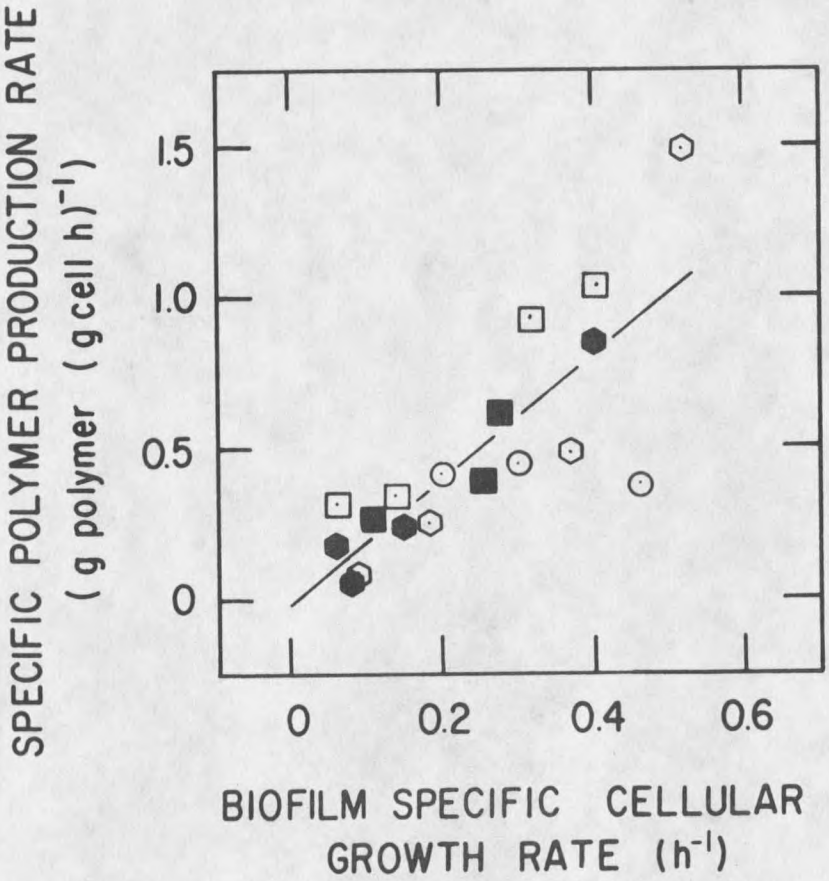

Figure 37. Plot of specific polymer production rate as a function of biofilm specific cellular growth rate. The straight line represents the best-fit described by Equation 9. (○,● 50 mg l^{-1}; □,■ 25 mg l^{-1}; and ⊙ 0.4 mg l^{-1} calcium).

immobilized culture from this study. This result suggests that Ps. aeruginosa may increase its polymer production rate when it is immobilized.

Stoichiometric Coefficients

The conversion of glucose into biomass can be described by the following equation (Busch, 1971):

$$24C_6H_{12}O_6 + 59O_2 + 17NH_3 \dashrightarrow 17C_5H_7NO_2 + 59CO_2 + 110H_2O \qquad (25)$$

Equation 25 represents the stoichiometric equation for the removal of glucose by a mixed microbial population in a batch reactor which is initially substrate saturated. According to Equation 25, one gram of oxygen is required for biochemical conversion of 0.91 g glucose (carbon equivalents) into biomass by mixed populations.

The stoichiometric ratio, $Y_{s/o}$, between glucose and oxygen for biochemical conversion of glucose into biomass by immobilized Ps. aeruginosa, in a continuous flow system, was obtained by plotting (Figure 38) specific substrate removal rate, q_s, as a function of specific oxygen removal rate, q_o. The slope of the estimated line is the stoichiometric ratio expressed as a g glucose carbon (g oxygen)$^{-1}$. The y-intercept of the best-fit line was 0.002 (SE = 0.025) and the slope equalled 0.92 (SE = 0.02). This result suggests that the stoichiometric relation between glucose and oxygen was constant and was independent of time, biofilm cellular mass, calcium concentrations in the dilution water, and the biofilm cellular growth rate.

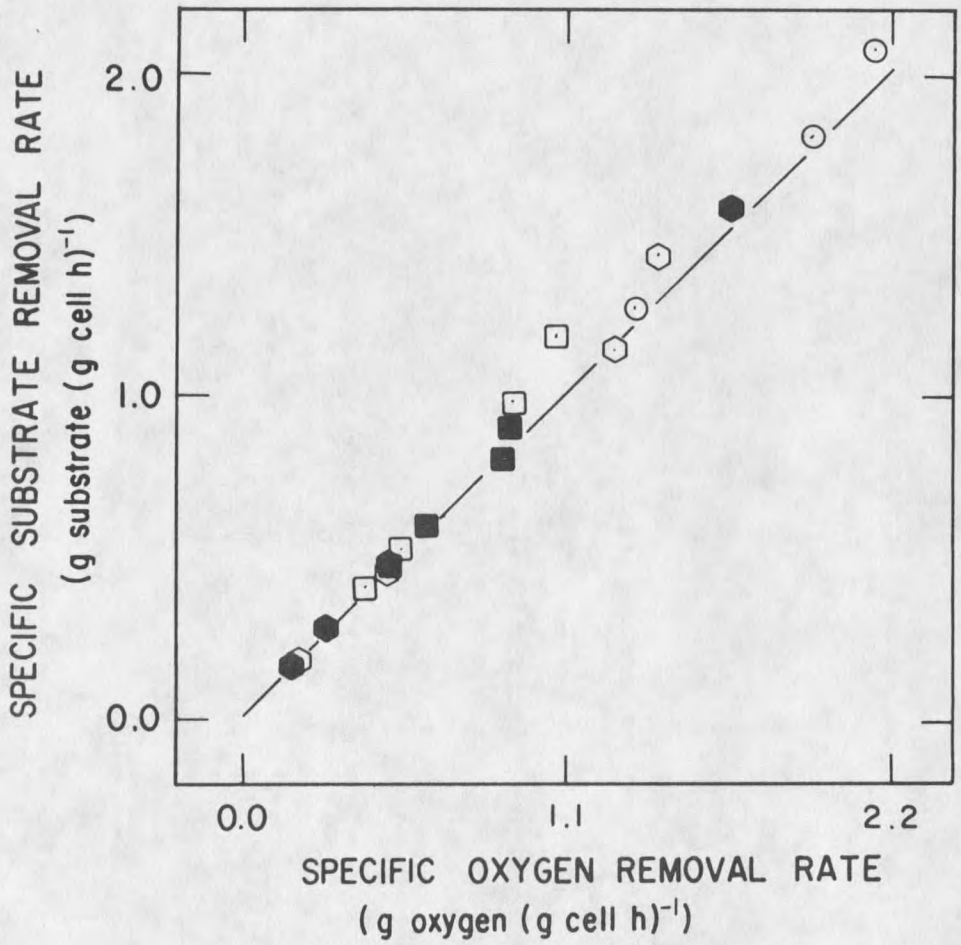

Figure 38. Change in specific substrate removal rate as a function of specific oxygen removal rate. The straight line represents the best linear fit. (○,● 50 mg l^{-1}; □,■ 25 mg l^{-1}; and ○ 0.4 mg l^{-1} calcium).

The stoichiometric coefficient, $Y_{s/o}$, obtained in the continuous flow, Ps. aeruginosa biofilm reactor (0.92 ± 0.02) was not significantly different from that obtained in batch culture (0.89 ± 0.06) of Ps. aeruginosa. This suggests that the minimum energy required for biochemical conversion of glucose into mass by suspended or immobilized cultures of Ps. aeruginosa is the same and is independent of calcium concentration. Also, the stoichiometric coefficient, $Y_{s/o}$, for Ps. aeruginosa was not significantly different from that obtained by Busch (1971) for an undefined mixed microbial population.

Substrate Diffusion

Since substrate is required for processes of cellular reproduction and extracellular polymer formation, the diffusion rate of substrate into the biofilm may be important. The linear relationship through the origin between specific substrate removal rate and specific oxygen removal rate (Figure 38) suggests that there was no significant substrate diffusional resistance through the Ps. aeruginosa biofilm at any calcium concentrations. Oxygen was assumed to be in excess because (1) the input water was saturated, (2) the annular reactor was operated at a residence time of 10 min, and (3) the transfer of oxygen from the ambient air to the acrylic annular reactor was significant and, thus, provided a continuous oxygen supply (Appendix F). Trulear (1983) reported that diffusion resistance of substrate through Ps. aeruginosa biofilm in the annular reactor at 200 rpm under glucose limitation was minimal.

Significant substrate diffusional resistance in mixed culture biofilms has been reported in the literature (Kornegay and Andrews, 1967; Lamotta, 1976; Hoehn and Ray, 1973). The results from this study and Trulear (1983) are contrary to results reported in the literature. An explanation of this apparent disagreement is due to the fact that (1) Ps. aeruginosa biofilm was developed in a well mixed annular reactor operated at low substrate concentration and (2) the mixed culture biofilms were considerably thicker (up to 1300 μm) as compared to the maximum biofilm thickness of 40 μm reported by Trulear (1983) for Ps. aeruginosa biofilm under similar operating conditions as in this study. Biofilm thickness was not measured in this study.

The results of this study suggest that substrate diffusion through the biofilm was not rate-limiting at any calcium concentration in the dilution water.

Calcium and Biofilm Structure

The addition of EGTA to Ps. aeruginosa and mixed culture biofilms resulted in the immediate detachment of a portion of biofilm from the surface. The detachment of biofilm material was presumably caused by removal of calcium important to the biofilm structure. Fletcher and Floodgate (1976) reported the disaggregation of extracellular polymer substances when attached microcolonies of a marine pseudomonad were transferred to media deficient in calcium and magnesium. Transmission electron microscopic analyses showed the condensed globules of EPS in the intercellular space after being fixed and stained with ruthenium red. A similar result was obtained in this study when a contiguous

portion of mixed culture biofilm from the tubular reactor was scraped from the surface and suspended in the growth media. Disaggregation of bioflocs was also observed when buffered EGTA was added to suspended biofilm flocs (mixed culture). Fletcher (1980) suggests that calcium may act as a cross-linking or charged screening agent for the ionic groups in the extracellular polymer substances. The results from this study suggest that calcium helps maintain the tertiary structure of these substances so that the interaction between adjacent sugars on different chains is promoted.

It is possible that other multivalent cations may also be important to the structure of the biofilm. The importance of magnesium to the biofilm structure can be determined by comparing the difference in the amount of biomass detached by the addition of EGTA and EDTA to Ps. aeruginosa biofilm developed under 0.4 mg l^{-1} calcium in the dilution water (Experiments 3 and 4, AR #7). Since EDTA is not a calcium specific chelant, the detachment of biofilm with EDTA might be connected with chelation of less strongly bound cations, such as magnesium, as well as calcium. The amount of biofilm detached as a result of EDTA addition (Experiment 4: AR #7) was slightly less than (Table 9) that detached by the addition of EGTA (Experiment 3; AR #7). Hence, it is unlikely that magnesium contributes significantly to the structural integrity of the biofilm. Since not all the biofilm is removed by chelant addition, other cohesive and adhesive mechanisms must exist.

It is unlikely that calcium is involved in direct bridging to a negatively charged substratum since some bacterial cells remained on

the surface after EGTA addition. Results from a separate study reported herein (Appendix H; Table 18) and those obtained by Fletcher (1980) also suggest that calcium is not involved in the direct bridging of cells to the negatively charged substratum.

Table 18. Experimental Results from Adsorption Studies Using *Pseudomonas* 224S.

	PCFU/field			
	Control slides		EGTA treated slides	
Expt. #	Slide number #1	#2	#3	#4
1	10.5±1.8	9.6±2.6	10.5±2.0	10.4±1.7
2	6.7±2.3	6.9±1.6	7.5±2.1	6.8±1.7

Calcium has been shown to be necessary for adsorption of aquatic bacteria (Marshall et al., 1971; Fletcher and Floodgate, 1973; Stanley, 1983). Fletcher (1980) observed that the adsorption of a marine pseudomonad was inhibited by the presence of EDTA, suggesting that the chelant removed surface-bound divalent cations conceivably involved in intercellular-ionic bridging. In experiments reported herein (Table 17), there was no visual evidence of *Ps. aeruginosa* adsorbed to batch growth flasks when grown in presence of EGTA. However, there was visual evidence that cells were adsorbed to the batch growth flasks which did not contain EGTA. The observation indicates that calcium was necessary for adsorption of *Ps. aeruginosa* to the glass surface.

CONCLUSIONS

The following conclusions can be drawn from this experimental study with *Ps. aeruginosa* biofilm within the range of the experimental conditions tested:

1. Calcium increases the rate and extent of biofilm mass accumulation.
2. Calcium increases the rate and extent of biofilm cellular carbon accumulation.
3. Calcium concentration in the biofilm increases with increasing calcium in the dilution water.
4. The elemental composition of the biofilm was not affected by increasing calcium concentration in the dilution water.
5. The stoichiometric ratio between glucose and oxygen for biochemical conversion of glucose into biomass by suspended or immobilized culture of *Ps. aeruginosa* was constant and was independent of time, cellular mass, calcium concentration in the medium, and specific cellular growth rate.
6. The specific substrate and oxygen removal rate in the low calcium (0.4 mg l^{-1}) experiment was higher than that in high calcium (25 and 50 mg l^{-1}) experiments.
7. Calcium contributes to the cohesiveness of *Ps. aeruginosa* and mixed culture biofilms.
8. EGTA and/or EDTA can remove a portion of established biofilms.

9. EGTA and/or EDTA did not affect overall microbial substrate utilization and, thus presumably, microbial activity in the biofilm.

LITERATURE CITED

LITERATURE CITED

Aiking, H., A. Stijnman, C. van Garderen, H. Van Heerikhuizen, and J. van't Riet. 1984. Inorganic phosphate accumulation and cadmium detoxification in Klebsiella aerogenes NCTC 418 growing in a continuous culture. Appl. Environ. Microbiol. 47:374-377.

Baier, R. E. 1975. Applied chemistry at protein surfaces, p. 1-25. In R. E. Baier (ed.), Advances in Chemistry Series, 145. American Chemical Society, Washington, D. C.

Baier, R. E., and L. Weiss. 1975. Applied chemistry at protein surfaces, p. 300-307. In R. E. Baier (ed.), Advances in Chemistry Series, 145. American Chemical Society, Washington, D. C.

Baier, R. E., and V. A. Depalma. 1977. Microfouling of metallic and coated metallic flow surfaces in model heat exchanger cells, Calspan Corporation Report, Buffalo, NY.

Baier, R. E. 1980. p. 59-104. In G. Bitton and K. C. Marshall (ed.), Adsorption of Microorganisms to Surfaces. John Wiley & Sons, Inc., New York.

Bakke, R. 1983. Dynamics of biofilm processes: substrate load variation, p. 53. M. S. Thesis, Montana State University, Bozeman.

Bakke, R., M. G. Trulear, J. A. Robinson, and W. G. Characklis. 1984. Activity of Pseudomonas aeruginosa in biofilms: steady state. Biotech. Bioeng. 26:1418-1424.

Bakken, L. R., and R. A. Olsen. 1983. Buoyant densities and dry matter contents of microorganisms: conversion of a measured biovolume into biomass. Appl. Environ. Microbiol. 45:1188-1195.

Bauer, S., and E. Ziv. 1976. Dense growth of aerobic bacteria in a benched-scale fermentor. Biotech. Bioeng. 18:81-94.

Bell, R. G., and D. J. Lantham. 1975. Influence of sodium chloride calcium ion and magnesium ion in the growth of marine Bdellovibrio sp. Estuarine Coastal Mar. Sci. 3:381-384.

Belliveau, J. W., and J. S. Lanyi. 1978. Calcium transport in Halobacterium halobium envelope vesicles. Arch. Biochem. Biophys. 186:89-105.

Brock, T. D. 1979. Biology of microorganisms, p. 802. Prentice Hall, Inc., Englewood Cliffs, NJ.

Brown, M. R., J. H. S. Foster, and J. R. Clamp. 1969. Composition of Pseudomonas aeruginosa slime. Biochem. J. 112:521-525.

Brown, M. J., and J. N. Lester. 1979. Metal removal in activated sludge: the role of bacterial extracellular polymers. Water Res. 13:817-837.

Buchanan, R. E., and N. E. Gibbon. 1974. Bergey's Manual of Determinative Bacteriology, p. 221-222. The Williams and Wilkins Co., Baltimore.

Buckmire, F. L. A. 1983. Selective accumulation of ions in cellular components of individual cells within colonies of Pseudomonas aeruginosa. Microbiol. Lett. 151-162.

Busch, A. W. 1971. Aerobic biological treatment of waste water. Oligodynamics Press, Houston, TX.

Campbell, A. K. 1983. Intracellular calcium: its universal role as regulator, p. 556. John Wiley & Sons Limited, New York.

Carlson, D. M., and L. W. Mathews. 1966. Polyuronic acids produced by Pseudomonas aeruginosa. Biochemistry 5:2817-2822.

Characklis, W. G. 1980. Biofilm development and destruction: final report, p. 250. Electric Power Research Institute, Palo Alto.

Characklis, W. G. 1981. Fouling biofilm development: a process analysis. Biotech. Bioeng. 23:1923-1960.

Cooksey, B., and K. E. Cooksey, 1980. Calcium is necessary for motility in diatom Amphora coffeaeformis. Plant Physiol. 65:129-131.

Cooksey, K. E. 1981. Requirement for calcium in the adhesion of a fouling diatom to glass. Appl. Environ. Microbiol. 41:1378-1382.

Corpe, W. A. 1964. Factors influencing growth and polysaccharide formation by strains of Chromobacterium violaceum. J. Bacteriol. 88:1433-1441.

Corpe, W. A., L. Matsuuchi, and B. Armbuster. 1976. In J. M. Sharpley and A. M. Kalpan (ed.), Proceedings of the Third International Biodegradation Symposium, p. 433-422. Applied Science, London.

Costerton, J. W. 1979. Pseudomonas aeruginosa in nature and diseases, p. 15-24. Proceedings of Pseudomonas aeruginosa International Symposium, Boston.

Couperwhite, I., and M. F. McCallum. 1974. The influence of EDTA on the composition of alginate synthesized by Azobacter vinelandii. Archives of Microbiology 97:73-80.

Doetsch, R. N., and T. M. Cook. 1973. Introduction to bacteria and their ecobiology, p. 371. University Park Press, Baltimore.

Drapeau, G. R., and R. A. MacLeod. 1965. Nature. 206-351.

Eagon, R. G. 1956. Studies on polysaccharide formation by Pseudomonas fluorescens. Can. J. Microbiol. 2:673-676.

Eagon, R. G. 1962. Composition of extracellular slime produced by Pseudomonas aeruginosa. Can. J. Microbiol. 8:585-586.

Evans, L. R., and A. Linker. 1973. Production and characterization of the slime polysaccharide of Pseudomonas aeruginosa. J. Bacteriol. 116:915-924.

Fletcher, M., and G. D. Floodgate. 1973. An electron-microscopic demonstration of an acidic polysaccharide involved in the adhesion of a marine bacterium to solid surfaces. J. Gen. Microbiol. 74:325-334.

Fletcher, M. 1980. Adherence of marine microorganisms to smooth surfaces, p. 347-374. In E. H. Beachy (ed.), Receptor and Recognition: Bacterial Receptors. Chapman and Hall, London.

Galanos, C., O. Luderitz, E. T. Reitschel, and O. Westphal. 1977. New aspects of chemistry and biology of bacterial lipopolysaccharides with special reference to their lipids A component. International Review of Biochemistry 14:239-335.

Grady, C. P., Jr., and H. C. Lim. 1980. Biological waste water treatment: theory and applications. p. 962. Marcel Dekker, Inc., New York, NY.

Hanson, R. S., and J. A. Phillips. 1981. Total carbohydrate by phenol reaction, p. 328-364. In P. Gerhardt et al. (ed.), Manuals of Methods of General Bacteriology. American Society for Microbiology, Washington, D. C.

Harrison, J. S. 1967. Process Biochem. 2:41.

Harvey, M., C. W. Forsberg, T. J. Beveridge, J. Pos, and J. R. Ogilvie. 1984. Methanogenic activity and structural characteristics of the microbial film on a needle-punched polyester support. Appl. Environ. Microbiol. 48:633-638.

Herbert, D. 1976. In A. C. R. Dean et al. (ed.), Continuous Culture 6, Applications and New Fields. Society of Chemical Industry, London.

Hobbie, J. E., R. J. Daley, and S. Jasper. 1977. Use of Nuclepore filters for counting bacteria by fluorescence microscopy. Appl. Environ. Microbiol. 35:858-862.

Hoehn, R. C., and A. D. Ray. 1973. Effects of thickness on bacterial film. J. Water Poll. Control Fed. 45:2302-2320.

Hojeberg, B., and J. Rydstrom. 1977. Ca^{2+}-dependent allosteric regulation of nucleotide transhydrogenase from Pseudomonas aeruginosa. Eur. J. Biochem. 77:235-241.

Howell, J. A., and B. Atkinson. 1976. Sloughing of microbial film in trickling filters. Water Res. 18:307-315.

Huang, J. C. C., and M. P. Starr. 1973. Effects of calcium and magnesium ions and host viability on growth of Bdellovibrios. Antonie van Leeuwenhoek 39:151-167.

Hunter, S. A. 1972. Inorganic nutrition. Annu. Rev. Microbiol. 26:311-346.

Jenkins, D. 1980. Activated sludge floc structure and its relation to process performance. National Science Foundation: Final Report, Washington, D. C., Project No. CME-768442.

Kenward, M. A., M. R. W. Brown, and J. J. Fryers. 1979. The influence of calcium or magnesium on the resistance to EDTA, or cold shock, and the composition of Pseudomonas aeruginosa grown in glucose- or magnesium-depleted batch cultures. J. Appl. Bacteriol. 47:489-503.

Kok, H. E., and J. A. Roels. 1980. Methods for statistical treatment of elemental and energy balances with application to steady-state continuous-culture growth of Saccharomyces cerevisiae CBS 426 in respiratory region. Biotech. Bioeng. 22:1097-1104.

Kornegay, B. H., and J. F. Andrews. 1967. Characteristics and kinetics of biological film reactors. Federal Water Pollution Control Administration Final Report, Research Grant WP-01181, Department of Environmental Systems Engineering, Clemson University, Clemson, SC.

Lamotta, E. J. 1976. Kinetics of growth and substrate uptake in a biological film system. Appl. Environ. Microbiol. 18:1359-1370.

Larsen, B., and A. Haug. 1971. Biosynthesis of alginate. Part I: Composition and structure of alginate produced by Azobacter vinelandii. Car. Res. 17:287-296.

Leive, L., V. K. Schoucin, and S. E. Mergenhagen. 1969. Physiological, chemical, and immunological properties of lipopolysaccharides released from E. coli by EDTA. J. Biol. Chem. 243:6384-6391.

Leive, L. 1974. The barrier function of gram-negative cell envelope. Annals of the New York Academy of Sciences. 235:109-129.

Loeb, G. I., and R. A. Neihof. 1975. Marine conditioning films, p. 319-335. In R. E. Baier (ed.), Applied Chemistry at Protein Interfaces. Amer. Chem. Soc., Advances in Chemistry Series 145, Washington, D. C.

Levine, B. A., and R. J. P. William. 1984. Calcium binding to proteins and anion centers, p. 3-55. In G. Spiro (ed.), Calcium in Biology. John Wiley & Sons Limited, New York.

Linker, A., and R. Jones. 1964. A polysaccharide resembling alginic acid from a Pseudomonas microorganism. Nature. 204:187-189.

Linker, A., and L. R. Evans. 1976. Unusual properties of glycurons [poly(glycosyluronic) compounds]. Car. Res. 47:179-187.

Luedeking, R., and E. L. Piret. 1959. A kinetic study of the lactic acid fermentation-batch processes at controlled pH. J. Biochem. Microbiol. Tech. Engrg. 1:393-412.

Lund, D. B., and C. Sandu. 1981. State-of-the art of fouling: heat transfer surfaces, p. 27-56. In B. Hallstrom, D. B. Lund, and Ch. Tragardh (ed.), Fundamentals and applications of surface phenomena associated with fouling and cleaning in food processing. Lund University, Tylosand, Sweden.

Luria, S. E. 1960. The bacterial protoplasm: composition and organization, p. 1-31. In I. C. Gunsalus and R. Y. Stanier (ed.), The Bacteria, Vol. 1: Structure. Academic Press, Inc., New York.

Marshall, K. C., R. Stout, and R. Mitchell. 1971. Mechanism of the initial events in the sorption of marine bacteria to surfaces. J. Gen. Microbiol. 68:337-348.

Marshall, K. C. 1979. p. 281-290. In M. Shilo (ed.), Strategies of microbial life in extreme environments. Dahlem Konferenzen Life Sciences Research Report 13, Varlag Chemie, Weinheim.

Mayberry, W. R., G. J. Prochazka, and W. J. Payne. 1968. Factors derived from studies of aerobic growth in minimal media. J. Bacteriol. 96:1424-1426.

Mian, F. A., T. R. Jarman, and R. C. Righelato. 1978. Biosynthesis of exopolysaccharide by Pseudomonas aeruginosa. J. Bacteriol. 134:418-422.

Monod, J. 1949. The growth of bacterial culture. Ann. Rev. of Microbiol. 3:371-394.

Moscona, A. A. 1968. Dev. Biol. 18:250.

Nelson, C. H. 1984. The influence of growth rate and cell concentration on bacterial attachment to surfaces in a continuous flow system, p. 80. M. S. Thesis, Montana State University, Bozeman.

Nelson, C. H., J. A. Robinson, and W. G. Characklis. 1985. Bacterial adsorption to smooth surfaces: rate, extent, and spatial pattern. Biotech. Bioeng. 27:1662-1667.

Reed, K. C., and F. L. Bygrave. 1975. Methodology for in vitro Ca^{2+} transport. Anal. Biochem. 67:44-54.

Robinson, J. A., M. G. Trulear, and W. G. Characklis. 1984. Cellular reproduction and extracellular polymer formation by Pseudomonas aeruginosa in continuous culture. Biotech. Bioeng. 26:1409-1417.

Roux, W. 1894. Arch. Entwickmch. 1:43-68.

Rutter, P. R. 1980. In A. S. C. Curtis, and J. D. Pitts (ed.), Cell adhesion and motility. Cambridge University Press, Cambridge.

Schindler, M., and M. J. Osborn. 1979. Interactions of divalent cations and polymyxin B with lipopolysaccharide. Biochemistry. 18:4425-4430.

Shankar, K., and R. C. Bard. 1952. The effect of metallic ions on the growth and morphology of Clostridium perfingenes. J. Bacteriol. 63:279-290.

Shaw, D. J. 1970. Introduction to colloidal and surface chemistry. Butterworths, London.

Shimizu, T., T. Furuki, T. Waki, and K. Ichikawa. 1978. J. Ferment. Technol. 56:207.

Shooter, R. A., and H. V. Wyatt. 1955. Mineral requirements for growth of Staphylococcus pyogens: effect of magnesium and calcium ions. Br. J. Exp. Pathol. 36:341-350.

Silver, S. 1977. Calcium transport in microorganisms, p. 49-103. In E. D. Weinberg (ed.), Microorganisms and Minerals. Marcel Dekker, Inc., New York.

Stahl, U., U. Kues, and K. Esser. 1983. Flocculation in yeast, an assay on the inhibition of cell aggregation. Eur. J. Appl. Microbiol. Biotech. 17:199-202.

Stanley, S. M. 1983. Factors affecting the reversible attachment of Pseudomonas aeruginosa to stainless steel. Can. J. Microbiol. 29:1493-1499.

Stouthamer, A. H. 1977. Theoretical calculations on the influence of the inorganic nitrogen source on parameters for aerobic growth of microorganisms. Antonie van Leeuwenhoek. 43:351-367.

Sukenik, A., W. Schroder, J. Lauer, G. Shelef, and C. J. Soeder. 1985. Coprecipitation of microalgal biomass with calcium and phosphate ions. Water Res. 19:127-129.

Sutherland, I. W. 1982. Biosynthesis of microbial exopolysaccharides, p. 80-142. In A. H. Rose and J. G. Morris (ed.), Advances in Microbial Physiology: volume 23. Academic Press, London.

Trulear, M. G., and W. G. Characklis. 1982. Dynamics of biofilm processes. J. Water Poll. Control Fed. 54:1288-1301.

Trulear, M. G. 1983. Cellular reproduction and extracellular polymer formation in the development of biofilms, p. 141. Ph.D. Thesis, Montana State University, Bozeman.

Turakhia, M. H., K. E. Cooksey, and W. G. Characklis. 1983. Influence of calcium-specific chelant on biofilm removal. Appl. Environ. Microbiol. 46:1236-1238.

Wacker, W. E. C., and R. J. P. William. 1968. Magnesium/calcium balances and steady states of biological systems. J. Theoret. Biol. 20:65-78.

Wang, H. Y., D. G. Mou, and J. R. Swartz. 1976. Thermodynamic evaluation of microbial growth. Biotech. Bioeng. 18:1811-1814.

Weinberg, E. D. 1977. Microorganisms and minerals, p. 491. Marcel Dekker, Inc., New York.

Weiss, L. 1974. Cellular pharmacology of lanthanum. Annu. Rev. Pharmacol. 14:343-354.

Wilkinson, J. R., and G. H. Stark. 1956. Proceedings of the Royal Physical Society, Edinburgh. 25:35.

Woods, D. E., D. C. Strauss, W. G. Johnson, Jr., V. K. Berry, and J. A. Bass. 1980. Role of pili in adherence of Pseudomonas aeruginosa to mammalian buccal epithelial cells. Infect. Immun. 29:1146-1151.

Wyatt, H. V. 1961. Cation requirements of He La cells in tissue cultures. Exp. Cell Res. 23:97-107.

Wyatt, H. V., G. W. Reed, and A. H. Smith. 1962. Calcium requirement for growth of Staphylococcus pyogenes. Nature. 195:100-101.

Wyatt, H. V. 1964. Cations, enzymes and control of cell metabolism. J. Theor. Biol. 6:441-479.

Zar, J. H. 1983. Biostatistical analysis, p. 718. Prentice Hall, Inc., Englewood Cliffs, NJ.

Zelver, N. 1979. Biofilm development and associated energy losses in water conduits. M. S. Thesis, Rice University, Houston, TX.

Zobell, C. E. 1943. The effect of solid surface upon bacterial activity. J. Bacteriol. 46:39-59.

NOMENCLATURE

NOMENCLATURE

A	Surface area	(L^2)
AR	Annular reactor	
D	Dilution rate	(t^{-1})
F	Volumetric flow rate	(L^3t^{-1})
F_R	Recycle flow rate	(L^3t^{-1})
k_b	Biofilm growth-associated polymer formation rate coefficient	$(M_pM_x^{-1})$
k'_b	Biofilm nongrowth-associated polymer formation rate coefficient	$(M_pM_x^{-1}t^{-1})$
k_c	Mass transfer coefficient	(t^{-1})
K_s	Saturation coefficient	(M_sL^{-3})
N_o	Diffusion flux of oxygen	$(M_oL^{-2}t^{-1})$
O_2	Effluent oxygen concentration	(M_oL^{-3})
O_{2i}	Influent oxygen concentration	(M_oL^{-3})
O_2^*	Saturated oxygen concentration	(M_oL^{-3})
p	Polymer carbon concentration	(M_pL^{-3})
p_b	Biofilm polymer carbon areal density	(M_pL^{-2})
p_i	Influent polymer carbon concentration	(M_pL^{-3})
R_D	Net rate of biomass detachment	$(ML^{-2}t^{-1})$
r_p	Specific polymer formation rate	$(M_pM_x^{-1}t^{-1})$
R_{dp}	Polymer carbon detachment rate from the biofilm	$(M_pL^{-2}t^{-1})$
R_{dx}	Cellular carbon detachment rate from the biofilm	$(M_xL^{-2}t^{-1})$

R_{pb}	Polymer carbon formation rate in the biofilm	$(M_p L^{-2} t^{-1})$
R_{xb}	Cellular carbon reproduction rate in the biofilm	$(M_x L^{-2} t^{-1})$
s	Glucose carbon concentration	$(M_s L^{-3})$
t	Time	(t)
TC	Total carbohydrate (glucose equivalents)	(ML^{-3})
TOC_b	Biofilm total organic carbon concentration	$(M_c L^{-2})$
TOC_{soln}	Liquid solution total organic carbon concentration	$(M_c L^{-3})$
TR	Tubular reactor	
V	Volume of the system	(L^3)
x	Cellular carbon concentration	$(M_x L^{-3})$
x_b	Biofilm cellular carbon area density	$(M_x L^{-2})$
x_i	Influent cellular carbon concentration	$(M_x L^{-3})$
x_T	Suspended biomass concentration	(ML^{-3})
$Y_{pb/o}$	Yield coefficient of polymer carbon from oxygen	$(M_p M_o^{-1})$
$Y_{pb/s}$	Yield coefficient of polymer carbon from substrate	$(M_p M_s^{-1})$
$Y_{s/o}$	Stoichiometric ratio between glucose carbon and oxygen	$(M_s M_o^{-1})$
$Y_{xb/o}$	Yield coefficient of cellular carbon from oxygen	$(M_x M_o^{-1})$
$Y_{xb/s}$	Yield coefficient of cellular carbon from substrate	$(M_x M_s^{-1})$
μ	Specific cellular growth rate	(t^{-1})
μ_b	Biofilm specific cellular growth rate	(t^{-1})
μ_m	Maximum specific growth rate	(t^{-1})

APPENDICES

APPENDIX A

RAW DATA: ANNULAR REACTOR EXPERIMENTS

APPENDIX A

RAW DATA: ANNULAR REACTOR EXPERIMENTS

1. AR #___ refers to annular reactor number.
2. BCC refers to biofilm cell count (# m^{-2}).
3. BCD refers to biofilm cell dimensions (μ_m x μ_m).
4. BM refers to dry biofilm mass (mg m^{-2}).
5. LCC refers to liquid phase cell count (# ml^{-1}).
6. LCD refers to liquid phase cell dimensions (μ_m x μ_m).
7. O_2 is effluent oxygen concentration (mg l^{-1}).
8. O_{2i} is influence oxygen concentration (mg l^{-1}).
9. p is polymer carbon concentration (mg l^{-1}).
10. p_b is biofilm polymer carbon areal density (mg m^{-2}).
11. s is effluent glucose carbon concentration (mg l^{-1}).
12. s_i is influent glucose carbon concentration (mg l^{-1}).
13. Time refers to time of experimental progression (h).
14. TOC refers to total organic carbon (mg l^{-1}).
15. TOC_b is biofilm total organic carbon (mg m^{-2}).

Table 19. Raw Data Experiment 3 (AR #7).

Time	48	97	140
Liquid phase			
s_i	6.56	6.56	6.56
s	1.15	0.82	0.82
Biofilm phase			
BM	332.5	610.5	919.6±30.5
TOC_b	316.1±15.3	222.6±8.9	397.4±13.5
x_b	39.1±5.6	43.2±6.0	118.6±16.8
P_b	277.1±16.2	179.3±10.7	278.8±21.5
BCC x 10^{-11}	5.4±0.8	5.8±0.8	16.0±2.3
BCD	1.60 x 0.7	1.65 x 0.7	1.65 x 0.70

Table 20. Raw Data Experiment 3 (AR #8).

Time	48	97	140
Liquid phase			
s_i	6.40	6.40	6.40
s	1.24	0.91	0.91
Biofilm phase			
BM	436.1	1042.9	1428.6±106.6
TOC_b	228.9±10.9	451.5±8.9	677.2±4.5
x_b	52.9±8.5	207.3±27.9	324.4±27.6
P_b	176.0±13.8	244.2±29.2	352.8±27.9
BCC x 10^{-11}	6.6±1.1	28.5±3.8	43.0±3.7
BCD	1.73 x 0.7	1.60 x 0.7	1.66 x 0.70

Table 21. Raw Data Experiment 4 (AR #7).

Time	57	96	140
Liquid phase			
s_i	4.83	4.83	4.83
s	0.66	0.77	0.54
Biofilm phase			
BM	407.0	667.7	742.1±276.3
TOC_b	131.3±0.0	680.4±135.0	375.2±4.5
x_b	20.8±1.5	29.9±2.9	61.3±8.4
P_b	110.5±1.5	650.5±135.1	313.9±45.8
BCC x 10^{-11}	2.9±0.2	4.1±0.4	8.2±1.1
BCD	1.60 x 0.7	1.60 x 0.7	1.65 x 0.70

Table 22. Raw Data Experiment 4 (AR #8).

Time	57	96	140
Liquid phase			
s_i	4.70	4.70	4.70
s	0.64	0.60	0.58
Biofilm phase			
BM	445.1	1538.9	2772.5
TOC_b	407.6±44.1	763.1±9.0	1297.2±0.0
x_b	84.6±12.3	297.1±31.9	646.7±76.7
P_b	323.1±45.7	465.9±33.1	650.6±76.7
BCC x 10^{-11}	10.4±1.5	37.5±4.0	85.0±10.1
BCD	1.80 x 0.7	1.75 x 0.7	1.68 x 0.70

Table 23. Raw Data Experiment 5 (AR #7).

Time	46	91	128	142
Liquid phase				
s_i	6.16	6.16	6.16	6.16
s	1.64	0.96	0.60	0.60
TOC	5.90±0.23	4.93±0.81	4.67±0.11	6.61±0.35
x	1.30±0.12	1.58±0.17	1.18±0.07	1.10±0.08
p	2.96±0.26	2.39±0.83	2.89±0.13	4.91±0.36
LCC x 10^{-6}	13.6±1.2	16.7±1.8	13.0±0.8	13.8±1.1
LCD	2.10 x 0.7	2.10 x 0.7	2.00 x 0.7	1.75 x 0.7
Biofilm phase				
BM	362.4	905.4	-	2162.7
TOC_b	383.5±105.2	496.7±41.6	-	1123.4±90.9
x_b	120.8±25.5	156.3±12.9	278.5*	223.4±19.9
p_b	262.6±108.2	340.4±43.5	375.7*	900.0±93.1
BCC x 10^{-11}	11.1±2.3	20.8±1.4	-	25.5±2.2
BCD	2.40 x 0.7	2.00 x 0.7	-	1.60 x 0.7

* time smoothed value

Table 24. Raw Data Experiment 5 (AR #8).

Time	46	73	105	140
Liquid phase				
s_i	6.00	6.00	6.00	6.00
s	2.57	0.92	0.76	0.76
TOC	6.50±0.23	7.08±0.21	5.23±0.48	5.40±0.00
x	1.08±0.11	1.52±0.26	1.27±0.12	0.77±0.09
p	2.84±0.25	4.63±0.34	3.19±0.49	3.86±0.09
LCC x 10^{-6}	12.9±1.3	18.5±3.2	15.6±1.5	9.8±1.1
LCD	1.85 x 0.7	1.80 x 0.7	1.80 x 0.7	1.75 x 0.7
Biofilm phase				
BM	-	553.2	1023.8	1583.4
TOC_b	-	305.0±4.1	597.7±27.5	807.8±80.8
x_b	69.2*	124.1±22.1	236.8±30.4	302.5±22.3
p_b	162.4*	180.8±22.4	360.9±40.9	505.3±83.8
BCC x 10^{-11}	-	15.2±2.7	31.2±4.1	41.4±3.1
BCD	-	1.80 x 0.7	1.63 x 0.7	1.60 x 0.7

* time smoothed value

Table 25. Raw Data Experiment 6 (AR #7).

Time	49	92	124	146
Liquid phase				
s_i	6.32	6.32	6.32	6.32
s	2.23	1.22	1.13	0.97
TOC	5.22±0.69	4.94±0.07	4.90±0.72	4.58±0.36
x	0.96±0.07	1.40±0.16	0.75±0.08	1.90±0.25
p	2.02±0.69	2.32±0.17	3.02±0.72	1.71±0.44
LCC x 10^{-6}	11.9±0.8	17.3±1.9	9.7±1.0	25.7±3.2
LCD	1.80 x 0.7	1.80 x 0.7	1.70 x 0.7	1.70 x 0.7
Biofilm phase				
BM	313.6	1068.3	-	2403.8
TOC_b	103.3±1.8	560.9±10.8	-	985.6±45.8
x_b	61.8±8.4	253.1±25.0	429.3*	733.3±72.9
p_b	41.5±8.6	307.8±27.3	293.4*	252.3±86.0
BCC x 10^{-11}	7.56±1.0	30.2±3.0	-	89.0±8.9
BCD	1.80 x 0.7	1.85 x 0.7	-	1.80 x 0.7

* time smoothed value

Table 26. Raw Data Experiment 6 (AR #8).

Time	49	72	105	140
Liquid phase				
s_i	6.04	6.04	6.04	6.04
s	2.15	1.38	1.13	1.03
TOC	7.38±0.23	4.47±0.37	5.46±0.26	4.56±0.80
x	1.34±0.11	1.38±0.19	1.73±0.14	1.67±0.28
p	3.89±0.25	1.71±0.41	2.60±0.29	1.86±0.85
LCC x 10^{-6}	16.6±1.3	17.5±2.4	22.0±1.7	20.0±3.4
LCD	1.82 x 0.7	1.76 x 0.7	1.78 x 0.7	1.80 x 0.7
Biofilm phase				
BM	375.2	413.4	1068.3	2251.0
TOC_b	174.9±17.4	193.9±9.5	540.5±30.2	922.0±40.7
x_b	65.1±6.6	97.7±26.9	260.5±30.3	606.8±66.8
p_b	109.8±18.6	96.3±28.5	280.0±42.8	315.2±78.2
BCC x 10^{-11}	7.6±0.8	12.3±3.4	33.8±3.9	83.7±9.2
BCD	1.90 x 0.7	1.75 x 0.7	1.70 x 0.7	1.60 x 0.70

Table 27. Raw Data Experiment 7 (AR #7).

Time	87	113	137
Liquid phase			
s_i	6.34	6.34	6.34
s	1.65	1.05	0.96
O_{2i}	7.2	7.2	7.2
O_2	5.08	4.63	4.63
TOC	2.80±0.21	3.25±0.00	4.01±0.45
x	0.42±0.02	1.31±0.11	1.22±0.11
p	0.73±0.21	0.89±0.11	1.83±0.46
LCC x 10^{-6}	2.0±0.2	16.1±1.4	15.8±1.4
LCD	1.90 x 0.7	1.80 x 0.7	1.70 x 0.7
Biofilm phase			
BM	-	273.2	617.5
TOC_b	205.6±6.4	314.8±10.8	515.1±17.5
x_b	52.4±0.0	70.5±9.2	101.8±17.1
P_b	153.2±6.4	244.3±14.2	413.2±24.5
BCC x 10^{-11}	5.9±2.7	9.1±1.2	13.7±2.4
BCD	1.80 x 0.7	1.80 x 0.7	1.70 x 0.7

APPENDIX B

RAW DATA: TUBULAR REACTOR DETACHMENT EXPERIMENTS

APPENDIX B

RAW DATA: TUBULAR REACTOR DETACHMENT EXPERIMENTS

1. TR refers to tubular reactor.
2. t is the time after chelant addition (min).
3 SS refers to effluent suspended solids (mg l^{-1}).
4. LCC refers to liquid phase cell count (# ml^{-1}).
5. TC refers to total carbohydrate (mg l^{-1}).
6. s is the effluent glucose carbon concentration (mg l^{-1}).
7. CSS refers to calculated suspended solids (mg l^{-1}).

Table 28. Raw Data TR Experiment 1.

t	SS	LCC X 10-6	TC	s	CSS
-30	2.0	4.99±1.10	5.65	-	0.230±0.05
0	-	-	-	0.04	-
1	5.1	5.56±1.00	-	0.07	0.257±0.05
2	6.7	7.78±1.37	6.09	-	0.359±0.06
3	6.4	7.20±1.00	5.56	-	0.332±0.05
4	7.8	-	-	-	-
5	13.8	16.70±1.39	7.53	-	0.772±0.06
10	18.1	29.00±5.22	8.16	-	1.340±0.02
15	27.1	30.70±4.10	13.18	0.00	1.419±0.19
45	33.8	46.20±6.60	17.80	-	2.135±0.30
75	31.8	38.20±4.82	15.06	-	1.765±0.22
105	24.7	34.80±2.88	14.06	0.00	1.608±0.13
180	19.0	23.40±3.39	6.65	-	1.081±0.16

Table 29. Raw Data TR Experiment 2.

t	SS	LCC X 10-6	TC	s	CSS
-30	11.0	-	9.97	0.07	-
0	8.0	1.60±0.43	5.16	0.03	0.074±0.02
3	34.8	7.86±1.15	-	-	0.363±0.05
5	60.0	9.47±1.09	6.02	0.00	0.438±0.05
8	87.2	-	13.80	0.00	-
10	155.5	20.00±3.44	20.47	0.03	0.924±0.16
12	144.4	-	25.90	0.00	-
15	182.5	-	29.24	0.00	-
20	189.5	73.20±20.0	34.80	0.00	3.382±0.92
35	-	65.80±1.00	65.80	0.00	3.040±0.05
52	283.8	58.00±10.1	46.16	0.00	2.680±0.50
72	200.0	-	39.98	0.00	-
95	190.0	66.20±8.73	39.67	-	3.060±0.40
120	-	36.00±5.10	-	-	1.663±0.23

APPENDIX C

RAW DATA: ANNULAR REACTOR DETACHMENT EXPERIMENTS

APPENDIX C

RAW DATA: ANNULAR REACTOR DETACHMENT EXPERIMENTS

1. AR #___ refers to annular reactor number.
2. t is the time after chelant addition (min).
3 SS refers to effluent suspended solids (mg l^{-1}).
4. LCC refers to liquid phase cell count (# ml^{-1}).
5. TC refers to total carbohydrate (mg l^{-1}).
6. s is the effluent glucose carbon concentration (mg l^{-1}).
7. CSS refers to calculated suspended solids (mg l^{-1}).

Table 30. Raw Data Detachment Studies Experiment 1 (AR #7).

t	SS	LCC X 10^{-6}	TC	s	CSS
0	1.95	0.33±0.14	0.0	0.70	0.052±0.02
14	1.94	0.50±0.12	0.0	0.64	0.079±0.02
30	-	-	0.0	0.61	-
60	2.00	0.50±0.22	0.0	0.64	0.079±0.04

Table 31. Raw Data Detachment Studies Experiment 1 (AR #8).

t	SS	LCC X 10-6	TC	s	CSS
0	1.61	0.35±0.13	0.0	0.67	0.055±0.02
2	5.26	-	-	-	-
3.5	7.07	6.21±1.01	-	-	0.985±0.16
5	13.20	17.70±1.67	2.31	-	2.810±0.26
7	12.44	7.34±2.78	2.03	-	1.164±0.44
10	10.70	-	3.01	-	-
12	8.90	-	-	-	-
14	9.32	3.20±1.21	-	0.64	0.507±0.19
17	-	2.30±1.21	3.01	-	0.364±0.19
21	6.55	-	-	-	-
25	4.67	-	2.45	-	-
30	-	0.96±0.25	-	0.64	0.153±0.04
50	1.41	-	-	-	-
60	-	0.82±0.25	1.89	0.64	0.131±0.04

Table 32. Raw Data Detachment Studies Experiment 2 (AR #7).

t	SS	LCC X 10-6	TC	s	CSS
0	1.50	0.27±0.08	3.14	0.60	0.043±0.01
15	1.60	0.09±0.03	-	-	0.014±0.01
30	-	0.14±0.07	3.50	0.64	0.022±0.01
60	2.00	-	1.92	0.50	-

Table 33. Raw Data Detachment Studies Experiment 2 (AR #8).

t	SS	LCC X 10-6	TC	s	CSS
0	1.19	0.90±0.24	1.92	0.96	0.143±0.04
2	5.50	2.33±0.98	3.71	-	0.370±0.16
3	13.50	-	3.00	-	-
4	15.00	3.80±1.30	4.57	-	0.063±0.21
7	29.98	15.20±1.41	6.22	-	2.410±0.22
11.5	26.10	12.90±1.57	-	-	2.040±0.25
13.5	21.52	6.33±0.87	5.79	-	1.004±0.14
19	17.50	7.61±0.55	-	-	1.207±0.09
30	9.34	-	3.00	-	-
40	7.22	2.78±1.05	3.57	-	0.441±0.17
50	3.21	-	-	-	-
60	4.10	1.22±0.30	2.28	0.64	0.193±0.05

Table 34. Raw Data Detachment Studies Experiment 3 (AR #7).

t	SS	TC	s
0	4.70	2.35	1.02
1.5	11.20	–	–
3.5	10.11	3.09	–
4.5	9.18	3.34	–
5.5	9.30	3.09	–
7.5	10.80	2.60	–
11.5	10.60	3.22	–
16	10.11	–	0.80
21	9.28	1.86	–
31	9.86	4.08	1.05
40	10.20	–	–
50	10.40	5.06	1.28
60	4.68	5.68	–

Table 35. Raw Data Detachment Studies Experiment 3 (AR #8).

t	SS	TC	s
0	1.54	4.45	0.90
1.5	38.40	–	–
3.5	–	14.32	–
4.5	–	14.90	–
5.5	63.75	–	–
8.5	65.90	13.09	–
12.5	39.35	10.70	–
16.5	28.80	–	–
20.5	14.00	6.79	0.71
30	9.33	5.70	0.90
40	7.00	–	0.80
50	2.70	4.45	–
60	1.51	–	0.80

Table 36. Raw Data Detachment Studies Experiment 4 (AR #7).

t	SS	TC	s
0	1.87	2.72	0.58
2	4.94	3.34	–
3.5	3.72	3.72	–
4.5	6.35	3.97	–
5.5	8.37	4.72	–
8.5	10.80	2.84	–
12.5	7.67	4.10	–
15	3.61	3.97	0.7
20	5.74	4.34	–
30	6.00	2.84	0.80
40	5.20	2.59	0.80
50	3.00	–	–
60	3.33	2.59	0.80

Table 37. Raw Data Detachment Studies Experiment 4 (AR #8).

t	SS	TC	s
0	4.64	1.47	0.64
1.5	28.40	6.23	–
2.5	23.30	7.86	–
3.5	41.00	7.74	–
4.5	43.50	7.98	–
5.5	42.72	7.48	–
8.9	38.20	7.74	–
12.5	24.32	–	–
15.5	34.51	7.74	–
20	21.67	4.10	0.64
30	10.90	3.97	–
40	6.20	2.97	–
50	3.20	–	0.67
60	3.51	2.71	0.67

Table 38. Raw Data Detachment Studies Experiment 6 (AR #7).

t	SS
0	6.40
2.5	51.70
3.5	56.88
4.5	66.93
5.5	58.75
8.5	53.03
12.5	38.80
16.5	38.10
20.5	16.11
30.5	11.11
40.5	7.50
50.5	7.70
56	3.70

APPENDIX D

EFFLUENT GLUCOSE AND OXYGEN DATA (AR EXPERIMENTS)

APPENDIX D

EFFLUENT GLUCOSE AND OXYGEN DATA (AR EXPERIMENTS)

Table 39. Effluent Glucose Data AR Experiment 1.

	Annular reactor # 7		Annular reactor # 8	
Time (h)	Effluent glucose mg/l	Glucose-carbon removal rate mg/l/min	Effluent glucose mg/l	Glucose-carbon removal rate mg/l/min
0	10.00	0.000	9.60	0.000
3	10.00	0.000	9.60	0.000
24	10.00	0.000	9.60	0.000
40	7.84	0.087	7.60	0.080
52	3.60	0.256	3.84	0.230
66	2.32	0.307	2.40	0.288
86	1.92	0.323	1.76	0.314

Table 40. Effluent Glucose Data AR Experiment 2.

	Annular reactor # 7		Annular reactor # 8	
Time (h)	Effluent glucose mg/l	Glucose-carbon removal rate mg/l/min	Effluent glucose mg/l	Glucose-carbon removal rate mg/l/min
0	10.40	0.000	9.60	0.000
3	10.40	0.000	9.60	0.000
27	10.40	0.000	8.64	0.038
40	6.40	0.160	8.00	0.064
50	5.20	0.208	3.20	0.246
65	2.40	0.320	1.68	0.317
93	1.60	0.352	1.60	0.320

Table 41. Effluent Glucose Data AR Experiment 3.

Time (h)	Annular reactor # 7 Effluent glucose mg/l	Annular reactor # 7 Glucose-carbon removal rate mg/l/min	Annular reactor # 8 Effluent glucose mg/l	Annular reactor # 8 Glucose-carbon removal rate mg/l/min
0	16.40	0.000	16.00	0.000
7	15.36	0.000	15.20	0.032
24	12.00	0.176	11.12	0.195
33	-	-	4.80	0.448
45	3.44	0.518	3.20	0.512
55	1.60	0.592	2.24	0.550
77	1.92	0.579	2.00	0.560
93	2.32	0.563	2.16	0.554
101	2.08	0.573	2.16	0.554
121	2.48	0.557	2.40	0.544
127	2.00	0.576	2.24	0.550

Table 42. Effluent Glucose Data AR Experiment 4.

	Annular reactor # 7		Annular reactor # 8	
Time (h)	Effluent glucose mg/l	Glucose-carbon removal rate mg/l/min	Effluent glucose mg/l	Glucose-carbon removal rate mg/l/min
0	12.08	0.000	11.76	0.000
8	11.68	0.016	8.32	0.138
22	9.12	0.118	6.48	0.211
27	7.28	0.192	4.72	0.282
33	4.80	0.291	3.04	0.349
45	2.64	0.378	1.60	0.406
49	1.60	0.419	1.60	0.406
70	1.68	0.416	1.60	0.406
78	1.44	0.426	1.44	0.413
96	1.92	0.406	1.60	0.406
119	1.68	0.416	1.52	0.410
140	1.36	0.429	1.44	0.413

Table 43. Effluent Glucose Data AR Experiment 5.

Time (h)	Annular reactor # 7 Effluent glucose mg/l	Annular reactor # 7 Glucose-carbon removal rate mg/l/min	Annular reactor # 8 Effluent glucose mg/l	Annular reactor # 8 Glucose-carbon removal rate mg/l/min
0	15.40	0.000	15.00	0.000
1	15.00	0.016	14.52	0.019
7	-	-	14.60	0.016
20	14.52	0.036	13.71	0.052
31	11.36	0.162	-	-
43	4.41	0.440	7.24	0.310
46	4.09	0.453	6.43	0.343
53	3.04	0.495	3.12	0.475
69	2.47	0.517	2.23	0.510
73	-	-	2.31	0.507
76	2.31	0.524	2.15	0.514
91	2.39	0.520	-	-
97	1.58	0.553	1.83	0.527
105	-	-	1.91	0.524
128	1.50	0.556	-	-
142	1.50	0.556	1.91	0.524

Table 44. Effluent Glucose Data AR Experiment 6.

	Annular reactor # 7		Annular reactor # 8	
Time (h)	Effluent glucose mg/l	Glucose-carbon removal rate mg/l/min	Effluent glucose mg/l	Glucose-carbon removal rate mg/l/min
0	15.80	0.000	15.10	0.000
1	15.65	0.006	14.63	0.019
21	14.23	0.063	13.76	0.054
30	12.03	0.151	11.79	0.132
45	6.36	0.378	6.28	0.353
49	5.57	0.409	5.37	0.389
53	4.15	0.466	4.07	0.441
70	-	-	3.44	0.466
73	3.52	0.491	-	-
79	3.13	0.507	3.13	0.479
92	3.05	0.510	-	-
94	-	-	2.66	0.498
105	-	-	2.81	0.491
117	2.42	0.535	2.58	0.501
124	2.81	0.520	-	-
144	2.42	0.535	2.58	0.501

Table 45. Effluent Oxygen Data AR Experiment 5.

		Annular reactor # 7		Annular reactor # 8	
Time (h)	Influent oxygen mg/l	Effluent oxygen mg/l	Oxygen removal rate mg/l/h	Effluent oxygen mg/l	Oxygen removal rate mg/l/h
7	7.5	7.5	0.00	7.5	0.00
20	7.2	6.8	5.58	6.9	4.18
31	7.1	6.4	9.76	6.7	4.89
49	7.1	4.7	33.46	5.5	22.31
69	7.1	4.8	32.06	5.2	26.49
76	7.1	4.5	36.25	4.9	30.67
97	7.0	4.5	34.85	4.9	29.28
116	7.3	4.5	39.03	-	-
126	7.3	4.0	46.00	4.5	39.03
139	7.0	4.1	40.43	-	-

Table 46. Effluent Oxygen Data AR Experiment 6.

		Annular reactor # 7		Annular reactor # 8	
Time (h)	Influent oxygen mg/l	Effluent oxygen mg/l	Oxygen removal rate mg/l/h	Effluent oxygen mg/l	Oxygen removal rate mg/l/h
6	7.4	7.4	0.00	7.4	0.00
24	7.3	7.0	4.88	7.0	4.88
31	7.3	6.5	11.15	6.5	11.15
55	7.3	5.2	29.28	5.4	26.49
79	7.3	4.8	34.15	4.8	34.85
94	7.2	5.1	29.28	4.9	32.06
118	7.1	4.9	30.67	4.8	32.06
139	7.3	4.6	37.64	4.6	37.64

APPENDIX E

RAW DATA: BATCH GROWTH EXPERIMENTS

APPENDIX E

RAW DATA: BATCH GROWTH EXPERIMENTS

Table 47. Oxygen Uptake Data Batch Experiment 1.

Time (h)	Oxygen uptake ($mg\ l^{-1}$) unit I	unit II	unit III
0	0.0	0.0	0.0
10	0.0	0.0	0.0
20	1.1	0.3	0.0
21	2.3	1.0	0.5
22	4.7	2.0	1.1
23	6.9	2.6	1.4
24	10.3	3.7	1.8
25	15.3	5.2	2.5
26	21.8	7.1	3.0
27	28.5	9.9	4.2
28	38.2	13.3	6.1
29	49.1	17.9	7.9
30	63.1	24.0	11.4
31	70.2	32.0	16.0
32	78.3	42.5	22.5
33	82.0	50.2	31.7
34	84.6	56.2	43.2
35	87.1	62.4	56.3
36	88.3	66.5	63.5
37	89.7	69.3	69.9
38	90.9	71.0	73.5
39	92.2	72.2	76.0
40	92.2	72.5	77.4
41	93.4	73.7	78.7
43	95.9	76.2	81.8
45	97.0	77.5	83.8
47	98.3	79.2	85.6
49	98.3	79.7	86.4
53	100.7	81.5	88.4
55	100.7	82.0	89.2

Table 48. Oxygen Uptake Data Batch Experiment 2.

Time (h)	Oxygen uptake ($mg\ l^{-1}$)		
	unit I	unit II	unit III
0.00	0.0	0.0	0.0
7.00	0.0	0.0	0.0
10.00	4.8	1.8	1.7
10.25	5.3	2.3	2.1
10.50	6.0	2.3	2.5
10.75	6.6	2.6	2.5
11.00	7.4	3.1	2.9
11.25	8.3	3.4	3.4
11.50	9.4	4.1	3.8
11.75	10.6	4.1	4.2
12.00	11.7	4.9	4.7
12.25	13.2	5.2	5.1
12.50	14.7	5.6	5.5
12.75	16.3	6.4	6.1
13.00	18.0	7.0	6.5
13.25	20.5	7.4	7.4
13.50	22.3	8.3	7.9
13.75	24.8	8.9	8.3
14.00	27.6	9.9	9.3
14.25	30.6	10.9	10.3
14.50	34.6	11.8	11.3
14.75	37.6	12.7	11.9
15.00	41.8	13.8	12.9
15.25	45.9	15.2	14.1
15.50	50.1	16.8	15.2
15.75	55.0	17.7	16.4
16.00	60.0	19.5	17.7
16.25	65.0	21.1	19.3
16.50	70.1	23.3	21.1
16.75	76.8	25.1	23.0

Table 48. Continued.

Time (h)	Oxygen uptake (mg l^{-1})		
	unit I	unit II	unit III
17.00	82.6	27.6	24.8
17.25	88.6	30.1	27.5
17.50	95.6	33.0	29.7
17.75	101.8	35.7	31.8
18.00	108.9	39.0	34.5
18.25	114.8	42.0	37.5
18.50	122.0	45.9	40.7
18.75	128.2	49.9	44.3
19.00	135.6	54.7	48.3
19.25	142.4	58.8	52.5
19.50	149.7	64.0	56.4
19.75	157.0	69.5	61.5
20.00	163.7	75.6	66.1
21.00	189.2	101.0	89.0
22.00	213.0	127.9	113.8
23.00	237.8	155.2	140.5
23.50	249.7	168.8	153.8
24.00	261.0	181.4	166.8
24.50	272.2	194.4	180.3
25.00	284.0	207.0	192.8
26.00	305.4	231.8	219.4
26.50	315.2	243.8	233.2
27.00	324.7	256.1	246.7
27.50	333.5	268.3	260.8
28.00	342.8	279.6	274.1
28.50	351.2	290.2	287.3
29.00	360.4	300.7	300.5
30.00	377.1	319.6	325.7
30.50	385.5	327.5	336.2
31.84	405.7	345.6	361.7

Table 49. Oxygen Uptake Data Batch Experiment 3.

Time (h)	Oxygen uptake ($mg\ l^{-1}$)		
	unit I	unit II	unit III
0.00	0.0	0.0	0.0
7.00	2.6	2.2	1.6
10.00	4.8	4.3	3.7
12.00	6.8	6.5	4.6
13.50	9.8	9.7	5.2
13.75	10.7	10.5	5.7
14.00	11.2	11.2	5.7
14.25	12.4	12.1	6.0
14.50	13.7	13.3	6.2
14.75	15.2	14.3	6.4
15.00	16.3	15.5	6.7
15.25	18.1	17.1	7.1
15.50	19.8	18.9	7.2
15.75	21.6	20.5	7.4
16.00	23.6	22.4	7.9
16.25	25.6	24.8	8.6
16.50	27.9	27.4	9.2
16.75	30.7	30.0	10.1
17.00	33.1	33.2	10.7
17.25	36.5	36.4	11.4
17.50	39.5	40.0	12.4
17.75	42.5	43.9	13.1
18.00	46.6	48.1	14.0
18.25	50.5	52.9	15.4
18.50	54.3	58.0	16.7
18.75	58.4	63.0	18.0
19.00	62.7	69.0	19.3
19.25	67.3	75.3	20.6
19.50	72.5	81.4	22.4
19.75	77.3	88.0	24.4

Table 49. Continued.

Time (h)	Oxygen uptake (mg l^{-1}) unit I	unit II	unit III
20.00	82.3	95.6	26.2
20.25	87.6	103.1	28.2
20.50	93.8	110.8	30.5
20.75	99.4	118.6	33.5
21.00	105.0	126.8	36.2
21.25	111.0	134.9	39.3
21.50	116.9	142.1	43.0
21.75	122.3	149.1	46.3
22.00	128.1	156.1	50.0
22.50	139.2	170.9	59.0
23.00	150.2	185.8	68.8
23.25	156.0	193.0	74.6
23.50	161.8	201.8	80.2
23.75	167.6	209.1	86.3
24.00	173.6	216.4	93.3
24.25	179.0	224.5	99.7
24.50	185.0	232.5	106.9
25.00	196.4	248.0	121.5
25.50	208.0	246.6	137.4
26.00	219.7	281.2	155.5
27.00	242.8	307.9	192.2
28.00	264.5	328.7	230.3
29.00	286.3	349.8	268.7
30.00	308.7	367.4	305.0
32.00	348.0	395.1	357.9
34.00	378.5	413.4	393.5
36.00	403.5	427.8	421.1
38.00	424.2	439.0	438.3
40.00	443.0	450.5	447.8
42.00	460.9	464.9	455.1

APPENDIX F

OXYGEN DIFFUSION STUDIES

APPENDIX F

OXYGEN DIFFUSION STUDIES

Objective

To determine the amount of oxygen diffusing into the annular reactor.

Method

The transfer of oxygen into the annular reactor can be determined by varying the concentration of oxygen in the dilution water (2-6 mg l^{-1}) and monitoring the changes in the effluent. Dissolved oxygen concentration in the dilution water was controlled by purging nitrogen gas. The flow rate of the purged water into the annular reactor was controlled at 60 ml min^{-1} using a variable speed peristaltic pump (Cole-Parmer Instrument Company, IL, model No. 7533-00). The flow rate water was monitored with an in-line flow meter (Gilmont Instruments Inc., Great Neck, NY, size No. 13). Rotational speed of the annular reactor was maintained at 250 rpm. The oxygen concentration was measured with a YSI model-54 oxygen meter. A material balance approach was used to account for the transfer of oxygen into the annular reactor. The mass balance (for oxygen) across annular reactor was as follows:

$$V\, dO_2/dt = F\,(O_{2i} - O_2) + N_o A \qquad (1)$$

net rate of accumulation in the reactor		net rate of output by flow		net flux of oxygen into the reactor

where,

V	=	volume of the system	(L^3)
F	=	flow rate of dilution water	(L^3t^{-1})
O_2	=	effluent oxygen concentration	(M_oL^{-3})
O_{2i}	=	influent oxygen concentration	(M_oL^{-3})
N_o	=	flux of oxygen into the system	$(M_oL^{-2}t^{-1})$
A	=	surface area	

Defining the oxygen flux into the reactor as:

$$N_o = k_c (O_2^* - O_2) V / A \qquad (2)$$

or,

$$dO_2/dt = D (O_{2i} - O_2) + k_c (O_2^* - O_2) \qquad (3)$$

where,

k_c	=	mass transfer coefficient	(t^{-1})
O_2^*	=	saturated oxygen concentration	(M_oL^{-3})
D	=	dilution rate	(t^{-1})

At steady state, k_c can be calculated from equation (3) as:

$$k_c = D (O_2 - O_{2i}) / k_c (O_2^* - O_2) \qquad (4)$$

Results:

The mass transfer coefficient, k_c, was calculated for a number of different influent oxygen concentrations (1.9 - 6.2 mg l^{-1}). The mass transfer coefficient was found to be 7.94 ± 0.64 h^{-1}.

Table 50. Experimental Data from Oxygen Transport Studies.

AR #	Temp. °C	Influent oxygen mg l^{-1}	Effluent oxygen mg l^{-1}	k_c h^{-1}
7	23	4.10	5.90	8.00
7	23	6.20	6.80	8.00
7	23	6.20	6.80	8.00
7	22	4.80	6.20	7.30
7	22	5.10	6.42	8.52
7	22	6.10	6.80	7.64
7	23	1.90	4.96	8.02
7	23	4.05	6.00	9.36
8	23	4.10	5.80	7.03
8	23	6.20	6.80	8.00
8	23	6.25	6.80	7.34
8	22	4.80	6.20	7.30
8	22	5.12	6.35	7.38
8	22	6.10	6.80	7.64
8	23	1.90	5.10	8.93
8	23	4.10	5.95	8.54

Average value of $k_c = 7.94 \pm .064\ h^{-1}$.

APPENDIX G

BATCH GROWTH EXPERIMENTS: EFFECT OF EGTA

APPENDIX G

BATCH GROWTH EXPERIMENTS: EFFECT OF EGTA

Objective

To determine the effect of EGTA (or free calcium) on the maximum specific growth rate, μ_m, of Pseudomonas aeruginosa.

Method

Batch growth (Glucose 1000 g m^{-3})

Absorbance at 660 nm

Procedure

Inoculate the batch growth medium (Table 51) with inoculum obtained from chemostat. Monitor the growth by measuring the change in absorbance of the medium at 660 nm.

Results

The addition of EGTA in the batch growth medium affected the maximum growth rate of Pseudomonas aeruginosa. Results of the two experiments are summarized in Table 17. EGTA was added to the medium to reduce the concentration of free calcium in the medium. The concentration of free calcium can be estimated using nomographs (Reed and Bygrave, 1975). These results indicate that the maximum specific growth rate of

Pseudomonas aeruginosa is influenced by free calcium in the medium. A t-test (Zar, 1984) was used to test the hypothesis that there is a significant difference in μ_m at different EGTA concentrations. There was a significant difference (at 95% confidence level) in μ_m between 0.000, 0.002, and 0.004 M EGTA concentrations. However, there was no significant difference in μ_m between 0.004 and 0.006 M EGTA concentrations.

Table 51. Composition of Batch Growth Medium.

Components	Concentration
$C_6H_{12}O_6$	1.000 g
NH_4CL	0.360 g
$MgSO_4$ $7H_2O$	0.100 g
Na_2HPO_4	0.210 g
KH_2PO_4	0.200 g
micronutrients	*
Tris	1.210 g
Distilled water	0.001 m^3
pH (pH units)	7.000

*For composition of the micronutrients see Table 3.

APPENDIX H

THE INFLUENCE OF CALCIUM ON MICROBIAL ADSORPTION

APPENDIX H

THE INFLUENCE OF CALCIUM ON MICROBIAL ADSORPTION

Objective

To determine if calcium is involved in the adsorption of bacteria to glass surface.

Microorganism: *Pseudomonas* 224S.

Method

Four glass slides were exposed to *Pseudomonas* 224S in a continuous flow microbial attachment reactor (Nelson, 1984). The aim of the experiment was to determine if EGTA (1 mM) can remove irreversibly adsorbed cells from the surface.

Staining Procedure

Following the adsorption experiment described by Nelson (1984), the slides were removed from the reactor and treated as follows: (1) rinsed with 10 ml of filtered distilled water per slide in a reproducible manner (Nelson, 1984; Marshall et al., 1971), (2) two slides were treated with 1 mM EGTA for 5 minutes and two with sterile water (control), (3) all the four slides were washed with 10 ml of distilled water, (4) next, the slides were stained with 1 ml of acridine orange solution per slide for 15 minutes, and (5) finally, the slides were

rinsed with 10 ml of 70% ethanol. The cells were counted using epifluorescence microscopy. The results are reported as potential colony forming units (PCFU) per microscope field. PCFU were defined as any group of cells in physical contact with each other, a cell in the process of dividing, or a single cell adsorbed to the microscope slide after a known exposure time (Nelson, 1984; Nelson et al., 1985).

Results

The results of two experiments, in which the clean slides were exposed for a known period of time, are summarized in Table 18. There was no detectable difference in PCFU/field between control and EGTA treated slides. This suggests that calcium was not involved in the adsorption of *Pseudomonas* 224S to the glass surface.

Turakhia, Mukesh H.
The influence of
calcium on biofilm...

DATE	ISSUED TO